# DYNAMICS OF ATOM-DIATOM REACTIONS AT LOW ENERGY

BY

JOHN ALBERT OLSON

A DISSERTATION PRESENTED TO THE GRADUATE COUNCIL OF
THE UNIVERSITY OF FLORIDA
IN PARTIAL FULFILLMENT OF THE REQUIREMENTS
FOR THE DEGREE OF DOCTOR OF PHILOSOPHY

UNIVERSITY OF FLORIDA

1982

Copyright 1982

by

JOHN ALBERT OLSON

# ACKNOWLEDGEMENTS

I would like to convey my sincere appreciation to my advisor, Professor David A. Micha. He played an essential role not only in selecting this problem but also in developing the formalism used to solve it. His patience, encouragement and support during this period of research is also gratefully acknowledged.

I would like to thank the other faculty members and graduate students in the Quantum Theory Project. The many seminars and discussions have been of great educational value. In particular I would like to thank Professor Yngve Öhrn. His courses on Quantum mechanics greatly stimulated my interest in this field. I also appreciate the help of Dr. Eduardo Vilallonga in some of the numerical aspects of this work.

I would like to express my sincere gratitude to Professor Per-Olov Löwdin for providing me the opportunity to attend the summer school in Sweden and Norway. His yearly organization of the Sanibel Symposium has also been of great educational value to me. His kind interest in me while at the Quantum Theory Project is warmly appreciated, I would also like to thank my family in Jacksonville, Florida, for providing support and for furnishing a place to go for an occasional rest.

Finally, I would like to thank the secretaries and staff of the Quantum Theory Project for both their typing skills and their organization of numerous social events.

# TABLE OF CONTENTS

Page

ACKNOWLEDGEMENTS ..... iii

ABSTRACT ..... vii

CHAPTER

1 INTRODUCTION ..... 1

- 1-1 General Problem ..... 1
- 1-2 Electronic Motions ..... 3
- 1-3 Nuclear Motions ..... 6

2 ELECTRONIC REPRESENTATIONS ..... 12

- 2-1 Introduction ..... 12
- 2-2 Electronic State Representations ..... 16
  - 2-2a The Adiabatic Representation ..... 19
  - 2-2b The Strictly Diabatic Representation ..... 20
  - 2-2c The Nearly Adiabatic Representation ..... 23
- 2-3 The Minimization Procedure ..... 25
- 2-4 The Two Electronic State Problem in One Dimension ..... 30
- 2-5 A Model Calculation ..... 34
- 2-6 Discussion ..... 47

3 GENERAL FORMALISM OF THE DYNAMICS ..... 49

- 3-1 The One Electronic State Problem ..... 49
- 3-2 General Time Independent Formalism ..... 54
- 3-3 The Eikonal Approximation ..... 58
- 3-4 The Short Wavelength Approximation ..... 62
- 3-5 Time Dependent Equations ..... 66
- 3-6 Solutions of the Equations ..... 72
- 3-7 Expressions for Observables ..... 81

4 THE ELECTRONIC PROBLEM FOR $H_3^+$ IN THE ADIABATIC REPRESENTATION ..... 84

- 4-1 General Considerations ..... 84
- 4-2 Method of Diatomics in Molecules ..... 87
- 4-3 The Eigenvalues ..... 95
- 4-4 The Eigenfunctions ..... 104
- 4-5 Non-Adiabatic Couplings ..... 107

5 THE NUCLEAR PROBLEM FOR COLLINEAR $H_3^+$ .......... 112

- 5-1 Hyperspherical Coordinates .......... 112
- 5-2 The Hamiltonian in the Almost Adiabatic Representation .......... 119
  - 5-2a The Electronic Transformation .......... 121
  - 5-2b The Equations of Motion .......... 124
- 5-3 The Hamiltonian in the Diabatic Representation .......... 128
  - 5-3a The Electronic Transformation .......... 128
  - 5-3b The Equations of Motion .......... 130

6 CALCULATIONS FOR $H_3^+$ .......... 134

- 6-1 Electronic Results .......... 134
  - 6-1a The Diatomic Potentials .......... 134
  - 6-1b Adiabatic Potential Energy Surfaces .......... 138
  - 6-1c Non-adiabatic Couplings .......... 143
  - 6-1d Model of Non-adiabatic Couplings .......... 152
- 6-2 Trajectory Calculations .......... 154
  - 6-2a Test Cases .......... 161
  - 6-2b $H_3^+$ Results .......... 187
- 6-3 Experimental Studies .......... 234
- 6-4 Theoretical Studies .......... 240
- 6-5 Comparisons .......... 243
- 6-6 Conclusions .......... 254

APPENDICES

1 HYPERSPHERICAL COORDINATES .......... 259

2 COMPUTER PROGRAM .......... 265

3 TOTAL ELECTRON TRANSFER PROBABILITY .......... 270

REFERENCES .......... 276

BIOGRAPHICAL SKETCH .......... 280

Abstract of Dissertation Presented to the Graduate Council
of the University of Florida in Partial Fulfillment of the
Requirements for the Degree of Doctor of Philosophy

# DYNAMICS OF ATOM-DIATOM REACTIONS AT LOW ENERGY

By

John Albert Olson

August 1982

Chairman: David A. Micha
Major Department: Chemistry

This work focuses on two fundamental problems in scattering theory. The first is centered around the electronic basis used to expand the solution of the time independent Schrödinger Equation. The other consists of how to handle the problem for the nuclear degrees of freedom when more than one electronic basis function is included in the expansion.

In chapter two it is shown that, in the adiabatic electronic representation, the Hamiltonian is not hermitean if more than one electronic basis function is included in the expansion. It is pointed out that in such

cases alternative electronic representations may be more suitable. The adiabatic and diabatic representations are reviewed and the "nearly adiabatic" representation and a representation based on a minimization procedure are introduced. Calculations are done to compare the results from the diabatic representation and the representation arising from the minimization procedure.

Chapter three considers the problem for the nuclear degrees of freedom in multi-surface systems. A "common" eikonal is used for the nuclear wave function satisfying the time independent Schrödinger equation. This "common" eikonal is obtained from a modified Hamilton-Jacobi equation that involves an average potential. Implementing the short wavelength approximation and transforming to a time dependent picture leads to a set of first order differential equations in time that determine the expansion coefficients. It is shown that these equations along with the differential equations obtained from the Hamilton-Jacobi like equation for the nuclear positions and momenta form a coupled set of first order differential equations in time that are formally equivalent to Hamilton's equations of motion.

This procedure is applied to the collinear $H_3^+$ system. Hyperspherical coordinates are used for the nuclear degrees of freedom and the adiabatic potential energy surfaces and electronic coupling terms are obtained from the method of Diatomics in Molecules. A transformation to the diabatic representation is made and the trajectories are calculated

in this representation. Typical trajectories are presented in chapter six and a comparison of the total electron transfer probability with those from a quantum mechanical study is made. The results are encouraging.

# CHAPTER 1
# INTRODUCTION

## 1-1 General Problem

This study primarily addresses the problem of molecular reactions where more than one electronic state is energetically accessible. These processes are usually referred to as non-adiabatic collisions. The collisions are assumed to take place between combinations of atomic or molecular fragments that can be either charged or neutral. Since the origins of the formalism to be presented are based in quantum mechanics, a few comments on the general quantum mechanical treatment of the problem seem appropriate.

The general solution to the Schrödinger equation involving both nuclear and electronic degrees of freedom is a function of the nuclear and electronic coordinates. Until programs are available to numerically solve these multidimensional equations, some form of approximation to the solution must be made. Generally, the solution is expanded in an electronic basis. This in itself does not simplify the problem but with the approximation to be discussed next, the electronic problem can be solved independently of the dynamics of the nuclei.

The approximation referred to above is the well-known Born-Oppenheimer approximation (Born and Oppenheimer, 1927).

This approximation is physically based on the fact that the electron's mass is orders of magnitude smaller than the mass of a nucleus and hence that the electronic motions are much faster than nuclear motions. Then one would expect that the dependence of the wave function describing electronic motion on nuclear variables could be neglected. In other words, this approximation assumes that the nuclear kinetic energy operator can treat the electronic wave functions as constants and leads to solutions of the electronic problem that depend only on the positions of the nuclei.

With this approximation, the electronic problem is solved with the positions of the nuclei held fixed. Since the electronic problem must be solved for each internuclear configuration, the electronic functions, energies, etc. are said to depend parametrically on the nuclear coordinates. Since the dependence of the nuclear wave function on the electronic coordinates has been ignored, the solution to the problem is in the form of a linear combination of products of electronic functions that depend parametrically on the nuclear coordinates and nuclear functions that depend only on the nuclear variables.

This approximation is an extreme simplification to the most general solution in that the electronic problem is solved without a full dynamical knowledge of the nuclei. In other words, this approximation assumes that the electronic problem can be solved independent of the nuclear velocities. This approximation may not be valid when the nuclear speeds are high (comparable to those of the electrons). But in this study, the nuclear speeds will be slow compared to electronic speeds so that this approximation will be assumed to hold to a high degree of accuracy.

From the preceding discussion, it is apparent that there are two essential steps to solving the problem. The first is to choose an electronic basis that is convenient for the calculation and to solve the electronic problem within the Born-Oppenheimer approximation. This will be the subject matter of the next section and chapter two. The second step is to expand the solution in this basis and solve for the nuclear expansion coefficients. This will be the topic of the last section of this chapter and chapter three.

## 1-2 Electronic Motions

As was discussed in the previous section, the solution of the full Schrödinger equation is expanded in an electronic basis and the electronic problem is solved with the nuclei held fixed. In general, the expansion in a set of n electronic states will result in a square nxn matrix representation of the electronic Hamiltonian, i.e. the full Hamiltonian without the nuclear kinetic energy operator. Couplings between the nuclear expansion coefficients will occur through the off-diagonal matrix elements of the electronic Hamiltonian and through the electronic matrix representation of the nuclear kinetic energy operator. Different electronic representations give rise to some or all of these couplings and a brief discussion of some of the more familiar representations and their properties follows.

One of the most widely used electronic representations is the adiabatic representation (Born and Oppenheimer, 1927; Born and Huang, 1954). This representation has both been extensively used in bound state calculations, i.e. in calculations where the dynamics of the nuclei can be ignored, and in scattering calculations. It is essentially characterized by giving a diagonal matrix representation of the electronic Hamiltonian.

The (diagonal) matrix elements, often referred to as eigenvalues, of this representation give rise to potential energy hypersurfaces. For adiabatic reactions, the reactants and products are both on the same potential energy hypersurface while for non-adiabatic reactions the surface for the reactants is different from that of the products. A consequence of this representation is that surfaces of the same electronic symmetry do not cross (Molnarwitach, 1961), i.e. couplings, in most cases, do not occur through the electronic Hamiltonian.

These surfaces are essential in many formulations of the problem. As mentioned in the previous section, the eigenvalues of this representation depend parametrically on the nuclear coordinates so that the electronic problem must be solved for each nuclear configuration. Since scattering calculations normally require many nuclear configurations, an ab initio treatment of the electronic problem would almost surely be prohibitive. This offers motivation and support for using more approximate procedures such as Diatomics in Molecules (Ellison, 1963) or Polyatomics in Molecules (Tully, 1977) which make use of either experimental or theoretical knowledge of the diatomics or polyatomics to construct the surfaces.

Since the electronic Hamiltonian is diagonal in this representation, the couplings between the nuclear expansion coefficients arise from the matrix representation of the nuclear kinetic energy operator and gradient in this basis. The inclusion of these terms in a scattering calculation leads to two main difficulties. First, efficient computer programs are not available for solving sets of equations that contain these terms and second, as has been noted (Smith, 1969), if all coupling terms are included, the Hamiltonian in this electronic basis is not hermitean. Although the first difficulty is a computational one that could be conceivably overcome, the second difficulty introduces theoretical problems such as nonconservation of energy and flux or the need to introduce a second set of nuclear coefficients that satisfy the adjoint operator of the original problem.

As can be surmised, this representation is probably not the most useful for processes that exhibit non-adiabatic effects. This representation is however still essential in that the solution of the electronic problem in this basis is well understood and theoretically sound. Other representations don't have this property so that they must be related to the adiabatic basis by way of unitary transformations in order to form a matrix representation of the electronic Hamiltonian. That is, the eigenvalues of the adiabatic representation are convenient to form a matrix representation of the electronic Hamiltonian in any electronic representation.

There are a variety of representations other than the adiabatic one that can be used in a scattering calculation. They are based on either completely or partially eliminating the couplings due to the nuclear kinetic energy operator or gradient or on minimizing the couplings in a way to be discussed later. These schemes have one thing in common in that coupling terms present in the adiabatic representation that are eliminated or minimized are replaced by electrostatic terms that give rise to a non-diagonal matrix representation of the electronic Hamiltonian.

The electronic problem will be the subject matter of chapter two. Four representations including the adiabatic one are discussed and some of their advantages and disadvantages are pointed out. It will be shown what care must be used in selecting the representation that would be most suitable for a scattering calculation.

## 1-3 Nuclear Motions

Once the electronic representation has been chosen there remains the problem of solving for the nuclear expansion coefficients. Generally they are solved for quantum mechanically, semi-classically or classically. Since quantum mechanical and semi-classical treatments of this problem are not topics of this study, only a brief discussion of these methods follows. Comments on these subjects will be restricted to be general and provide motivation for using the method to be developed.

Since the electronic problem was treated quantum mechanically, it would seem natural to treat the nuclear problem quantum mechanically too. Indeed, this does give dynamically consistent formalisms but all quantum mechanical approaches to this problem have a serious disadvantage. Since the nuclei have vibrational, rotational and translational degrees of freedom, a quantum mechanical approach even for inelastic collisions would require expanding the nuclear expansion coefficients in at least internal states corresponding to the vibrational and rotational degrees of freedom. Since normally many internal states are energetically accessible, this expansion leads to a large number of coupled differential equations to be solved simultaneously. This is actually one of the simpler cases in that if a partial wave expansion is made a normally much larger set of equations is obtained.

The problem becomes even more difficult for reactive collisions. In this case there is more than one asymptotic Hamiltonian to be considered. Expansions in internal states for each asymptotic Hamiltonian must be made. Not only does the number of coupled equations increase but basis elements corresponding to different asymptotic Hamiltonians are not necessarily orthogonal and can lead to problems such as overcompleteness.

It would seem then that even though a quantum mechanical approach is theoretically appealing, it leads to some very fundamental difficulties. Even if approximations were introduced to reduce the number of coupled equations, it would be helpful to introduce a formalism that would avoid these difficulties as much as possible. Before pursuing this however a few comments on the semiclassical approach to non-adiabatic collisions without nuclear rearrangements will be made.

Semi-classical approaches to non-adiabatic processes without nuclear rearrangement have been used extensively and many good reviews are available on this subject (McDowell and Coleman, 1970). These approaches normally start with the time dependent Schrödinger equation for the electronic Hamiltonian and assume that the trajectories of the nuclei are known. One then needs to solve a set of first order differential equations in time for the expansion coefficients of the electronic wave function. Simultaneous integration of these equations gives these coefficients as a function of time and their values at the final time are related to the probability of non-adiabatic transitions for the collision.

As mentioned in the preceding paragraph, the nuclear trajectories in these approaches are assumed known. These lead to different approximations such as the impact parameter method (high velocity approximation) or the perturbed stationary state method (low velocity limit). Besides the limitations caused by not determining the trajectories from ab initio considerations the extension of these approaches to include nuclear rearrangement is not trivial.

Since the masses of the nuclei are so much heavier than those of the electrons, it would seem possible that some or all of the nuclear degrees of freedom could be treated classically. This approach has been successful for the case of one potential energy surface, i.e. in the absence of couplings between nuclear and electronic degrees of freedom. For such systems, the nuclei evolve according to classical equations of motion on a quantum mechanical potential energy surface. The initial conditions of the trajectories are obtained by taking a Monte Carlo sampling of the possible initial states of the system. This approach is however not as straightforward when more than one surface is included.

A primary concern in this study is to develop a formalism that extends the classical treatment of nuclear degrees of freedom to systems that are characterized by more than one electronic state. This avoids the difficulty of expansions in internal states required by quantum mechanical treatments. Also assumptions about the nuclear trajectories are not needed since they are determined from classical equations of motion. This also has the advantage that individual trajectories give a clear conceptual picture of the collision event.

Briefly, the approach to be used here starts with the time independent Schrödinger equation. The wave function is expanded in a set of electronic states. The nuclear expansion coefficients are written as products of an amplitude and a common phase which is proportional to the eikonal. The gradient of the eikonal is required to satisfy the Hamilton-Jacobi equation whose potential is determined from the quantum mechanical equations. Upon implementing the short wavelength approximation and making a transformation into time, it is found that the nuclear expansion coefficients satisfy first order differential equations in time and that the gradients of the eikonal become the classical moments of the nuclei. If a convenient form for the nuclear expansion coefficients is chosen, it is found that not only the nuclear positions and momenta but also the expansion coefficients satisfy Hamilton's equations of motion.

Although other approaches (Meyer and Miller, 1979) have obtained similar results, the author considers this treatment to be on a more sound theoretical foundation. The development of this formalism will be the subject matter of chapter three.

The formalism of chapters two and three is applied to the collinear $H_3^+$ system. This system was chosen partly because of the presence of large non-adiabatic coupling terms. Also, due to the relatively light masses of the nuclei, this system should provide a good test of the theory. It is also interesting from the viewpoint that not only do elastic and inelastic processes occur but it also exhibits reactions and or rearrangements. Finally $H_3^+$ is adequately described with two electronic states which is a natural starting point for an application of the theory.

The electronic and nuclear parts of the problem for $H_3^+$ will be developed in chapters four and five respectively. The electronic problem will be solved with the method of Diatomics in Molecules and the nuclear problem will be solved in hyperspherical coordinates. This convenient choice of coordinate system will be discussed at length in Appendix one.

This study will conclude with a presentation of the calculations in chapter six. A brief background on previous experimental and theoretical studies for the $H_3^+$ system will also be given. A comparison with a quantum mechanical calculation (Top and Heer, 1977) for collinear $H_3^+$ will be made and this work will close with some comments and conclusions.

# CHAPTER 2
# ELECTRONIC REPRESENTATIONS

## 2-1 Introduction

The adiabatic approximation has played a central role in the study of molecular processes since its introduction by Born and Oppenheimer (Born and Oppenheimer, 1927, Born and Huang, 1954). The approximation introduces a basis of electronic states that provide an adiabatic representation for electronic operators. Non-adiabatic collisions, originally studied by Landau, Zener and Stueckelberg, (Landau, 1932; Zener, 1932; Stueckelberg, 1932; Nikitin, 1970) require information on the momentum couplings of the adiabatic representation. Many models have been developed to incorporate the couplings (Child, 1979; Tully, 1976, Garrett and Truhlar, 1980, Delos, 1981).

In cases where the adiabatic couplings can not be ignored, a different electronic basis and corresponding representation may prove to be useful. One such alternative is a diabatic representation (Smith, 1969) defined so that momentum couplings are exactly eliminated and transitions occur only through Coulomb interactions of electrons and nuclei. This is done by introducing the eigenstates of the momentum operator. In its original version this representation was criticized because the electronic states of the new representation could not change with intermolecular distance, except for phase factors (Gabriel and Taulbjerg, 1974). Working however with finite bases one can define a diabatic representation by requiring that the matrix of the momentum operator is zero. This introduces a matrix unitary transformation from the adiabatic to the diabatic set of states which does change with intermolecular distance. Given this matrix, one can transform the matrix of Coulomb interactions to the new basis.

Although this procedure is mathematically rigorous, it may lead to complications in the physical description of collisional processes. As we shall see, depending on the magnitude of the momentum couplings in the original adiabatic representation, the diagonal elements of the Coulomb interaction matrix in the new diabatic representation may be far from physically meaningful. For large momentum couplings these diagonal elements may repeatedly cross; while for small momentum couplings they may be far from adiabatic potentials in regions where these are physically meaningful. The latter problem can be particularly significant in studies of reactive atom-diatom collisions because the new representation may give the correct description of the reactant potentials but a completely unphysical one for the product potentials.

These difficulties result from using finite bases and from the differential equation satisfied by the unitary transformation, which is of first order in the intermolecular position variables. It follows that given the known boundary conditions for large distances the transformation and diabatic potentials are mathematically determined for all shorter distances, which does not leave any room for physical considerations.

The aims of the present chapter are to introduce a new diabatic representation which leads to physically well behaved potentials (in the sense to be described), and to show how it is constructed around pseudocrossings. It starts with the adiabatic potentials and couplings which are obtained in electronic structure calculations. The procedure is based on the minimization of coupling terms, and provides a criterion to determine the range of kinetic energies over which it is justifiable to neglect couplings altogether.

Other diabatic representations are possible and have been introduced by means of physical arguments (O'Malley, 1967). For energetic atom-atom collisions, several of the representations have been extended to incorporate electron translation factors in order to satisfy asymptotic conditions (Delos and Thorson, 1979; Delos, 1981). These extensions shall not be considered because the immediate aims refer to thermal and hyperthermal collisions. Adiabatic and diabatic representations have also been introduced for atom-diatom collisions (Baer, 1975, Top and Baer, 1977a).

Numerical studies of electronic states in various representations include calculations of potentials and their couplings for atom-atom (Redmon and Micha, 1974, Nimrich and Truhlar, 1975; Evans, Cohen and Lane, 1971) and atom-diatom systems (Rebentrost and Lester, 1977, Tully, 1980). A great deal of related work has also been done on diabatic molecular orbitals and their energies (Lichten, 1963, Briggs, 1976, McCarroll, 1976), to which the developments in this chapter could also be applied.

To illustrate some of the numerical aspects, some results are briefly mentioned for $H_3^+$ and $FH_2$ in the collinear conformations. For a basis of two electronic states (the two lowest states of $^1\Sigma$ symmetry for $H_3^+$; the lowest $^1\Sigma$ and $^3\Sigma$ states for $FH_2$), the transformation from the adiabatic to a diabatic basis depends on the integral

$$\int_D dX \tau^a(X)$$

where $\tau^a$ is the momentum coupling in the nuclear variables X, and D is their domain. As shall be seen in Section 2-4, the standard diabatic representation (Smith, 1969) works well when the integral equals $\pi/2$ but not when it differs appreciably from $\pi/2$. For atom-diatom mass-weighted Jacobi variables (Z,z) for the intermolecular and internal coordinates, a transformation to polar coordinates $r = (Z^2 + z^2)^{1/2}$ and $\theta = \tan^{-1}(z/Z)$ leads to values of

$$\int_{\theta_<}^{\theta_>} d\theta \tau^a(\theta;r)$$

which for $H_3^+$ go from 0.3 to 1.6 as r varies from 4 a.u. to 12 a.u. (Tully, 1976), while for $FH_2$ they stay around 0.7

as r varies from 8 a.u. to 12 a.u. (Tully, 1980). Other numerical examples can be found in the recent literature on adiabatic-diabatic transformations for slow nuclear degrees of freedom, where the integrals are instead larger than $\pi/2$ and multiple crossings occur (Baer, Drolshagen and Toennies, 1980).

Given the wide variety of problems where pseudo-crossings may occur, this chapter shall not concentrate on a given physical system but shall instead construct a model of potentials and couplings with parameters that will be varied around physical values. The shape of the potentials and couplings are similar to those calculated (Tully, 1976) for $H_3^+$ and the physical parameters relate also to this system.

The adiabatic, diabatic and nearly adiabatic representations will be briefly developed in Section 2-2. This will be followed in Section 2-3 with a general development of the minimization procedure. Section 2-4 will give a detailed treatment of the two electronic state problem in one dimension. A comparison of the results for two of the diabatic procedures will be given in Section 2-5 and the chapter will close with a discussion.

## 2-2 Electronic State Representations

We consider to begin with a molecular system with n nuclei, in a center-of-mass reference frame. Introducing cartesian coordinates and the nuclear position vectors

$\{\underset{\sim}{y}_i,\ i=1 \text{ to } n\}$, the nuclear kinetic energy operator is expressed as

$$\hat{T}_{nu} = -\sum_{i=1}^{n} (2m_i)^{-1}\ \partial^2/\partial \underset{\sim}{y}_i^2 \qquad (2\text{-}1)$$

where $m_i$ is the mass of the $i^{th}$ nucleus and we have used atomic units ($\hbar=1$). Introducing a change of variables,

$$\underset{\sim}{x}_i = (m_i/M)^{\frac{1}{2}}\ \underset{\sim}{y}_i \qquad (2\text{-}2)$$

where M is the total mass, gives

$$\hat{T}_{nu} = -(2M)^{-1} \sum_{i=1}^{n} \partial^2/\partial \underset{\sim}{x}_i^2 \quad . \qquad (2\text{-}3)$$

Defining next a nuclear momentum operator in vector form with n orthogonal components and written as

$$\hat{\underset{\sim}{P}}_{nu} = -i\ \left(\frac{\partial}{\partial \underset{\sim}{x}_1},\ \frac{\partial}{\partial \underset{\sim}{x}_2},\ \cdots,\ \frac{\partial}{\partial \underset{\sim}{x}_n}\right) = -i\ \frac{\partial}{\partial \underset{\sim}{X}} \qquad (2\text{-}4)$$

where $\underset{\sim}{X} = (\underset{\sim}{x}_1,\ .\ .\ .\ \underset{\sim}{x}_n)$, the kinetic energy operator becomes

$$\hat{T}_{nu} = (2M)^{-1}\ \hat{\underset{\sim}{P}}_{nu} \cdot \hat{\underset{\sim}{P}}_{nu} = -(2M)^{-1}\partial^2/\partial \underset{\sim}{X}^2 \quad . \qquad (2\text{-}5)$$

For the special case of systems with two nuclei, the momentum operator in the center-of-mass coordinate system would simply be

$$\hat{\underset{\sim}{P}}_{nu} = -i\,\partial/\partial\underset{\sim}{R} \quad , \qquad (2\text{-}6)$$

where $\underset{\sim}{R}$ is the relative position vector between the nuclei. For the three-nuclei system, mass weighted Jacobi coordinates also satisfy the above conventions.

Solutions of the time independent Schrodinger equation satisfy

$$(\hat{H}-E)\,|\Psi(\underset{\sim}{X})> = 0 \quad , \qquad (2\text{-}7)$$

where

$$\hat{H} = \hat{T}_{nu}(\partial/\partial\underset{\sim}{X}) + \hat{H}_{el}(\underset{\sim}{X}) \quad , \qquad (2\text{-}8)$$

$\hat{T}_{nu}$ and the nuclear positions $\underset{\sim}{X}$ were defined above and $\hat{H}_{el}$ is the electronic Hamiltonian including nuclear-nuclear repulsion terms. The bracket notation refers to the electronic coordinates and involves an integration only over electronic coordinates. Invoking a separation of electronic and nuclear variables leads to the solution having the general form

$$|\Psi(\underset{\sim}{X})> = \sum_{i} |\Phi_i(\underset{\sim}{X})>\psi_i(\underset{\sim}{X}) \qquad (2\text{-}9)$$

where one requires that the electronic functions, $\Phi_i$, form a complete, orthonormal set at each $\underset{\sim}{X}$.

Substituting Eq. (2-9) into Eq. (2-7) and multiplying from the left by $\langle\phi_j(\underset{\sim}{X})|$ leads to

$$\sum_i \{\langle\phi_j(\underset{\sim}{X})|\hat{T}_{nu}|\phi_i(\underset{\sim}{X})\rangle\psi_i(\underset{\sim}{X}) + \langle\phi_j(\underset{\sim}{X})|\hat{H}_{e\ell}|\phi_i(\underset{\sim}{X})\rangle\psi_i(\underset{\sim}{X})\} = E\psi_j(\underset{\sim}{X}) \tag{2-10}$$

where $\hat{T}_{nu}$ operates on all factors to the right. The development thus far is completely general but not of much use. More useful representations may be obtained by requiring the electronic functions to obey additional properties besides those of completeness and orthonormality and these will be briefly discussed below.

## 2-2a The Adiabatic Representation

This highly useful and widely used representation (Born and Oppenheimer, 1927; Born and Huang, 1954) is based on the requirement that the electronic functions satisfy

$$\langle\phi_i^a|\hat{H}_{e\ell}|\phi_j^a\rangle = \delta_{ij}V_{jj}^a(\underset{\sim}{X}) \tag{2-11}$$

where the superscript "a" denotes the adiabatic representation. Using this basis in Eq. (2-10) leads to

$$\sum_i \langle\phi_j^a|\hat{T}_{nu}|\phi_i^a\rangle\psi_i^a(\underset{\sim}{X}) + V_{jj}^a(\underset{\sim}{X})\psi_j^a(\underset{\sim}{X}) = E\psi_j^a(\underset{\sim}{X}) \quad , \tag{2-12}$$

where $\hat{T}_{nu}$ operates on all factors to the right. As is well known, adiabatic potential surfaces $V_{jj}^a$ of the same symmetry do not cross. They can however exhibit "avoided crossings" which can lead to a breakdown of descriptions of nuclear motions.

### 2-2b The Strictly Diabatic Representation

The diabatic representation (Smith, 1969) is based on the requirement that the electronic basis elements satisfy

$$<\phi_i^d|\hat{P}_{nu}|\phi_j^d> = 0 \text{ for all } i,j \qquad (2\text{-}13)$$

where the superscript "d" indicates diabatic quantities. This representation will be referred to as "strictly diabatic" when compared with our representation, or as diabatic when the meaning is obvious. A general form for the basis which would satisfy the above requirement around a chosen point $\underset{\sim}{X}_o$ would be $\{|\phi_i^d(\underset{\sim}{X}_o)>\}$. This basis can be related to the adiabatic basis by a unitary transformation. In matrix notation one would have

$$|\underset{\approx}{\phi}^d(\underset{\sim}{X}_o)> = |\underset{\approx}{\phi}^a(\underset{\sim}{X})\ \underset{\approx}{A}(\underset{\sim}{X},\underset{\sim}{X}_o) \qquad (2\text{-}14)$$

where $|\underset{\approx}{\phi}^k> = (|\phi_1^k>\ldots|\phi_n^k>)$ $k=d,a$ and $\underset{\approx}{A}$ is a nxn matrix. From Eq. (2-13) one finds that the transformation must satisfy

$$\hat{P}_{nu}\underset{\approx}{A}(\underset{\sim}{X},\underset{\sim}{X}_o) + <\underset{\approx}{\phi}^a|\hat{P}_{nu}|\underset{\approx}{\phi}^a>\underset{\approx}{A}(\underset{\sim}{X},\underset{\sim}{X}_o) = \underset{\approx}{0} \qquad (2\text{-}15)$$

with the boundary condition $\underset{\approx}{A}(\underset{\sim}{X}_o,\underset{\sim}{X}_o) = \underset{\approx}{A}_o$. Expanding the solution of Eq. (2-10) in this basis and performing a little algebra (see Baer for details) (Baer, 1975; Top and Baer, 1977a) leads to a final result, in matrix notation, of the form

$$\hat{\underset{\approx}{T}}_{nu}\underset{=}{\psi}^{d}(\underset{\sim}{X}) + \underset{\approx}{V}^{d}\underset{=}{\psi}^{d}(\underset{\sim}{X}) = E\underset{=}{\psi}^{d}(\underset{\sim}{X}) \qquad (2\text{-}16)$$

where

$$\underset{\approx}{V}^{d}(\underset{\sim}{X}) = \underset{\approx}{A}^{+}(\underset{\sim}{X},\underset{\sim}{X}_{o})\underset{\approx}{V}^{a}(\underset{\sim}{X})\underset{\approx}{A}(\underset{\sim}{X},\underset{\sim}{X}_{o}) \qquad (2\text{-}17)$$

$$\underline{\psi}^{d}(\underset{\sim}{X}) = \{\psi_{j}^{d}(\underset{\sim}{X})\} \text{ , a column matrix,} \qquad (2\text{-}18)$$

and the elements of the diagonal matrix $\underset{=}{V}^{a}$ are defined by Eq. (2-11).

As was mentioned previously, this procedure rigorously eliminates the momentum coupling terms between electronic states. It does not however guarantee physically well behaved potentials corresponding to those electronic states. The following example should help clarify what is meant by physically well behaved potentials.

Consider the hypothetical case depicted in Fig. (1) of a one dimensional two electronic state system. In regions (a) and (c) the momentum coupling between electronic states should be small since the potentials are relatively far apart. One would therefore expect that the adiabatic

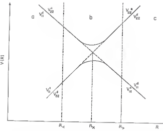

Fig. (1) Schematic representation of a pseudocrossing. Solid curves correspond to adiabatic potentials, dashed lines intersecting at $R_x$ correspond to diabatic potentials. The superscripts "a" and "d" signify adiabatic and diabatic, respectively.

approximation would be valid in these regions. In region (b) the potentials do approach each other relatively closely so the adiabatic approximation would no longer be valid and one should either include the momentum coupling terms in the adiabatic basis or use a diabatic representation. Then physically well behaved diabatic potentials should fulfill the following conditions. In region (c), as shown in Fig. (1), the diagonal elements of the diabatic potential matrix $V_{11}^d$ and $V_{22}^d$ should coincide with the adiabatic potentials $V_{11}^a$ and $V_{22}^a$, respectively. In region (a) $V_{11}^d$ and $V_{22}^d$ should coincide with $V_{22}^a$ and $V_{11}^a$, respectively. In region (b) the diagonal elements of the diabatic potential matrix should vary smoothly and exhibit a single crossing. Finally, the off diagonal matrix elements $V_{12}^d$ and $V_{21}^d$ should vanish in regions (a) and (c) far from the crossing.

As is seen in Eq. (2-15), the transformation matrix $\underset{\sim}{A}(\underset{\sim}{X},\underset{\sim}{X}_o)$ satisfies a first order differential equation and one therefore has only one boundary condition at one's disposal. This will ensure proper behavior in one of the regions in Fig. (1), usually chosen to be region (c), but the behavior in the other regions will depend on the coupling terms $<\underset{\sim}{\phi}^a|\hat{P}_{nu}|\underset{\sim}{\phi}^a>$ so that this procedure does not in general guarantee diabatic states that satisfy the above conditions.

## 2-2c The Nearly Adiabatic Representation

As was pointed out in Section 1-2, one of the difficulties that arise when using an arbitrary electronic representation is that Eq. (2-10) is not necessarily Hermitian. The non-Hermitian components arise from the first term on the left hand side of Eq. (2-10). It can be shown (Smith, 1969) that for a complete electronic basis that is real and orthonormal

$$\langle\underset{\approx}{\phi}|\hat{T}_{nu}|\underset{=}{\phi}\rangle = (2M)^{-1}(\hat{P}_{nu}\cdot\langle\underset{\approx}{\phi}|\hat{P}_{nu}|\underset{\approx}{\phi}\rangle + \langle\underset{\approx}{\phi}|\hat{P}_{nu}|\underset{=}{\phi}\rangle\cdot\langle\underset{\approx}{\phi}|\hat{P}_{nu}|\underset{\approx}{\phi}\rangle) \ .$$

(2-19)

Since $\hat{P}_{nu}$ is imaginary and $\langle\underset{\approx}{\phi}|\hat{P}_{nu}|\underset{\approx}{\phi}\rangle$ is an imaginary antisymmetric matrix, the first term on the right hand side of Eq. (2-19) is real and antisymmetric while the second is real and symmetric. Thus the first term is non-Hermitian and would cause difficulties if it were not neglectable.

An obvious way to restore Hermiticity would be to choose an electronic basis that satisfies

$$\hat{P}_{nu}\cdot\langle\underset{\approx}{\phi}^{n}|\hat{P}_{nu}|\underset{\approx}{\phi}^{n}\rangle = \underset{\approx}{0} \qquad (2\text{-}20)$$

where the superscript "n" stands for nearly adiabatic. Relating this to the adiabatic representation via a unitary transformation, i.e.

$$\underset{\approx}{\phi}^{n} = \underset{=}{\phi}^{a}\underset{\approx}{C} \qquad (2\text{-}21)$$

leads to, with some simplification,

$$\underset{\approx}{C}^{\dagger}\hat{P}_{nu}^{2}\underset{\approx}{C} + (\hat{P}_{nu}\underset{\approx}{C}^{\dagger})\cdot\hat{P}_{nu}\underset{\approx}{C} + \underset{\approx}{C}^{\dagger}(\hat{P}_{nu}\cdot\langle\underset{=}{\phi}^{a}|\hat{P}_{nu}|\underset{=}{\phi}^{a}\rangle)\underset{\approx}{C} = \underset{\approx}{0}. \qquad (2\text{-}22)$$

With the form of $\hat{P}_{nu}$ given by Eq. (2-4) one sees that the transformation satisfies a second order differential equation. Since there are two boundary conditions, use of this representation could ensure proper behavior of the electronic potentials on both sides of the pseudocrossing.

It should be noted that since second order partial differential equations are usually difficult to solve, the usefulness of this representation may be somewhat limited. It should however provide an alternative in cases where the non-Hermitian term in the adiabatic representation can not be ignored and the strictly diabatic representation gives unphysical results.

## 2-3 The Minimization Procedure

Physically ill behaved diabatic potentials can be a serious drawback in studies of scattering processes. The procedure to be developed here starts from a different point of view. Instead of completely neglecting the momentum coupling terms, our procedure requires well behaved diabatic potentials. It introduces a unitary transformation with parameters to be variationally chosen, and then minimizes the momentum coupling in the pseudocrossing region.

Since the electronic Hamiltonian is usually only known in the adiabatic representation, a unitary transformation between the representations is necessary. In this procedure, a transformation $\underset{\approx}{B}$ will be chosen to guarantee physically well behaved potentials and will in general depend on a set of parameters $\{\alpha_i,\ i = 1 \text{ to } k\}$ to be determined. The two bases can be related through

$$\underset{\approx}{\phi}^m(\underset{\sim}{X};\alpha_1\ldots\alpha_k) = \underset{\approx}{\phi}^a(\underset{\sim}{X})\underset{\approx}{B}(\underset{\sim}{X};\alpha_1\ldots\alpha_k) \qquad (2\text{-}23)$$

where the superscript "m" denotes the electronic representation obtained through a minimization procedure. Using this basis in Eq. (2-10) and suppressing the arguments leads to

$$\langle\underset{\approx}{\phi}^m|\hat{T}_{nu}|\underset{\approx}{\phi}^m\rangle\underset{\approx}{\psi}^m + \langle\underset{\approx}{\phi}^m|\hat{H}_{e\ell}|\underset{\approx}{\phi}^m\rangle\underset{\approx}{\psi}^m = E\underset{\approx}{\psi}^m \qquad (2\text{-}24)$$

where the unitarity of $\underset{\approx}{B}$ has been used and $\hat{T}_{nu}$ operates on all factors to its right. From the discussion in the preceding section one has

$$\hat{T}_{nu} = \hat{P}_{nu}^2/(2M) \qquad (2\text{-}25)$$

so that by using Eq. (2-23) in Eq. (2-24) one has

$$(\hat{P}_{nu}^2/2M)\underset{\approx}{\psi}^m + M^{-1}\underset{\sim}{P}^m\cdot\hat{P}_{nu}\underset{\approx}{\psi}^m + \underset{\approx}{K}^m\underset{\approx}{\psi}^m + \underset{\approx}{V}^m\underset{\approx}{\psi}^m = E\underset{\approx}{\psi}^m \qquad (2\text{-}26)$$

where

$$\underset{\approx}{P}^m = \underset{\approx}{B}^{\dagger}\langle\underset{\approx}{\phi}^a|\hat{P}_{nu}|\underset{\approx}{\phi}^a\rangle\underset{\approx}{B} \quad , \qquad (2\text{-}27)$$

$$\underset{\approx}{T}^{m} = (2M)^{-1}\underset{\approx}{B}^{\dagger}\langle\underset{\sim}{\phi}^{e}|\hat{P}^{2}_{nu}|\underset{\sim}{\phi}^{e}\rangle\underset{\approx}{B} \quad , \tag{2-28}$$

$$\underset{=}{V}^{m} = \underset{=}{B}^{\dagger}\underset{=}{V}^{e}\underset{=}{B} \tag{2-29}$$

and $\hat{P}_{nu}$ operates on all factors to its right.

Since the momentum coupling terms in this representation are not identically zero, the usefulness of the representation will depend on whether they can be neglected. To make them as small as possible our procedure determines the coefficients, $\alpha_i$, so as to minimize the positive expression $\mathrm{tr}(\underset{\approx}{P}^{m\dagger}\cdot\underset{\approx}{P}^{m})$, where tr indicates the trace operation, in a domain D. Explicitly for each $\alpha_i$, one requires that

$$\frac{\partial}{\partial\alpha_i}\int_D d\underset{-}{X}\ \mathrm{tr}\,(\underset{\approx}{P}^{m\dagger}\cdot\underset{\approx}{P}^{m}) = 0 \qquad i=1,2,\ldots,k \tag{2-30}$$

where the domain of integration, D, is the region where the adiabatic momentum coupling is significant. From Eq. (2-27) and remembering the assumed form of $\hat{P}_{nu}$ discussed in Section 2-2, one has

$$\underset{\approx}{P}^{m} = \underset{\approx}{B}^{\dagger}\underset{\approx}{P}^{e}\underset{\approx}{B} + \underset{\approx}{B}^{\dagger}\hat{P}_{nu}\underset{\approx}{B} \tag{2-31}$$

where

$$\underset{\approx}{P}^{e} = \langle\underset{\approx}{\phi}^{e}|\hat{P}_{nu}|\underset{\approx}{\phi}^{e}\rangle \tag{2-32}$$

and the orthonormality of the adiabatic basis set was used. The adjoint matrix is given by

$$\underset{\approx}{P}^{m\dagger} = \underset{\approx}{B}^{\dagger}\underset{\approx}{P}^{a\dagger}\underset{\approx}{B} + (\hat{P}_{nu}\underset{\sim}{B})^{\dagger}\underset{\approx}{B} \qquad (2\text{-}33)$$

so that Eq. (2-26) becomes

$$\frac{\partial}{\partial\alpha_i}\int_D dX\,\mathrm{tr}[(\underset{\approx}{B}^{\dagger}\underset{\approx}{P}^{a\dagger}\underset{\approx}{B} + (\hat{P}_{nu}\underset{\sim}{B})^{\dagger}\underset{\approx}{B})(\underset{\approx}{B}^{\dagger}\underset{\approx}{P}^{a}\underset{\approx}{B} + \underset{\approx}{B}^{\dagger}\hat{P}_{nu}\underset{\sim}{B})] = 0 \qquad (2\text{-}34)$$

where $\hat{P}_{nu}$ operates only on the first factor to its right.

It should be emphasized that this procedure only minimizes the momentum coupling terms. Whether or not they can be neglected will depend on the particular system being investigated and the relevant collision energies. In general, these couplings can be neglected if the terms in the Schrödinger equation involving couplings between nuclear functions by $\hat{P}_{nu}$, i.e $\frac{1}{M}\underset{\approx}{P}^{m} \cdot \hat{P}_{nu}$ , are negligible compared to the couplings of the nuclear functions by the potential $\underset{\approx}{V}^{m}$. An estimate of $\hat{P}_{nu}\underset{\sim}{\psi}^{m}$ is given by $\sqrt{2mE_{rel}(\underset{\sim}{X})}\underset{\sim}{\psi}^{m}$ where $E_{rel}(\underset{\sim}{X})$ is the local relative kinetic energy. Since $\underset{\approx}{P}^{m}$ is a real antisymmetric matrix (provided the electronic functions $|\underset{\sim}{\phi}^{m}\rangle$ are assumed to be real), one has

$$|M^{-1}P_{ij}^{m}\sqrt{2ME_{rel}}| << |V_{ij}^{m}| \qquad (2\text{-}35)$$

as a condition for neglecting momentum couplings. This expression should be helpful in determining the range of the relative kinetic energy where the momentum coupling can be neglected.

Neglecting the $\underset{\approx}{K}^{m}$ coupling terms should also be justified. Defining

$$\underset{\approx}{K}^{a} = (2M)^{-1}\langle\underset{\approx}{\phi}^{a}|\hat{P}_{nu}^{2}|\underset{\approx}{\phi}^{a}\rangle \qquad (2\text{-}36)$$

and assuming the adiabatic basis is complete, $\underset{\approx}{K}^{m}$ can be related to $\underset{\approx}{K}^{a}$ by Eq. (2-28) with $\underset{\approx}{K}^{a}$ obtained by letting $\hat{P}_{nu}$ operate on $\langle\underset{\approx}{\phi}^{a}|\hat{P}_{nu}|\underset{\approx}{\phi}^{a}\rangle$ to give

$$\underset{\approx}{K}^{a} = (2M)^{-1}(\hat{P}_{nu}\underset{\approx}{P}^{a} + \underset{\approx}{P}^{a}\cdot\underset{\approx}{P}^{a}) \qquad (2\text{-}37)$$

where the $\underset{\approx}{P}^{a}\cdot\underset{\approx}{P}^{a}$ term comes from the completeness of $\underset{\approx}{\phi}^{a}$. Since the literature usually only reports couplings between the lowest electronic states, this expression may not be useful. If a valence bond, Diatomics in Molecules or other method, was used to obtain the $\underset{\sim}{X}$-dependent expansion coefficients for the electronic states, the $\underset{\approx}{K}^{a}$ terms could be obtained by numerical methods. Once $\underset{\approx}{K}^{a}$ has been calculated, it is straightforward via Eq. (2-28) to determine $\underset{\approx}{K}^{m}$. A justification for neglecting it would depend on whether

$$|K_{ij}^{m}| << |V_{ij}^{m} - E\delta_{ij}| \qquad (2\text{-}38)$$

for each i,j where E is now the total energy. In the examples given later in this paper, only a functional form for $\underset{\sim}{F}^{e}$ will be obtained and the terms $\underset{\sim}{K}^{m}$ will not be considered. Normally, though, if the coupling from $\hat{P}_{nu}$ is small, one would expect that the coupling from $\hat{P}_{nu}{}^{2}$ would be at least as small.

## 2-4 The Two Electronic State Problem in One Dimension

In the previous section a general development of the minimization procedure was presented. Since many systems that exhibit non-adiabatic effects can be treated as processes occurring on two electronic potential curves, a more detailed treatment of the two-state case will now be given. For simplicity it will be restricted to one dimension, indicated by the radial variable R.

A general form for the real unitary transformation matrix for this case is given by

$$\underset{\sim}{B}(R,\alpha) = \begin{pmatrix} \cos \gamma^{m}(R;\alpha) & \sin \gamma^{m}(R;\alpha) \\ -\sin \gamma^{m}(R;\alpha) & \cos \gamma^{m}(R;\alpha) \end{pmatrix} \qquad (2\text{-}39)$$

with $\gamma^{m}(R_{>};\alpha) = 0$, $\gamma^{m}(R_{<};\alpha) = \frac{\pi}{2}$ and where the parameter $\alpha$ is to be determined. In one dimension, the momentum operator is given by

$$\hat{P}_{nu} = -i \; d/dR \qquad (2\text{-}40)$$

and the antisymmetric matrix of the adiabatic momentum coupling terms has the form

$$\underset{\sim}{F}^a = \begin{pmatrix} 0 & -i\tau^a(R) \\ i\tau^a(R) & 0 \end{pmatrix} \qquad (2\text{-}41)$$

where

$$\tau^a(R) = \langle \phi_1^a | d\phi_2^a/dR \rangle \quad . \qquad (2\text{-}42)$$

Using Eqs. (2-39) through (2-42) in Eq. (2-34) leads to

$$\frac{\partial}{\partial\alpha} \int_D dR[\tau^a(R) + \gamma^m(R;\alpha)']^2 = 0 \qquad (2\text{-}43)$$

where the "prime" denotes differentiation with respect to R. The domain of integration in this case will be the interval $[R_<, R_>)$ (see Fig. (1)) where $\tau^a(R)$ is significant. In analogy to Eq. (2-41) one has

$$\underset{\sim}{F}^m = \begin{pmatrix} 0 & -i\tau^m(R;\alpha) \\ i\tau^m(R;\alpha) & 0 \end{pmatrix} \qquad (2\text{-}44)$$

where, from Eq. (2-31),

$$\tau^m(R,\alpha) = \tau^a(R) + \gamma^m(R,\alpha)' \qquad (2\text{-}45)$$

Assuming the integrand in Eq. (2-43) to be continuous gives

$$\int_{R_<}^{R_>} dR[\tau^a(R) + \gamma^m(R;\alpha)']\partial\gamma^m(R;\alpha)'/\partial\alpha = 0 \quad . \qquad (2\text{-}46)$$

A functional form of $\gamma^m$ that varies smoothly from zero for large R to $\pi/2$ for small R (see the discussion in Section 2-1) was introduced by choosing

$$\gamma^m(R;\alpha) = (\pi/4)[1-\tanh\alpha(R-R_x)] \qquad (2\text{-}47)$$

where $R_x$ is the point where the diabatic surfaces cross. Then

$$\gamma^m(R;\alpha)' = -(\pi/4)\,\alpha\,\mathrm{sech}^2\alpha(R-R_x) \qquad (2\text{-}48)$$

and

$$\partial\gamma^m(R;\alpha)'/\partial\alpha = (\pi/2)\,\mathrm{sech}^2\alpha(R-R_x)\cdot[\alpha(R-R_x)\tanh\alpha(R-R_x)-1/2] \;. \qquad (2\text{-}49)$$

Using Eqs. (2-48) and (2-49) in Eq. (2-46) leads to

$$\int_{R_<}^{R_>} dR\;\mathrm{sech}^2\alpha(R-R_x)\,[\gamma^n(R) - (\pi/4)\,\mathrm{sech}^2\alpha(R-R_x)] \qquad (2\text{-}50)$$

$$\times\quad [\alpha(R-R_x)\tanh\alpha(R-R_x) - 1/2] = 0 \;.$$

Equation (2-50) does not give an analytical solution for the parameter $\alpha$ so that a numerical procedure must be implemented to determine the value of $\alpha$ such that the integral is less than a small positive number.

In the next section, the results of this procedure will be compared to those obtained from the strictly diabatic procedure presented in Section 2-2. For the two electronic state problem in one dimension, the transformation matrix for the strictly diabatic procedure can also be expressed as

$$\underset{\approx}{A}(R,R_o) = \begin{pmatrix} \cos \gamma^d(R,R_o) & \sin \gamma^d(R,R_o) \\ -\sin \gamma^d(R,R_o) & \cos \gamma^d(R,R_o) \end{pmatrix} . \qquad (2\text{-}51)$$

However, the angle $\gamma^d$ is given by (Baer, 1975, Top and Baer, 1977)

$$\gamma^d(R,R_o) = \int_{R_o}^{R} dR\tau^e(R) \qquad (2\text{-}52)$$

where $\gamma^d(R_o,R_o) = 0$. Equation (2-52) was obtained by multiplying Eq. (2-15) from the left by $\underset{\approx}{A}^{\dagger}(R,R_o)$ which eliminates the sine and cosine factors, and by solving the resulting differential equation for $\gamma^d$.

One can easily determine from the form of the transformation matrix that $\underset{\approx}{V}^u$ is given by the elements

$$V^u_{11}(R) = V^e_{11}(R)\cos^2\gamma^u(R,c) + V^e_{22}(R)\sin^2\gamma^u(R,c) \qquad (2\text{-}53)$$

$$V^u_{22}(R) = V^a_{11}(R)\sin^2\gamma^u(R,c) + V^d_{22}(R)\cos^2\gamma^u(R,c) \qquad (2\text{-}54)$$

$$V_{12}^{u}(R) = V_{21}^{u}(R) = (V_{11}^{a}-V_{22}^{a})\sin\gamma^{u}(R,c)\cdot\cos\gamma^{u}(R,c) \qquad (2\text{-}55)$$

where $(u,c)$ equals $(m,\alpha)$ or $(d,R_0)$, respectively.

Equation (2-52) emphasizes the point made in the last part of Section 2-2b that the behavior of the diabatic potentials $\underline{V}^{d}$ depend on the momentum coupling $\tau^{a}(R)$. Letting $R_0$ equal $R_>$ in Fig. (1), one sees that unless the integral in Eq. (2-52) from $R_<$ to $R_>$ is equal to $\pi/2$, the diabatic potentials will not coincide with adiabatic potentials in region (a). One also has that the diabatic $V_{ii}^{d}$ will cross whenever

$$\gamma^{d}(R,R_0) = \pm(2n+1)\pi/4 \quad , \; n = 0,1,2,\ldots \qquad (2\text{-}56)$$

and that depending on $\tau^{a}(r)$, they can cross more than once. These undesirable features do not occur in this procedure since it started with a proper form of $\gamma^{m}$.

## 2-5 A Model Calculation

In the following calculations $\tau^{e}(R)$ was given the form of a Gaussian and written explicitly as

$$\tau^{e}(R) = \tau_{x}\, e^{-b(R-R_x)^2} \qquad (2\text{-}57)$$

where $R_x$ is in the region of the pseudocrossing. Using Eq. (2-57) in Eq. (2-52) leads to the result

$$\gamma^{d}(R,R_0) = \tau_{x}\sqrt{\pi/(4b)}\,(\mathrm{erf}[\sqrt{b}(R-R_x)]-\mathrm{erf}[\sqrt{b}(R_0-R_x)]) \qquad (2\text{-}58)$$

where erf(x) (Abramowitz and Stegun, 1972) is the error function. To obtain the parameter in $Y^m$, Eq. (2-50) was integrated numerically using Simpson's rule (Abramowitz and Stegun, 1972) and variable step sizes.

Morse potentials (Morse, 1929), defined by

$$V_{ii}^{a}(R) = D_i\{\exp[-2a_i(R-R_i^0)]-2\exp[-a_i(R-R_i^0)]\}$$

$i=1,2$, were used for the adiabatic potential curves $V_{11}^a$ and $V_{22}^a$. $V_{11}^a$ was chosen to roughly correspond to $H_2$ giving a well depth, $D_1$, of .176 a.u. with a minimum located at $R_1^0 = 1.4$ a.u. and a value of $a_1$ of .801 a.u. $V_{22}^a$ was rather arbitrarily chosen to give a well defined avoided crossing at a distance of 2.2 a.u. This is somewhat like the pseudocrossing between $H^+$-$H_2$ and $H$-$H_2^+$ (Tully and Preston, 1971). The values used were .139 a.u. for $D_2$, 2.1 a.u. for $R_2^0$ and 1.8 a.u. for $a_2$.

The value of b used in Eq. (2-57) for $\tau^a(R)$ was 50 a.u. and $R_x$ was set equal to 2.2 a.u. With this choice of b, the Gaussian in Eq. (2-57) has a half width of approximately 0.2 a.u. This choice of b reflects the rather sharp avoided crossing of the adiabatic potentials. Three different values of $\tau_x$ were used in this study all with b = 50 a.u. The value of $\tau_x$ = 10 a.u. roughly corresponds to the results shown in Fig. (2) in the paper by Tully and Preston (Tully and Preston, 1971). The values of $\tau_x$ equal to 7.5 a.u. and 5 a.u. were included for comparisons.

For $\tau_x$ equal to 10 a.u. the value of the parameter $\alpha$ satisfying Eq. (2-50) was found to be 10.89 a.u. The results of Eqs. (2-53) through (2-55) for u=m and d are shown in Fig. (2). One notices that the diagonal curves, $V_{11}^{d}$ and $V_{22}^{d}$ cross twice and they don't coincide with the adiabatic curves for small values of R. Also as seen in Fig. (3) the off diagonal matrix elements $V_{12}^{d}$ diverge. This procedure clearly avoids these disparities.

The momentum couplings $\tau^{m}$ given by Eq. (2-45) and $\tau^{a}$ from Eq. (2-57) are compared in Fig. (4). One sees that this procedure reduces the couplings by about a factor of three. Also shown in the figure is the absolute value of the derivative with respect to R of $\gamma^{m}$, which would be equal to $\tau^{a}$ in the strictly diabatic case. From Eq. (2-35), the range of energy where these couplings can be neglected is given by

$$E_{rel} << (M/2)\,|V_{12}^{m}/P_{12}^{m}| \ . \tag{2-60}$$

From Fig. (3) and (4), estimates of $V_{12}^{m}$ and $P_{12}^{m}$ are given by .002 a.u. and 3 a.u. Using that the reduced mass M of the $H^{+}$-$H_2$ system is 1836 a.u., and substituting the values in Eq. (2-60) justify neglecting the momentum coupling if $E_{rel}$ is much less than about .0004 a.u. (or .25 kcal/mole). Then for very low collision energies our procedure would be useful whereas for higher energies an adiabatic representation may be more convenient. This requirement of very low energies is due partially to the small reduced mass for $H^{+}$-$H_2$, and should not be as severe for other systems with larger reduced masses.

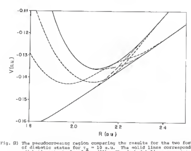

Fig. (2) The pseudocrossing region comparing the results for the two formulations of diabatic states for $\tau_x$ = 10 a.u. The solid lines correspond to the adiabatic potentials of Eq. (59). The dash-dot lines correspond to the diabatic potentials of Eqs. (53) and (54) with u = m. The dashed lines correspond to the diabatic potentials of Eqs. (53) and (54) with u = d.

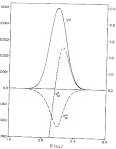

Fig. (3) A comparison of the off diagonal potential matrix elements for the two formulations of diabatic states for $\tau_X = 10$ a u. The dash-dot and dashed curves correspond to $V_{12}^{d}$ and $V_{12}^{d}$ in Eq. (55) respectively. $\tau^a$ given by Eq. (57) corresponds to the solid line and is included for comparison

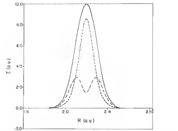

Fig. (4) A comparison of the momentum couplings in the adiabatic and diabatic representations for $\tau_x = 10$ a.u. The solid curve corresponds to $\tau^a$ in Eq. (57). The dash-dot line corresponds to the absolute value of $\gamma^m(R;\alpha)'$ in Eq. (48).

For $\tau_x$ equal to 7.5 a.u. the value of the parameter $\alpha$ was found to be 9.172 a.u. The diagonal elements of $\underset{\approx}{V}^{d}$ and $\underset{\approx}{V}_{M}$ are compared in the crossing region in Fig. (5). Although the strictly diabatic curves $V_{11}^{d}$ do not have multiple crossings in this case, they stilll don't give the correct behavior for small R. As shown in Fig. (6), the off diagonal elements of $\underset{\approx}{V}^{d}$ again diverge.

The momentum couplings $\tau^{a}$ and $\tau^{m}$ are compared in Fig (7). One notices that the momentum coupling is reduced by a factor of about seven. With a value of .002 a.u. for $V_{12}^{m}$ and 1 a.u. for $F_{12}^{m}$, the energy range where the momentum coupling can be neglected is given now by $E_{rel} << .007$ a.u. (or 4.4 kcal/mole). Thus for this case the energy range has considerably increased.

Figures (8) through (10) show the results for $\tau_x = 5$ a.u. In this case $\alpha$ is 6.840 a.u. Fig. (8) again demonstrates the improper behavior for small R of the $V_{11}^{d}$'s. One also notices that as $\tau_x$ is decreased the crossing from this procedure occurs over a larger region. This coincides with the larger spread in $V_{12}^{m}$ shown in Fig. (9). One also notices the divergence of $V_{12}^{d}$ in this figure. As noted previously, this will always occur if the integral of $\tau^{a}(R)$ doesn't equal $\pi/2$

The coupling terms are compared in Fig. (10) where one sees that this procedure reduces couplings by a factor of around ten. With $V_{12}^{m}$ and $F_{12}^{m}$ equal to .002 a.u. and .5 a.u., respectively, the energy must be much less than .03 a.u.

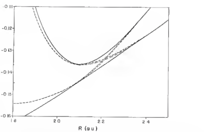

Fig. (5) The pseudocrossing region comparing the results for the two formulations of diabatic states for $r_x$ = 7.5 a.u. The solid lines correspond to the adiabatic potentials of Eq. (59). The dash-dot lines correspond to the diabatic potentials of Eqs. (53) and (54) with u = m. The dashed lines correspond to the diabatic potentials of Eqs. (53) and (54) with u = d.

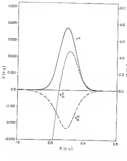

Fig.(6) A comparison of the off diagonal potential matrix elements for the two formulations of diabatic states for $\tau_x = 7.5$ a.u. The dash-dot and dashed curves correspond to $V_{12}^m$ and $V_{12}^d$ in Eq. (55) respectively. $\tau^s$ given by Eq. (57) corresponds to the solid line and is included for comparison.

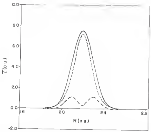

Fig. (7) A comparison of the momentum couplings in the adiabatic and diabatic representations for $\tau_X$ = 7.5 a.u. The solid curve corresponds to $\tau^A$ in Eq. (57). The dash-dot line corresponds to the absolute value of $\gamma^D(R,\alpha)'$ in Eq. (48).

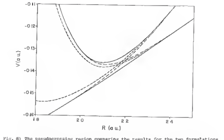

Fig. (8) The pseudocrossing region comparing the results for the two formulations of diabatic states for $r_X$ = 5 a.u. The solid lines correspond to the adiabatic potentials of Eq. (59). The dash-dot lines correspond to the diabatic potentials of Eqs. (53) and (54) with u = m. The dashed lines correspond to the diabatic potentials of Eqs. (53) and (54) with u = d.

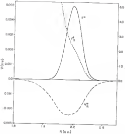

Fig. (9) A comparison of the off diagonal potential matrix elements for the two formulations of diabatic states for $\tau_x = 4$ a.u. The dash-dot and dashed curves correspond to $V^q_{12}$ and $V^d_{12}$ in Eq. (55) respectively. $\tau^a$ given by Eq. (57) corresponds to the solid line and is included for comparison

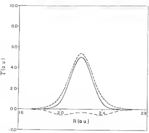

Fig. (10) A comparison of the momentum couplings in the adiabatic and diabatic representations for $\tau_X = 5$ a.u. The solid curve corresponds to $\tau^a$ in Eq. (57). The dash-dot line corresponds to the absolute value of $\gamma^m(R;\alpha)'$ in Eq. (48).

(or 19 kcal/mole). Thus again the range in energy where the momentum couplings can be neglected has considerably increased.

## 2-6 Discussion

This chapter has proposed an alternative procedure to construct electronic states. This procedure is based on choosing a transformation from the adiabatic representation into another that will ensure the proper behavior of the potentials away from the crossing region. The new transformation depends on a set of parameters which are obtained through Eq.(2-30). It was shown in Section 2-4 that this procedure led to a rather simple treatment of the two state problem in one dimension while the results demonstrated that it gives well behaved potentials and reduced momentum couplings.

The transformation only depends on the momentum couplings through the set of parameters $\{a_i\}$. The problem is thus broken up into two parts: (1) the determination of the parameters (which gives also the momentum couplings), and (2) the use of the transformation matrix to obtain the diabatic representation. In contrast, in the strictly diabatic transformation a numerical procedure must be implemented to determine the transformation at each point $\underline{X}$. The transformations in this treatment are always analytical so that numerical procedures need only be used once to determine the parameters.

As was emphasized earlier, whether the momentum couplings can be neglected or not depends on the system being investigated and the collision energy. An appealing aspect of the present procedure is that it allows us to estimate the range of energy where it can be used. If the collision energy is not in this range, one could use either the adiabatic representation with its diagonal electronic Hamiltonian matrix or the diabatic representation, Eq. (2-15), with the possibility of unrealistic potentials.

Several related problems can be studied along the present lines. In particular, a numerical treatment of the similar problem for three electronic states in one dimension would be useful. Extensions of the formalism would also be helpful in describing reactive scattering.

# CHAPTER 3
# GENERAL FORMALISM OF THE DYNAMICS

## 3-1 The One Electronic State Problem

As an introduction to the more general formalism to be presented in the following sections of this chapter, a brief development of the simpler one electronic state problem is presented using this formalism. It is hoped that this will provide a background that will aid in understanding the more general cases to be considered later. This case should also provide a more transparent connection between the formalism and classical mechanics since the results lead to classical trajectories for the nuclear particles on an electronic potential energy surface, which is a well known method for handling such systems.

This procedure, for obvious reasons, originates from a time independent treatment of the problem. Explicitly, one seeks the solutions of the time independent Schrödinger equation,

$$\hat{H}|\Psi(\underset{\sim}{R})> = E|\Psi(\underset{\sim}{R})> \qquad (3-1)$$

where

$$\hat{H} = \hat{T}_{nu}(\underset{\sim}{R},\frac{\partial}{\partial \underset{\sim}{R}}) + \hat{H}_{el}\ (\underset{\sim}{R}) \quad , \qquad (3-2)$$

and the notation was previously defined in Section 2-2. Since there is only one electronic state, i.e. no couplings, the adiabatic representation will be used. Using the Born-Oppenheimer approximation, the solutions to Eq. (3-1) are written as

$$|\Psi(\underset{\sim}{R})> = |\phi(\underset{\sim}{R})>\psi(\underset{\sim}{R}). \qquad (3\text{-}3)$$

Replacing this in Eq. (3-1), multiplying from the left with $<\phi(\underset{\sim}{R})|$ and integrating over electronic variables lead to

$$\hat{T}_{nu}\psi(\underset{\sim}{R}) + V(\underset{\sim}{R})\psi(\underset{\sim}{R}) = E\psi(\underset{\sim}{R}) \qquad (3\text{-}4)$$

where

$$V(\underset{\sim}{R}) = <\phi(\underset{\sim}{R})|\hat{H}_{el}|\phi(\underset{\sim}{R})>, \qquad (3\text{-}5)$$

i.e. the adiabatic potential energy surface. It has been assumed that the electronic functions are real and normalized. Equation (3-4) is the usual time independent Schrödinger equation for one electronic state systems which is the starting point for many treatments of this problem.

Using the nuclear coordinate system described in Section 2-2, Eq. (3-4) becomes

$$-\frac{\hbar^2}{2m}\nabla^2\psi(\underset{\sim}{R}) + V(\underset{\sim}{R})\psi(\underset{\sim}{R}) = E\psi(\underset{\sim}{R}) \qquad (3\text{-}6)$$

A form for the solution of Eq. (3-6) is apparent if one considers the case of $V(\underset{\sim}{R})$ equal zero. In this case the solutions are just travelling waves. A form similar to this will be chosen for the case of a nonzero potential. This is referred to as the Eikonal Approximation and the solution is written as

$$\psi(\underset{\sim}{R}) = \chi(\underset{\sim}{R})e^{\frac{i}{\hbar}S(\underset{\sim}{R})} . \qquad (3\text{-}7)$$

where $S(\underset{\sim}{R})$ is the eikonal, assumed along with $\chi(\underset{\sim}{R})$ to be real. Using this in Eq. (3-6) leads to, after some simplification,

$$-\frac{\hbar^2}{2m}\nabla^2\chi + \frac{(\nabla S)^2}{2m}\chi - \frac{i\hbar}{m}(\nabla S)\cdot(\nabla\chi) - \frac{i\hbar}{2m}(\nabla^2 S)\chi + (V-E)\chi = 0 \qquad (3\text{-}8)$$

where the $\underset{\sim}{R}$ dependence has been suppressed. The essential need at this point is to find an auxiliary equation involving the eikonal that will lead, on a transformation into time, to a straightforward classical interpretation of it. An expression that will be seen to fulfill this is obtained by requiring that the gradient of the eikonal satisfy a Hamilton-Jacobi like equation, i.e. define

$$\frac{(\nabla S)^2}{2m} + \overline{W} = E \qquad (3\text{-}9)$$

where $\overline{W}$ is to be determined. Using this in Eq. (3-8) gives

$$-\frac{\hbar^2}{2m}\nabla^2\chi - \frac{i\hbar}{m}(\nabla S)\cdot(\nabla\chi) - \frac{i\hbar}{2m}(\nabla^2 S)\chi + (V - \overline{W})\chi = 0 \quad . \tag{3-10}$$

An expression for $\overline{W}$ is obtained from the real part of Eq. (3-10) and one finds that

$$\overline{W} = V - \frac{\hbar^2}{2m}\frac{\nabla^2\chi}{\chi} \tag{3-11}$$

The imaginery part of Eq. (3-10) would lead to an expression for the flux but since it is not necessary for this discussion, the treatment of it will be deferred to a later section.

The next step involves implementing the short wavelength approximation. This approximation essentially assumes that the nuclear wave functions, $\chi$, vary slowly so that terms involving $\nabla^2\chi$ can be neglected. It can be shown (this will be treated in detail in Section 3-5) that if this approximation is used in Eq. (3-10) and a transformation into time is made, $\chi$ will satisfy a first order differential equation in time. Even though the case being considered here is trivial in that no electronic transitions take place, similar results, i.e. first order differential equations, will be obtained in the general case. Further, as will be shown in Section 3-6, for $\chi$ expressed in several convenient forms, these differential equations will result in $\chi$ being determined by Hamilton's equations of motion.

Using the short wavelength approximation in Eq. (3-11) and replacing the result in Eq. (3-9) leads to

$$\frac{(\nabla S)^2}{2m} + V = E \quad . \tag{3-12}$$

On transforming into time, the gradients of the eikonal become the nuclear momenta, $\underset{\sim}{P}(t)$, and the nuclear positions become functions of time, $\underset{\sim}{R}(t)$, so that Eq. (3-12) becomes

$$\frac{\underset{\sim}{P}(t)^2}{2m} + V(\underset{\sim}{R}(t)) = E \tag{3-13}$$

Defining the Hamiltonian,

$$H(\underset{\sim}{R}(t),\ \underset{\sim}{P}(t)) = \frac{\underset{\sim}{P}(t)^2}{2m} + V(\underset{\sim}{R}(t)), \tag{3-14}$$

choosing the initial positions $\underset{\sim}{R}(t_{in})$ and momenta $\underset{\sim}{P}(t_{in})$ such that

$$H(\underset{\sim}{R}(t_{in}),\ \underset{\sim}{P}(t_{in})) = E \tag{3-15}$$

and requiring that

$$\frac{d\underset{\sim}{R}}{dt} = \frac{\partial H}{\partial \underset{\sim}{P}} \tag{3-16}$$

and

$$\frac{d\underline{P}}{dt} = - \frac{\partial H}{\partial \underline{R}} \qquad (3\text{-}17)$$

i.e. that the nuclear positions and momenta satisfying Hamilton's equations of motion result in conservation of total energy (this can be easily seen by taking the total time derivative of the Hamiltonian and using Eqs. (3-16) and (3-17)).

The preceding discussion has demonstrated that, for the one-surface case, this formalism leads to the well known classical trajectory method. That is, the nuclei are treated as classical particles that evolve on a quantum mechanical potential energy surface. This should aid in seeing through some of the complications that arise in the more general cases to be considered next.

## 3-2 General Time Independent Formalism

In the preceding section, development of the one-surface case was presented and it was shown that the formalism led to the method of classical trajectories. The rest of this chapter will develop the formalism for a system of n electron states. The formalism will be developed without reference to a particular coordinate system in order to emphasize the generality of the procedure and avoid cumbersome notation.

In order to avoid assumptions about the time dependence of the nuclear positions and momenta, this procedure originates in a time independent formalism. Specifically, one seeks the solutions of the time independent Schrödinger equation which satisfy

$$(\hat{H}-E)\,|\Psi\rangle = 0 \tag{3-18}$$

where $|\ \rangle$ refers to electronic coordinates, $\langle\ |\ \rangle$ indicates integration over electronic coordinates,

$$\hat{H} = -\frac{\hbar^2}{2m}\nabla^2 + \hat{H}_{e\ell} \tag{3-19}$$

and the terms in Eq. (3-19) were defined in Section 2-2. For brevity, the dependence on nuclear coordinates has been suppressed. As was discussed in chapters one and two, one expands the solution of Eq. (3-18) in an electronic basis. In order to further clarify the problem of non-Hermiticity mentioned in Sections 1-2 and 2-2c, a specific electronic representation will not be used at this point. The basis will, however, be assumed to be real, complete and orthonormal. Expanding in this arbitrary electronic basis leads to

$$|\Psi\rangle = |\underset{\sim}{\phi}\rangle\,\underset{\sim}{\psi} \tag{3-20}$$

where $|\underset{\sim}{\phi}\rangle$ is a 1xn row matrix and $\underset{\sim}{\psi}$ is a nx1 column matrix. Using Eq. (3-20) in Eq. (3-18), multiplying from the left by $\langle\underset{\sim}{\phi}|$ and integrating over electronic coordinates gives

$$\underset{\approx}{K}\underset{\sim}{\psi} + \frac{\hbar}{i}\,\underset{\approx}{v}\cdot\nabla\underset{\sim}{\psi} - \frac{\hbar^2}{2m}\nabla^2\underset{\sim}{\psi} + \underset{\approx}{V}\underset{\sim}{\psi} - E\underset{\sim}{\psi} = \underset{\sim}{0} \tag{3-21}$$

where

$$\underset{\approx}{K} = \langle\underset{\approx}{\phi}| - \frac{\hbar^2}{2m}\nabla^2|\underset{\approx}{\phi}\rangle \quad , \tag{3-22}$$

$$\underset{\approx}{v} = \langle\underset{\approx}{\phi}|\frac{\hbar}{im}\nabla|\underset{\approx}{\phi}\rangle = \underset{\approx}{v}^{\dagger} \quad , \tag{3-23}$$

$$\underset{\approx}{V} = \langle\underset{\approx}{\phi}|\hat{H}_{el}|\underset{\approx}{\phi}\rangle = \underset{\approx}{V}^{\dagger} \tag{3-24}$$

and one must remember that, due to the presence of the gradient, the matrix $\underset{\approx}{v}$ must be treated as a vector. Obviously Eqs. (3-22) through (3-24) define nxn square matrices.

As was mentioned previously, Eq. (3-21) is not in general Hermitian. The terms that give rise to this come from Eq. (3-22). Since

$$\nabla^2\langle\underset{\approx}{\phi}|\underset{\approx}{\phi}\rangle = \underset{\approx}{0} \quad , \tag{3-25}$$

which gives

$$\nabla\cdot\langle\nabla\underset{\approx}{\phi}|\underset{\approx}{\phi}\rangle + \langle\nabla\underset{\approx}{\phi}|\nabla\underset{\approx}{\phi}\rangle + \langle\underset{\approx}{\phi}|\nabla^2\underset{\approx}{\phi}\rangle = \underset{\approx}{0} \tag{3-26}$$

it is not difficult to show, by making use of the completeness of the electronic basis, that

$$\underset{\approx}{K} = \frac{1}{2}\left(\frac{\hbar}{i}\nabla\cdot\underset{\approx}{v} + m\underset{\approx}{v}\cdot\underset{\approx}{v}\right) \quad . \tag{3-27}$$

As was discussed in Section 2-2c, this is not Hermitian because the first term on the right hand side of Eq. (3-27) is real and antisymmetric. If this term were present in the Hamiltonian, serious difficulties would arise since energy and flux would not be conserved.

In order to avoid the difficulties mentioned above, the electronic basis will be assumed to satisfy

$$\nabla\cdot\underset{\approx}{v} = \underset{\approx}{0} \quad . \tag{3-28}$$

This is the same electronic basis that was discussed in Section 2-2c. It was shown there that the unitary transformation relating it to the adiabatic basis satisfies Eq. (2-22), which in this notation (the superscript n used in Section 2-2c has been suppressed)

$$\underset{\approx}{C}^{\dagger}\nabla^2\underset{\approx}{C} + \nabla\underset{\approx}{C}^{\dagger}\cdot\nabla\underset{\approx}{C} + \underset{\approx}{C}^{\dagger}(\nabla\cdot\underset{\approx}{d}^{m})\underset{\approx}{C} = \underset{\approx}{0} \tag{3-29}$$

where

$$\underset{\approx}{d}^{m} = \langle\underset{\approx}{\phi}^{m}|\nabla\underset{\approx}{\phi}^{m}\rangle \quad .$$

Then in this electronic representation the nuclear wave functions satisfy

$$-\frac{\hbar}{2m}\nabla^2\underset{\approx}{\psi} + \frac{\hbar}{i}\underset{\approx}{v}\cdot\nabla\underset{\approx}{\psi} + \frac{m}{2}\underset{\approx}{v}\cdot\underset{\approx}{v}\underset{\approx}{\psi} + \underset{\approx}{V}\underset{\approx}{\psi} - E\underset{\approx}{\psi} = \underset{\approx}{0} \,. \tag{3-30}$$

This equation is Hermitian and provides the starting point for the developments to be presented in the next sections.

### 3-3 The Eikonal Approximation

As in the one surface case, the next step in this treatment involves using the Eikonal Approximation. The form of the solution is chosen to be the product of an amplitude written as a nx1 column matrix of complex elements and a common phase that is proportional to the eikonal. A common phase is used because it will lead to common momenta and positions for all electronic channels. Explicitly, the form of the nuclear wave function is chosen to be

$$\underset{\sim}{\psi}(\underset{\sim}{R}) = \underset{\sim}{\chi}(\underline{R})\,e^{\frac{i}{\hbar}S(\underline{R})} \tag{3-31}$$

where $S(\underline{R})$ is the eikonal. Using Eq. (3-31) in Eq. (3-30) leads to

$$\frac{-\hbar^2}{2m}\nabla^2\underset{\sim}{\chi} - \frac{i\hbar}{m}(\nabla S)\cdot(\nabla\underset{\sim}{\chi}) - \frac{i\hbar}{2m}(\nabla^2 S)\underset{\sim}{\chi} + \frac{(\nabla S)^2}{2m}\underset{\sim}{\chi}$$

$$+ (\nabla S)\cdot\underset{\approx}{v}\underset{\sim}{\chi} + \frac{\hbar}{i}\underset{=}{v}\cdot\nabla\underset{\sim}{\chi} + \frac{m}{2}\underset{\sim}{v}\cdot\underset{\approx}{v}\underset{\sim}{\chi} + \underset{\approx}{V}\underset{\sim}{\chi} - E\underset{\sim}{\chi} = \underset{\sim}{0} \quad . \tag{3-32}$$

As in Section 3-1, the gradient of the eikonal is required to satisfy a Hamilton-Jacobi like equation which gives

$$\frac{(\nabla S)^2}{2m} + \bar{W} = E \tag{3-33}$$

where $\overline{W}$ is to be determined. Using Eq. (3-33) in Eq. (3-32) results in

$$-\frac{\hbar}{2m}\nabla^2\underset{\approx}{\chi} - \frac{i\hbar}{m}(\nabla S)\cdot(\nabla\underset{\approx}{\chi}) - \frac{i\hbar}{2m}(\nabla^2 S)\underset{\approx}{\chi} + (\nabla S)\cdot\underset{\approx}{v}\underset{\approx}{\chi}$$

$$+ \frac{\hbar}{i}\underset{\sim}{v}\cdot\nabla\underset{\approx}{\chi} + \frac{m}{2}\underset{\sim}{v}\cdot\underset{\approx}{v}\underset{\approx}{\chi} + \underset{\approx}{V}\underset{\approx}{\chi} - \overline{W}\underset{\approx}{\chi} = \underset{\approx}{0} \quad . \tag{3-34}$$

An expression for $\overline{W}$ can be obtained by multiplying Eq. (3-34) from the left by $\underset{\approx}{\chi}^\dagger$, multiplying the adjoint of Eq. (3-34) from the right by $\underset{\approx}{\chi}$ and adding the results. Doing this one finds that

$$\overline{W} = \frac{1}{2}(\underset{\approx}{\chi}^\dagger\underset{\approx}{\chi})^{-1}\Big(2\underset{\approx}{\chi}^\dagger\underset{\approx}{V}\underset{\approx}{\chi} + \frac{i\hbar}{m}\nabla S\cdot((\nabla\underset{\approx}{\chi}^\dagger)\underset{\approx}{\chi} - \underset{\approx}{\chi}^\dagger\nabla\underset{\approx}{\chi})$$

$$- \frac{\hbar}{2m}(\underset{\approx}{\chi}^\dagger\nabla^2\underset{\approx}{\chi} + (\nabla^2\underset{\approx}{\chi}^\dagger)\underset{\approx}{\chi}) + \frac{\hbar}{i}(\underset{\approx}{\chi}^\dagger\underset{\sim}{v}\cdot\nabla\underset{\approx}{\chi} - (\nabla\underset{\approx}{\chi}^\dagger)\cdot\underset{\approx}{v}\underset{\approx}{\chi})$$

$$+ m\underset{\approx}{\chi}^\dagger\underset{\sim}{v}\cdot\underset{\approx}{v}\underset{\approx}{\chi} + 2\nabla S\cdot\underset{\approx}{\chi}^\dagger\underset{\approx}{v}\underset{\approx}{\chi}\Big) \quad . \tag{3-35}$$

This expression for $\overline{W}$ may seem to be a bit complicated and perhaps a few comments on its general properties may be helpful.

Considering an initial channel where one of the amplitudes equals one and all others are zero, then if an initial time is chosen so that the interactions between the fragments and the couplings $(\underset{\approx}{v})$ are zero and the amplitudes are constant, the expression for $\overline{W}$ reduces to a single potential energy surface. This is certainly what one would expect. As time increases and the fragments enter the interaction zone, the amplitudes are free to change. In this case there are three contributions to $\overline{W}$. The first contribution comes from the first term on the right hand side of Eq. (3-35). This can be viewed as an average potential with the weights determined from the amplitudes. The second contribution comes from the next two terms in Eq. (3-35) and arises from the variations of $\underset{\sim}{\chi}$. If the elements of $\underset{\sim}{\chi}$ are slowly varying, this second contribution may be "small" enough to neglect. The final contribution comes from the last three terms which depend on the electronic couplings. At a final time when the amplitudes are again constant and the electronic couplings and interactions between the fragments are zero, $\overline{W}$ is again given by the first term on the right hand side of Eq. (3-35). However $\overline{W}$ for the final state is now an average potential with the weights determined by the final values of the amplitudes. The implications of this will be discussed in a later section after a transformation to time has been made.

An expression for the flux is obtained by multiplying Eq. (3-34) from the left by $\underset{\sim}{\chi}^\dagger$, multiplying the adjoint of Eq. (3-34) from the right by $\underset{\sim}{\chi}$ and subtracting the results. Carrying out the algebra leads to

$$-\frac{i\hbar}{m}[(\nabla^2 S)\underset{\sim}{\chi}^\dagger\underset{\sim}{\chi} + (\nabla S)\underset{\sim}{\chi}^\dagger\cdot\nabla\underset{\sim}{\chi} + (\nabla S)\cdot(\nabla\underset{\sim}{\chi}^\dagger)\underset{\sim}{\chi}] + \frac{\hbar^2}{2m}[(\nabla^2\underset{\sim}{\chi}^\dagger)\underset{\sim}{\chi} - \underset{\sim}{\chi}^\dagger\nabla^2\underset{\sim}{\chi}] + \frac{\hbar}{i}[\underset{\sim}{\chi}^\dagger\underset{\approx}{v}\cdot\nabla\underset{\sim}{\chi} + (\nabla\underset{\sim}{\chi}^\dagger)\cdot\underset{\approx}{v}\underset{\sim}{\chi}] = 0 \quad . \qquad (3\text{-}36)$$

Defining

$$\underline{j}_1 = \frac{(\nabla S)}{m}\, \underline{\chi}^{\dagger} \underline{\chi} \quad , \qquad (3\text{-}37)$$

$$\underline{j}_2 = \underline{\chi}^{\dagger} \underline{\underline{v}} \underline{\chi} \quad , \qquad (3\text{-}38)$$

and

$$\underline{j}_3 = \frac{i\hbar}{2m} \left(\underline{\chi}^{\dagger} \nabla \underline{\chi} - (\nabla \underline{\chi})^{\dagger} \underline{\chi}\right) \qquad (3\text{-}39)$$

and recalling that the electronic basis satisfies Eq. (3-28) one obtains

$$\nabla \cdot \underline{j} - \nabla \cdot \underline{j}_2 = 0 \qquad (3\text{-}40)$$

where

$$\underline{j} = \underline{j}_1 + \underline{j}_3 \quad . \qquad (3\text{-}41)$$

From Eq. (3-40) one sees that there are three terms in the expression for flux. The first term $\underline{j}_1$ defined by Eq. (3-37) is the most transparent. At the initial time when $\underline{\underline{v}}$ is the zero matrix and $\underline{\chi}$ is constant, Eq. (3-40) reduces to the gradient of $\underline{j}_1$ equal to zero. $\underline{j}_1$ is just the product of a velocity term given by $(\nabla S)/m$ times the number density of particles given by $\underline{\chi}^{\dagger} \underline{\chi}$. At later times when $\underline{\underline{v}}$ is non-zero and $\underline{\chi}$ is changing, the flux has additional terms involving electronic couplings and variations of $\underline{\underline{\chi}}$. If $\underline{\underline{\chi}}$ is slowly varying, it may be possible to neglect the last term in Eq. (3-40) so that the flux will be given by Eq. (3-41).

As has been suggested throughout this section, if use is made of the slowly varying nature of $\underline{\underline{\chi}}$, the expressions for $\overline{W}$ and $\underline{j}$ are considerably simplified. This will be the topic of the next section.

### 3-4 The Short Wavelength Approximation

In the previous section, the Eikonal approximation was used and it was found that the nuclear wave function, $\underline{\underline{\chi}}$, satisfied Eq. (3-34). This section will make use of the slowly varying nature of $\underline{\underline{\chi}}$ in order to introduce a physically motivated approximation to Eq. (3-34). This will in turn simplify the expressions for $\overline{W}$ and the flux.

The approximation referred to above is the well known short wavelength approximation (Newton, 1966). This approximation is based on the classical behavior of the nuclear particles. From Eq. (3-33) one has

$$|\nabla S| = \sqrt{2m(E-\overline{W})} \tag{3-42}$$

so that a characteristic wavelength can be defined as

$$\lambda = \frac{\hbar}{|\nabla S|} = \frac{\hbar}{\sqrt{2m(E-\overline{W})}} \quad . \tag{3-43}$$

In a full classical treatment of the trajectories, $\hbar$ would be zero so that the wavelength would also be zero as it should. The short wavelength approximation assumes that

$$\bar{\lambda} << 1 \qquad (3\text{-}44)$$

which is normally valid except around turning points where $E = \bar{W}$. Obviously, from Eq. (3-43), as the total energy is increased this approximation becomes better so that it is in actuality a high energy approximation.

In a similar fashion one can define "characteristic wavelengths" for the amplitudes as

$$\frac{|\nabla \chi_j|}{|\chi_j|} = \lambda_{j,1}^{-1} \qquad (3\text{-}45,a)$$

and

$$\frac{|\nabla^2 \chi_j|}{|\nabla \chi_j|} = \lambda_{j,2}^{-1} \qquad (3\text{-}45,b)$$

for an arbitrary electronic channel j. If the amplitudes are assumed to be slowly varying functions, their "wavelengths" should be large compared to $\bar{\lambda}$ so that with Eq. (3-44) one would have that

$$\lambda_{j,1}^{-1} << \bar{\lambda}^{-1} \qquad (3\text{-}46)$$

and

$$\,^{-1}_{j,2} \ll \lambda^{-1} \quad . \qquad (3\text{-}47)$$

Using these conditions in Eq. (3-34) leads to

$$-\frac{i\hbar}{m}(\nabla S)\cdot(\nabla\underline{\chi}) - \frac{i\hbar}{2m}(\nabla^2 S)\underline{\chi} + (\nabla S)\cdot\underline{\underline{v}}\underline{\chi} + \frac{m}{2}\,\underline{\underline{v}}\cdot\underline{\underline{v}}\underline{\chi} + \underline{\underline{V}}\underline{\chi} - \overline{W}\underline{\chi} = \underline{0} \quad . \qquad (3\text{-}48)$$

Carrying through the same procedure that was used to obtain Eq. (3-35) results in

$$\overline{W} = \frac{1}{2}(\underline{\chi}^{+}\underline{\chi})^{-1}\Big(2\underline{\chi}^{+}\underline{\underline{V}}\underline{\chi} + \frac{i\hbar}{m}(\nabla S)\cdot\big((\nabla\underline{\chi}^{+})\underline{\chi} - \underline{\chi}^{+}\nabla\underline{\chi}\big)$$

$$+ 2(\nabla S)\cdot\underline{\chi}^{+}\underline{\underline{v}}\underline{\chi} + m\underline{\chi}^{+}\underline{\underline{v}}\cdot\underline{\underline{v}}\underline{\chi}\Big) \quad . \qquad (3\text{-}49)$$

Assuming that the second term on the right hand side of Eq. (3-49) is negligible gives

$$\overline{W} = (\underline{\chi}^{+}\underline{\chi})^{-1}\underline{\chi}^{+}\left(\underline{\underline{V}} + \nabla S\cdot\underline{\underline{v}} + \frac{m}{2}\,\underline{\underline{v}}\cdot\underline{\underline{v}}\right)\underline{\chi} \quad . \qquad (3\text{-}50)$$

The general properties of $\overline{W}$ discussed in the previous section still hold here. Suffice it to say that the approximations used to obtain Eq. (3-50) have considerably simplified the determination of $\overline{W}$ in that only a knowledge of the amplitudes and not their variations is needed.

The flux is determined by using the same procedure that led to Eq. (3-36). Carrying through the algebra results in

$$\frac{(\nabla^2 S)}{m}\,\underline{\underline{\chi}}^{\dagger}\underset{\sim}{\chi} + \frac{(\nabla S)}{m}\cdot\underline{\underline{\chi}}^{\dagger}\nabla\underset{\sim}{\chi} + \frac{(\nabla S)}{m}\,(\nabla\underline{\underline{\chi}}^{\dagger})\underline{\underline{\chi}} = 0 \qquad (3\text{-}51)$$

or

$$\nabla\cdot\mathcal{J}_1 = 0 \qquad (3\text{-}52)$$

where $\mathcal{J}_1$ is given by Eq. (3-37). Equation (3-52) is an expression for the conservation of current. In the case of one electronic surface, Eq. (3-37) reduces to

$$\mathcal{J}_1 = \chi^2\,\frac{\nabla S}{m} \qquad (3\text{-}53)$$

which is a well known result (Messiah, 1966).

Equations (3-48), (3-50) and (3-52) are the main results of this section. One notices that Eq. (3-48) does not contain terms involving $\nabla^2\underline{\underline{\chi}}$. It will be shown in the next section that, because of this, the amplitudes will satisfy first order differential equations in time. This is a pleasing aspect since Hamilton's equations of motion are also first order differential equations in time.

Another point worth mentioning has to do with the form of $\overline{W}$. At a later stage in this development, $\overline{W}$ will be used to construct a "classical" Hamiltonian and one sees from Eq. (3-50) that $\overline{W}$ depends on the amplitudes.

Then the "classical" Hamiltonian will not only depend on the traditional variables but also on the nuclear amplitudes as well. This suggests, already at this point, that all the nuclear dynamics could perhaps be determined through Hamilton's equations of motion.

### 3-5 Time Dependent Equations

The developments of the preceding sections of this chapter were done with a time independent formalism. This section shall be concerned with transforming these previous results into a time dependent picture. The use of the word time is somewhat arbitrary but it will be seen later that the parameter, which the nuclear variables are a function of, plays the role of a "classical" time.

In making a transformation into time one has

$$\underset{\sim}{R} \rightarrow \underset{\sim}{R}(t) \quad , \tag{3-54}$$

$$\nabla S \rightarrow \nabla S(t) = \underset{\sim}{P}(t) \tag{3-55}$$

and

$$\underset{\approx}{X}(\underset{\sim}{R}(t)) \rightarrow \underset{\approx}{A}(t) \quad . \tag{3-56}$$

Matters are somewhat simplified if a coordinate system is chosen such that one of the orthogonal unit vectors, say $\underset{\sim}{e}$, is in the direction of $\underset{\sim}{P}$ (see Fig. 11). Then one has

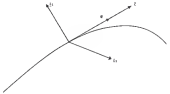

Fig. (11) Schematic of coordinate system assumed in making a transformation into time.

$$\nabla^2 S = \nabla\cdot\underset{\sim}{P} = \frac{dP}{ds} = \frac{dt}{ds}\frac{dP}{dt} = \frac{m}{P}\frac{dP}{dt} \quad , \tag{3-57}$$

where

$$P = |\underset{\sim}{P}| \quad , \tag{3-58}$$

or

$$\nabla^2 S = m\frac{d}{dt}(\ln P) \quad . \tag{3-59}$$

Furthermore,

$$\frac{\underset{\sim}{P}}{m}\cdot\nabla\underset{\approx}{\chi} = \frac{ds}{dt}\frac{d}{ds}\underset{\approx}{\chi} = \frac{ds}{dt}\frac{dt}{ds}\frac{d\underset{\approx}{A}}{dt} = \frac{d\underset{\approx}{A}}{dt} \tag{3-60}$$

so that Eq. (3-48) becomes

$$\frac{\hbar}{i}\frac{d\underset{\approx}{A}}{dt} + \left(\frac{\hbar}{2i}\frac{d}{dt}\ln P - \overline{W}\right)\underset{\approx}{A} + \left(\underset{\approx}{V} + \underset{\sim}{P}\cdot\underset{\approx}{v} + \frac{m}{2}\,\underset{\approx}{v}\cdot\underset{\approx}{v}\right)\underset{\approx}{A} = \underset{\approx}{0} \quad . \tag{3-61}$$

By the now standard technique, one can show that

$$\overline{W} = (\underset{\approx}{A}^{\dagger}\underset{\approx}{A})^{-1}\underset{\approx}{A}^{\dagger}\left(\underset{\approx}{V} + \underset{\sim}{P}\cdot\underset{\approx}{v} + \frac{m}{2}\,\underset{\approx}{v}\cdot\underset{\approx}{v}\right)\underset{\approx}{A} \quad . \tag{3-62}$$

A somewhat simpler differential equation that Eq. (3-61) results if one defines

$$\underset{\approx}{A}(t) = \underset{\approx}{C}(t)\exp\frac{i}{\hbar}\left(\int_{t_1}^{t} dt'\left(\overline{W}(t') - \frac{\hbar}{i}\frac{d}{dt'}\ln P^{1/2}\right)\right) \quad , \tag{3-63}$$

where $t_1$ is the initial time, so that

$$\frac{\hbar}{i}\frac{d\underset{\approx}{C}}{dt} + (\underset{\approx}{V} + \underset{\sim}{p}\cdot\underset{\approx}{v} + \frac{m}{2}\,\underset{\approx}{v}\cdot\underset{\approx}{v})\underset{\approx}{C} = \underset{\approx}{0} \quad . \tag{3-64}$$

It is also relatively easy to show that

$$\overline{W} = (\underset{\approx}{C}^{\dagger}\underset{\approx}{C})^{-1}\underset{\approx}{C}^{\dagger}(\underset{\approx}{V} + \underset{\sim}{p}\cdot\underset{\approx}{v} + \frac{m}{2}\,\underset{\approx}{v}\cdot\underset{\approx}{v})\underset{\approx}{C} \quad . \tag{3-65}$$

By multiplying Eq. (3-64) from the left by $\underset{\approx}{C}^{\dagger}$ and the adjoint of Eq. (3-64) from the right by $\underset{\approx}{C}$ and adding the results, one finds that

$$\frac{d}{dt}(\underset{\approx}{C}^{\dagger}\underset{\approx}{C}) = 0 \tag{3-66}$$

i.e. the probability is conserved. Equation (3-63) can also be written as

$$\underset{\approx}{A}(t) = \left(\frac{P_1}{P}\right)^{\frac{1}{2}} e^{\frac{i}{\hbar}\int_{t_1}^{t} dt'\,\overline{W}(t')}\,\underset{\approx}{C}(t) \tag{3-67}$$

which shows that the amplitudes have the correct asymptotic form. The amplitudes $\underset{\approx}{C}$ are more convenient to work with because they avoid the singularities that occur in $\underset{\approx}{A}$ at the turning points where $P$ is zero.

The main result thus far is given by Eq. (3-64). If the trajectories and moments are known functions of time, the amplitudes are determined from a set of coupled first order differential equations in time. The remainder of this section will deal with how to determine the trajectories and momenta which will also lead to some general relations between the real and imaginary parts of the amplitudes.

As was mentioned in Section (3-3), requiring that the gradient of the eikonal satisfy Eq. (3-33) would be suggestive when making a transformation into time. Using Eq. (3-55) in Eq. (3-33) gives

$$\frac{P^2}{2m} + \overline{W} = E \quad . \tag{3-68}$$

Defining the "Hamiltonian" as

$$\overline{H}(R,\underset{-}{P},\underset{=}{C}) = \frac{P^2}{2m} + \overline{W} \tag{3-69}$$

and requiring that

$$\frac{d\overline{H}}{dt} = 0 \tag{3-70}$$

would result in the conservation of energy. The dependence of the "Hamiltonian" on the amplitudes is a manifestation of its non-classical nature. Recalling that the amplitudes were assumed to be complex and writing the real and imaginary parts as $C_j^R$ and $C_j^I$ respectively which are independent variables leads to

$$\frac{d\bar{H}}{dt} = \left(\frac{\partial\bar{H}}{\partial\underline{R}}\right)\frac{d\underline{R}}{dt} + \left(\frac{\partial\bar{H}}{\partial\underline{P}}\right)\frac{d\underline{P}}{dt} + \frac{1}{\hbar}\sum_j\left(\left(\frac{\partial\bar{H}}{\partial C_j^R}\right)\frac{\hbar}{i}\frac{dC_j^R}{dt} + \left(\frac{\partial\bar{H}}{\partial C_j^I}\right)\frac{\hbar}{i}\frac{dC_j^I}{dt}\right) \quad (3\text{-}71)$$

where the partial derivatives are evaluated holding everything but the variable in question constant and $\bar{H}$ is assumed not to depend explicitly on t. If one requires that

$$\frac{d\underline{R}}{dt} = \frac{\partial\bar{H}}{\partial\underline{P}} \quad , \qquad (3\text{-}72)$$

$$\frac{d\underline{P}}{dt} = -\left(\frac{\partial\bar{H}}{\partial\underline{R}}\right) \quad , \qquad (3\text{-}73)$$

$$\frac{\hbar}{i}\frac{dC_j^R}{dt} = \frac{\partial\bar{H}}{\partial C_j^I} \quad , \qquad (3\text{-}74)$$

and

$$\frac{\hbar}{i}\frac{dC_j^I}{dt} = -\frac{\partial\bar{H}}{\partial C_j^R} \qquad (3\text{-}75)$$

then energy would be conserved. Equations (3-72) and (3-73) are in the form of Hamilton's classical equations of motion and provide a prescription for determining the trajectories and momenta. Equations (3-74) and (3-75) are interesting in that if the real and imaginary parts of the amplitude are chosen to be conjugate variables, then with trajectories and moments satisfying equations (3-72) and (3-73) respectively, energy is conserved.

It is not difficult to show that for the amplitudes expressed in terms of their real and imaginary parts Eqs. (3-74) and (3-75) are equivalent to Eq. (3-64). The advantage offered by Eq. (3-64) is that the form of the amplitudes is not specified. It will be shown later that the flexibility in choosing the form of the amplitudes will lead to other sets of canonical variables that have a straightforward physical interpretation.

The next section shall be concerned with finding solutions of Eq. (3-64). Several different forms for the solution will be developed and it will be seen that they satisfy Eqs. (3-74) and (3-75). Having more than one form is certainly not surprising. It is in a way equivalent to the problem in classical mechanics of having more than one choice of coordinates some of which lead to a simpler treatment of the problem.

3-6 Solutions of the Equations

This section will develop solutions to Eq. (3-64) for two forms of the amplitudes. It will be shown how these forms can be used to construct canonical variables that satisfy Eqs. (3-74) and (3-75). It will also be emphasized that care must be used in selecting a set of canonical variables in that some of them can lead to inherent difficulties that arise from the form of the Hamiltonian.

---

The matrix $\underset{\sim}{C}$ is in general a nx1 column matrix of complex numbers. A general way of writing such a matrix is to let

$$\underset{\sim}{C}(t) = e^{-\frac{i}{\hbar}\underset{\sim}{\gamma}(t)}\,\underset{\sim}{c}(t) \qquad (3\text{-}76)$$

where $\underset{\sim}{\gamma}$ is a real square diagonal nxn matrix and $\underset{\sim}{c}$ is a real nx1 column matrix. Using Eq. (3-76) in Eq. (3-64) and rearranging terms give

$$\frac{d}{dt}\,\underset{\sim}{c} = \frac{i}{\hbar}\left(\frac{d}{dt}\,\underset{\sim}{\gamma}\right)\underset{\sim}{c} - \frac{i}{\hbar}\,e^{\frac{i}{\hbar}\underset{\sim}{\gamma}}\left(\underset{\sim}{V} + \underset{\sim}{P}\cdot\underset{\sim}{v} + \frac{m}{2}\,\underset{\sim}{v}\cdot\underset{\sim}{v}\right)e^{-\frac{i}{\hbar}\underset{\sim}{\gamma}}\,\underset{\sim}{c} \quad . \qquad (3\text{-}77)$$

It is not difficult to show that the j<sup>th</sup> component satisfies

$$\dot{c}_j = \frac{i}{\hbar}\,\dot{\gamma}_j c_j - \frac{i}{\hbar}\,e^{\frac{i}{\hbar}\gamma_j}\sum_{k=1}^{n}\left(V_{jk} + \underset{\sim}{P}\cdot v_{jk}\right.$$

$$\left. + \frac{m}{2}(\underset{\sim}{v}\cdot\underset{\sim}{v})_{jk}\right)e^{-\frac{i}{\hbar}\gamma_k}\,c_k \quad . \qquad (3\text{-}78)$$

An equation for $c_j$ can be found by multiplying Eq. (3-78) from the left by $c_j$, multiplying the complex conjugate of Eq. (3-78) from the left by $c_j$ and adding the results. Doing this results in

$$2c_j \frac{dc_j}{dt} = \frac{i}{\hbar} c_j e^{-\frac{i}{\hbar}\gamma_j} \sum_{k=1}^{n} U_{kj} e^{\frac{i}{\hbar}\gamma_k} c_k - \frac{i}{\hbar} c_j e^{\frac{i}{\hbar}\gamma_j} \sum_{k=1}^{n} U_{jk} e^{-\frac{i}{\hbar}\gamma_k} c_k \tag{3-79}$$

where

$$U_{jk} = V_{jk} + \underline{F}\cdot v_{jk} + \frac{m}{2} \sum_{\ell} v_{j\ell}\cdot v_{\ell k} \quad . \tag{3-80}$$

With the form of C given by Eq. (3-76), one has that

$$\overline{W} = (\underline{\underline{C}}^{\dagger}\underline{\underline{C}})^{-1} \underline{\underline{C}}^{\dagger} e^{\frac{i}{\hbar}\underline{\underline{\gamma}}} \underline{\underline{U}} e^{-\frac{i}{\hbar}\underline{\underline{\gamma}}} \underline{\underline{C}} \tag{3-81}$$

where the elements of $\underline{\underline{U}}$ were defined in Eq. (3-80). It is straightforward to show that

$$\frac{\partial \overline{W}}{\partial \gamma_j} = (\sum_j c_j)^{-1} (\frac{i}{\hbar} c_j e^{\frac{i}{\hbar}\gamma_j} \sum_{\ell} U_{j\ell} e^{-\frac{i}{\hbar}\gamma_\ell} c_\ell - \frac{i}{\hbar} c_j e^{-\frac{i}{\hbar}\gamma_j} \sum_{\ell} U_{\ell j} e^{\frac{i}{\hbar}\gamma_\ell} c_\ell) \quad . \tag{3-82}$$

Comparing Eqs. (3-79) and (3-82) gives

$$\frac{2c_j}{\sum_j c_j^2}\frac{dc_j}{dt} = -\frac{\partial \bar{H}}{\partial \gamma_j} \tag{3-83}$$

or by defining

$$P_j = \frac{c_j^2}{\sum_j c_j^2} \tag{3-84}$$

and recalling from Eq. (3-66) that

$$\frac{d}{dt}\sum_j c_j^2 = 0 \tag{3-85}$$

one obtains

$$\frac{dP_j}{dt} = -\frac{\partial \bar{H}}{\partial \gamma_j} \quad . \tag{3-86}$$

One would expect at this point that $\gamma_j$ and $P_j$ are canonical variables and that they should satisfy equations similar to (3-74) and (3-75) respectively. The other relation can be obtained by subtracting the results that were used to obtain Eq. (3-79). This results in a differential equation for $\gamma_j$ and one finds that

$$\frac{d\gamma_j}{dt} = \frac{i}{2c_j}\left(e^{\frac{i}{\hbar}\gamma_j}\sum_{k=1}^{n} U_{jk}e^{-\frac{i}{\hbar}\gamma_k}c_k + e^{-\frac{i}{\hbar}\gamma_j}\sum_{k=1}^{n} U_{kj}e^{\frac{i}{\hbar}\gamma_k}c_k\right) \quad . \tag{3-87}$$

Since, from Eq. (3-84),

$$c_j = \left(\sum_{k=1}^{n} c_k\right)^{\frac{1}{2}} P_j^{\frac{1}{2}}$$

$\overline{W}$ as a function of $P_j$ and $\gamma_j$ becomes

$$\overline{W} = \left(e^{\frac{i}{\hbar}\gamma_1} P_1^{\frac{1}{2}} \cdots e^{\frac{i}{\hbar}\gamma_n} P_n^{\frac{1}{2}}\right) \underset{=}{U} \begin{pmatrix} e^{-\frac{i}{\hbar}\gamma_1} P_1^{\frac{1}{2}} \\ \cdot \\ \cdot \\ \cdot \\ e^{-\frac{i}{\hbar}\gamma_n} P_n^{\frac{1}{2}} \end{pmatrix} \quad . \qquad (3\text{-}88)$$

Then

$$\frac{\partial \overline{W}}{\partial P_j} = \frac{1}{2} P_j^{-\frac{1}{2}} e^{\frac{i}{\hbar}\gamma_j} \sum_{k=1}^{n} U_{jk} e^{-\frac{i}{\hbar}\gamma_k} P_k^{\frac{1}{2}}$$

$$+ \frac{1}{2} P_j^{-\frac{1}{2}} e^{-\frac{i}{\hbar}\gamma_j} \sum_{k=1}^{n} U_{kj} e^{\frac{i}{\hbar}\gamma_k} P_k^{\frac{1}{2}} \qquad (3\text{-}89)$$

or

$$\frac{\partial \overline{W}}{\partial P_j} = \frac{1}{2C_j}\left(e^{\frac{i}{\hbar}\gamma_j} \sum_{k=1}^{n} U_{jk} e^{-\frac{i}{\hbar}\gamma_k} c_k + e^{-\frac{i}{\hbar}\gamma_j} \sum_{k=1}^{n} U_{kj} e^{\frac{i}{\hbar}\gamma_k} c_k\right) \quad . \qquad (3\text{-}90)$$

Comparing equations (3-87) and (3-90) gives the desired result in that one has

$$\frac{d\gamma_j}{dt} = \frac{\partial H}{\partial P_j} \quad . \tag{3-91}$$

Then as was expected, $\gamma_j$ and $P_j$ form a set of canonical variables. Expressing the total time derivative of the Hamiltonian in this set of variables and using Eqs. (3-86) and (3-91) lead to energy conservation.

An interesting aspect of these variables is seen by considering Eq. (3-89). Since the terms on the right hand side contain the quantity $P_j^{-\frac{1}{2}}$, there is an essential singularity in this equation if $P_j$ is equal to zero. This can be very troublesome since normally one starts in a pure electronic state where all probabilities, $P_j$, are zero except one of them which is set equal to one. Trying to integrate this set of coupled equations that contain singularities at the boundary conditions is clearly not meaningful.

Even though this set of variables has the difficulty that was mentioned above they are easily understood in a physical sense. Indeed, it is gratifying to see that the quantum mechanical probability, $P_j$, and phase, $\gamma_j$, turn out to be canonical variables in a "classical" description. Although other sets of canonical variables which avoid these difficulties are used to do the calculations, it is convenient to construct the probabilities and phases as a guide to a straightforward physical interpretation of the collision process.

Another form for the amplitudes is obtained by letting

$$\underline{\underline{C}} = \alpha \underline{\underline{X}} + i\beta \underline{\underline{Y}} \quad . \tag{3-92}$$

Using this form of the amplitude in Eq. (3-64) gives

$$\frac{ah}{i} \frac{d\underline{\underline{X}}}{dt} + b\beta \frac{d\underline{\underline{Y}}}{dt} + \alpha \underline{\underline{U}}\,\underline{\underline{X}} + i\beta \underline{\underline{U}}\,\underline{\underline{Y}} = \underline{\underline{0}} \tag{3-93}$$

where the elements of $\underline{\underline{U}}$ are defined by Eq. (3-80) and $\underline{\underline{X}}$ and $\underline{\underline{Y}}$ are real nx1 column matrices. It is straightforward to show that the $j^{th}$ component satisfies

$$\frac{ah}{i} \frac{dX_j}{dt} + h\beta \frac{dY_j}{dt} + \alpha \sum_k U_{jk}X_k + i\beta \sum_k U_{jk}Y_k = 0 \quad . \tag{3-94}$$

A differential equation for $X_j$ is obtained by subtracting Eq. (3-94) from its complex conjugate which gives

$$\frac{dX_j}{dt} = \frac{-i}{2ah} \left(\alpha \sum_k (U_{jk} - U^*_{jk})X_k + i\beta \sum_k (U_{jk} + U^*_{jk})Y_k\right. \quad . \tag{3-95}$$

In a similar fashion, the differential equation for $Y_j$ is found by adding Eq. (3-94) to its complex conjugate and one finds that

$$\frac{dY_j}{dt} = -\frac{1}{2\hbar\beta}\{\alpha \sum_k (U_{jk} + U_{jk}^{*})X_k + i\beta \sum_k (U_{jk} - U_{jk}^{*})Y_k \quad . \qquad (3\text{-}96)$$

Equations (3-95) and (3-96) provide first order differential equations for determining the amplitudes but the task still remains to determine sets of canonical variables. In order to find sets of canonical variables, it is necessary to find an expression for $\overline{W}$. To somewhat simplify matters, Eq. (3-65) will be used and it will be assumed that

$$\underset{\sim}{C}^{\dagger}\underset{\sim}{C} = 1 \quad . \qquad (3\text{-}97)$$

The results of this analysis do not depend on this assumption in that if Eq. (3-97) was not satisfied, then new variables weighted by the inverse of the square root of Eq. (3-97) could be formed that would also satisfy Eqs. (3-95) and (3-96). Using Eqs. (3-97) and (3-92) in Eq. (3-65) gives

$$\overline{W} = \sum_k (\alpha X_k - i\beta Y_k) \sum_\ell U_{k\ell}(\alpha X_\ell + i\beta Y_\ell) \quad . \qquad (3\text{-}98)$$

It is not difficult to show that

$$\frac{\partial \overline{W}}{\partial Y_j} = -i\beta\{\alpha \sum_k (U_{jk} - U_{jk}^{*})X_k + i\beta \sum_k (U_{jk} + U_{jk}^{*})Y_k \qquad (3\text{-}99)$$

and

$$\frac{\partial \overline{W}}{\partial X_j} = \alpha(\alpha \sum_k (U_{jk} + U_{jk}^*)X_k + i\beta \sum_k (U_{jk} - U_{jk}^*)Y_k \qquad (3\text{-}100)$$

where use was made of the property that

$$U_{jk} = U_{kj}^* \quad . \qquad (3\text{-}101)$$

Equations (3-99) and (3-100) are similar to Eqs. (3-95) and (3-96) respectively and for certain choices of $\alpha$ and $\beta$, $X_j$ and $Y_j$ will play the role of canonical variables.

By comparing Eq. (3-95) to Eq. (3-99) and Eq. (3-96) to Eq. (3-100) one finds that $X_j$ and $Y_j$ will form a canonical set of variables if

$$\alpha\beta = \frac{1}{2\hbar} \quad . \qquad (3\text{-}102)$$

Two obvious choices of $\alpha$ and $\beta$ that satisfy Eq. (3-102) are given by letting

$$\alpha = \beta = \frac{1}{\sqrt{2\hbar}} \qquad (3\text{-}103)$$

and

$$\alpha = 1 \quad , \qquad (3\text{-}104)$$

$$\beta = \frac{1}{2\hbar} \quad . \qquad (3\text{-}105)$$

These, of course, are not the only possibilities. The case where $\alpha$ and $\beta$ are given by Eq. (3-103) will be referred to as the symmetric form and this form was used in doing the calculations.

One notices that Eqs. (3-99) and (3-100) do not contain singularities in the variables $X_j$ and $Y_j$ so that the difficulties that occurred when using the probability and phase as canonical variables are avoided. As was mentioned earlier, the probability and phase do have the advantage of being easy to physically interpret and of being formed quite easily by using the relations

$$P_j = \alpha^2 X_j^2 + \beta^2 Y_j^2 \qquad (3\text{-}106)$$

and

$$\gamma_j = - \hbar \tan^{-1}\left(\frac{\beta Y_j}{\alpha X_j}\right) \quad . \qquad (3\text{-}107)$$

The solution of the problem will then consist of integrating the coupled equations given by the expressions (3-72) and (3-73) and the corresponding ones for the amplitudes. The amplitudes will be chosen to have the form of Eq. (3-92). The probabilities and phases are found by using Eqs. (3-106) and (3-107).

## 3-7 Expressions for Observables

As was pointed out in Section 3-3, one of the curious features of this formalism is that the trajectories end up on an average potential energy surface with the weights determined by the probabilities $P_j$. This may seem to be a serious drawback because experimentally, the system begins and ends up in a definite electronic state. This feature is not unique to this formalism in that this problem also occurs in other semi-classical treatments of multi-surface systems.

Trajectories that do go from one surface to another can be found by considering the quantum mechanical expressions for the transition matrix or scattering matrix which can be expressed in terms of the initial and final states of the system. The problem then consists of finding trajectories that go smoothly from the initial to the final state. Several procedures have been developed for finding these trajectories but they are quite complicated and not easy to implement. A further discussion of this problem will be presented in chapter six.

The approach to be used in this work is based on accepting average potentials for the trajectories and on using the $P_j$'s to construct a total electronic transition probability. The problem is that there are many "classical" trajectories that correspond to the same quantum mechanical initial state. One would then expect that some sort of an average of these "classical" probabilities, $P_j$, would correspond to the quantum mechanical probability.

This becomes more clear if one considers the case of a collinear collision between an atom and a diatomic molecule. The "classical" initial state would consist of specifying a total energy, E, which is the sum of the vibrational energy, $E_n$, of the diatomic and the relative kinetic energy, the distance between the atom and the center of mass of the diatomic, the vibrational coordinate of the diatomic, the direction of the diatomic momentum and the initial amplitudes. The quantum mechanical initial state, however, would represent the diatomic by a wave function, $\psi_n$, corresponding to the $n^{th}$ vibrational state. The total electronic transition probability can be written as

$$P_{j'\to j}(E,E_n) = \int dX\, P_{j'\to j}(E,E_n,X)\,|\psi_n(X)|^2 \qquad (3\text{-}108)$$

where X is the vibrational coordinate. Equation (3-108) provides a prescription for determining the total electronic transition probability. Final probabilities for different values of X are calculated and the total probability is obtained by averaging the final probabilities with the weights given by Eq. (3-108).

The procedure for determining total probabilities in the general case is essentially the same. For variables that are treated quantum mechanically by probability distributions, one determines the final probabilities for a number of values of the variable and averages them with the weights dependent on the probability distribution.

# CHAPTER 4
# THE ELECTRONIC PROBLEM FOR $H_3^+$ IN THE ADIABATIC REPRESENTATION

## 4-1 General Considerations

As has by now become apparent, the potential energy surfaces play a crucial role in the formalism that has been developed. It was pointed out in chapter two that it is convenient to solve the electronic problem in the adiabatic representation because there exists a number of theoretically sound procedures for solving the problem in this representation. These procedures can in general be divided into three categories based on whether they are ab initio, semi-empirical or empirical in nature. The ab initio approach is of course a first principles procedure while the other two make use of experimental information.

Naturally, an ab initio approach would be theoretically more appealing. There are however two main limitations that must be considered. The first has to do with the number of electrons. Roughly the time for a calculation increases as the fourth power of the number of atomic basis functions. Thus the cost could become prohibitive for systems with many electrons. The second limitation comes from the number of nuclear configurations that are needed to obtain a reasonable potential energy surface. If ten configurations were necessary for the case of a diatomic molecule, the surface for a triatomic system would require in the neighborhood of a thousand nuclear configurations. Even if the electronic calculation were to only take ten seconds per configuration, the surface would still require nearly three hours of calculation time. These limitations are inherent in the ab initio approach and from the second limitation alone it is unlikely that this approach would be feasible for obtaining the surfaces.

At the other extreme of the spectrum lie empirical approaches to the problem. These approaches are based on using arbitrary functions to construct a potential energy surface. The function's parameters are adjusted until the surface passes through either experimentally known or theoretically calculated points. Even though these approaches bypass the need to do a quantum mechanical calculation, quite a bit of guesswork is involved. If these approaches were used on systems that didn't contain a wealth of experimental or theoretical information there would exist a significant risk of obtaining unreliable results.

The final class of approaches to be considered here are the semi-empirical ones. These approaches have the advantage of starting with the time independent Schrödinger equation. This can not only lead to a better understanding of the approximations used but also offer some insight into its limitations. The number of semi-empirical approaches is staggering and in a way reflects the great diversity of physical systems being studied.

As is well known, most of the effort in an electronic calculation is spent in evaluating the two center electron integrals. The common trait of semi-empirical approaches is that they either simplify or reduce the number of those integrals. A well known approach that simplifies the exchange integral is the Xα method (Slater, 1971). There are a number of other methods such as CNDO that simplify the problem by reducing the number of electron integrals.

One of the possible difficulties that arise in using most semi-empirical methods is that they usually employ only one electronic configuration, i.e. a single antisymmetrized product of molecular orbitals. This may give a good description of the surface for some regions of the internuclear coordinates but usually does not adequately describe the entire surface, which is necessary for the scattering calculation. Although there are semi-empirical methods that employ configuration interactions, the number of internuclear configurations needed to determine the surface would more than likely make using these procedures too costly.

The method that will be employed here is called Diatomics in Molecules. It was introduced by Ellison (Ellison, 1963) and later generalized to include directional bonding (Kuntz and Roach, 1972; Tully, 1973). It has fairly recently been used to construct a number of potential surfaces for triatomic systems. Two of the many examples are the surfaces for $LiH_2$ and $FH_2$ (Tully, 1973a).

This method utilizes the fact that the electronic Hamiltonian can be written in terms of atomic and diatomic Hamiltonians. This leads, as will be seen in the next section, to a solution which is expressed in terms of an overlap matrix and atomic and diatomic energies. The ground and excited energy levels of the diatomics are obtained through either experiment or theory. Whether or not the electronic problem can be solved with this approach depends on the availability of the diatomic energy levels.

Another advantage of this method comes from the form of the electronic basis functions. Since the basis functions are expressed as an antisymmetrized product of atomic orbitals, a little manipulation of the antisymmetrizer leads to a valence bond description of the electronic problem. Thus, this method has built into it the correct electronic description of the reactants and products.

In the following section the formalism for Diatomics in Molecules will be briefly developed. This formalism will be applied to the $H_3^+$ system and the eigenvalues and eigenfunctions will be the topic of Sections 4-3 and 4-4 respectively. Section 4-5 will focus on the non-adiabatic couplings which are a convenient by-product of this method.

## 4-2 Method of Diatomics in Molecules

The goal of Diatomics in Molecules (DIM) is to make use of the energies of the diatomics that comprise the polyatomic to construct the polyatomic energies. If the diatomic energies are all known experimentally, this procedure eliminates the necessity of doing an electronic calculation except perhaps for overlaps. In most applications the internuclear dependence of the overlaps is neglected so that the electronic calculation is avoided altogether and the electronic problem is solved with only a knowledge of the diatomic energies.

Since there are already a number of detailed treatments of this subject available in the literature (Ellison, 1963; Tully, 1973b), only a brief outline of the method will be presented here. This will hopefully have the advantage of displaying the main conclusions without resorting to the rather cumbersome formalism that is inherent in more detailed treatments. The development presented here will somewhat follow the one given by Tully (Tully, 1980).

The basis functions in this procedure are chosen to be antisymmetrized products of atomic functions. For a system composed of n electons and N nuclei where at least three nuclei are assumed to be present, the basis functions can be written as

$$\phi_m(1,\cdots,n) = \hat{A}_n\phi_m(1,\cdots,n) \qquad (4\text{-}1)$$

where $\hat{A}_n$ is the n electron antisymmetrizer and the $\phi_m$ are defined as (Moffitt, 1951)

$$\phi_m(1,\cdots,n) = \eta_m^{(A)}(1,\cdots,n_A)\,\eta_m^{(B)}(n_A + 1,\cdots,n_A + n_B)$$

$$\cdots\eta_m^{(N)}(n - n_N + 1,\cdots,n) \qquad (4\text{-}2)$$

where the atomic functions $\eta$ are assumed to be antisymmetric. The notation has been somewhat changed here in order to emphasize the importance of assigning electrons to particular nuclei. The bracket will still be used to indicate integration over the relevant electronic coordinates. Expanding the total wave function in terms of the basis of Eq. (4-1) gives

$$\Psi_\ell(1,\cdots,n) = \sum_m \phi_m(1,\cdots,n)\,\Gamma_{m\ell} \qquad (4\text{-}3)$$

where $\Gamma_{\ell m}$ are the expansion coefficients. Using Eq. (4-3) in the time independent Schrödinger equation leads to

$$\underset{\sim}{H}\underset{\sim}{\Gamma} = \underset{\sim}{S}\underset{\sim}{\Gamma}\underset{\sim}{E} \qquad (4\text{-}4)$$

where the adiabatic energies are given by the diagonal matrix $\underset{\sim}{E}$,

$$H_{mm'} = \langle\phi_m|\hat{A}_n\hat{H}|\phi_{m'}\rangle \qquad (4\text{-}5)$$

and

$$S_{mm'} = \langle\phi_m|\phi_{m'}\rangle \quad . \qquad (4\text{-}6)$$

Equation (4-5) was obtained by using the property that the antisymmetrizer commutes with the Hamiltonian.

The next step in this procedure is to partition the Hamiltonian into components that are atomic and diatomic in nature. This can be accomplished by writing (Ellison, 1963)

$$\hat{H} = \sum_{K=1}^{N} \sum_{L>K}^{N} \hat{H}^{(KL)} - (N-2) \sum_{K=1}^{N} \hat{H}^{(K)} \qquad (4\text{-}7)$$

where $\hat{H}^{(KL)}$ is the Hamiltonian for the isolated diatomic which is comprised of the nuclei K and L and the electrons assigned to those nuclei. A similar definition holds for $\hat{H}^{(K)}$. In the electronic basis defined by Eq. (4-1), the operator $\hat{H}$ has the following matrix representation

$$\underline{\underline{H}} = \sum_{K=1}^{N} \sum_{L>K}^{N} \underline{\underline{H}}^{(KL)} - (N-2) \sum_{K=1}^{N} \underline{\underline{H}}^{(K)} \qquad (4\text{-}8)$$

where

$$H_{mm'}^{(K)} = \langle \phi_m | \hat{A}_n \hat{H}^{(K)} | \phi_{m'} \rangle \qquad (4\text{-}9)$$

and

$$H_{mm'}^{(KL)} = \langle \phi_m | \hat{A}_n \hat{H}^{(KL)} | \phi_{m'} \rangle \quad . \qquad (4\text{-}10)$$

Since the total antisymmetrizer does not commute with the fragment Hamiltonians, $\hat{H}^{(KL)}$ and $\hat{H}^{(K)}$, Eq. (4-8) is not term by term Hermitian. The sum will however remain Hermitian if a complete set of electronic states are used.

Equation (4-8) is of utmost importance in this theory. One sees from Eqs. (4-9) and (4-10) that the total Hamiltonian is now expressed in terms of fragment Hamiltonians whose operators correspond to isolated atomic and diatomic systems. The solution to the problem will consist of making transformations of the electronic basis given by Eq. (4-1) to bases that diagonalize the fragment Hamiltonians, i.e. whose eigenvalues correspond to the experimental or theoretical energies.

In order to show how these transformations are done, a brief development for the operator $\hat{H}^{(K)}$ is presented here. For clarity, the basis functions are written in the form

$$\phi_m^{(K)} = \phi_n^{(\overline{K})} \eta_m^{(K)} \qquad (4\text{-}11)$$

where $\phi_m^{(\overline{K})}$ is the product of all atomic functions not centered on atom K and $\eta_m^{(K)}$ is the atomic function centered on atom K. Of course, the electrons are still assigned according to Eq. (4-1). Assuming that the electronic basis is complete, one has

$$\hat{H}^{(K)} \phi_m^{(K)} = \sum_{\ell} \phi_{\ell}^{(\overline{K})} \eta_{\ell}^{(K)} \Delta_{\ell m}^{(K)} \qquad (4\text{-}12)$$

where the $\Delta^{(K)}_{\ell m}$ are the expansion coefficients. Substituting Eq. (4-12) into Eq. (4-9) gives

$$\underset{\approx}{H}^{(K)} = \underset{\approx}{S}\underset{\approx}{\Delta}^{(K)} \tag{4-13}$$

where the elements of $\underset{\approx}{S}$ were defined in Eq. (4-5). The important thing to recognize in Eq. (4-13) is that the matrix $\underset{\approx}{\Delta}^{(K)}$ depends only on the atom K. Then it should be possible to relate $\underset{\approx}{\Delta}^{(K)}$ to the eigenvalue problem of $\hat{H}^{(K)}$ for isolated atom K by means of a transformation. Since the atomic basis is assumed to be complete and $\hat{H}^{(K)}$ operates only on atom K one also has that

$$\hat{H}^{(K)}\eta^{(K)}_{m} = \sum_{\ell} \eta^{(K)}_{\ell}\Delta^{(K)}_{\ell m} \tag{4-14}$$

Defining

$$h^{(K)}_{mm'} = \langle\eta^{(K)}_{m}|\hat{H}^{(K)}|\eta^{(K)}_{m'}\rangle \tag{4-15}$$

and

$$\sigma^{(K)}_{mm'} = \langle\eta^{(K)}_{m}|\eta^{(K)}_{m'}\rangle \tag{4-16}$$

one obtains the matrix equation

$$\underset{\approx}{h}^{(K)} = \underset{\approx}{\sigma}^{(K)}\underset{\approx}{\Delta}^{(K)} \quad . \tag{4-17}$$

Considering the eigenvalue problem for isolated atom K, one has in matrix notation

$$\hat{H}^{(K)}\underline{\underline{\chi}}^{(K)} = \underline{\underline{\chi}}^{(K)}\underline{\underline{\varepsilon}}^{(K)} \tag{4-18}$$

where $\underline{\underline{\chi}}^{(K)}$ and $\underline{\underline{\varepsilon}}^{(K)}$ are the matrices of eigenvectors and eigenvalues respectively and $\underline{\chi}^{(K)}$ is a row matrix. The two basis can be related by means of a transformation so that

$$\underline{\underline{\chi}}^{(K)} = \underline{\underline{\eta}}^{(K)}\underline{\underline{\gamma}}^{(K)} \tag{4-19}$$

where $\underline{\underline{\eta}}^{(K)}$ is also a row matrix. Multiplying Eq. (4-18) from the left by $\underline{\underline{\eta}}^{(K)\dagger}$, integrating over electronic variables and using Eq. (4-19) gives

$$\underline{\underline{h}}^{(K)}\underline{\underline{\gamma}}^{(K)} = \underline{\underline{\sigma}}^{(K)}\underline{\underline{\gamma}}^{(K)}\underline{\underline{\varepsilon}}^{(K)} \quad . \tag{4-20}$$

Since

$$\underline{\underline{\gamma}}^{(K)}\underline{\underline{\gamma}}^{(K)\dagger} = \underline{\underline{\sigma}}^{-1} \tag{4-21}$$

Eq. (4-20) becomes

$$\underline{\underline{h}}^{(K)} = \underline{\underline{\sigma}}^{(K)}\underline{\underline{\gamma}}^{(K)}\underline{\underline{\varepsilon}}^{(K)}\underline{\underline{\gamma}}^{(K)\dagger}\underline{\underline{\sigma}}^{(K)} \tag{4-22}$$

so that on comparing Eqs. (4-17) and (4-22) one finds that

$$\underset{\sim}{\Delta}^{(K)} = \underset{\sim}{\gamma}^{(K)} \underset{\sim}{\varepsilon}^{(K)} \underset{\sim}{\gamma}^{(K)\dagger} \underset{\sim}{S}^{(K)} \qquad (4\text{-}23)$$

In an analogous fashion one arrives at

$$\underset{\sim}{H}^{(KL)} = \underset{\sim}{S}\underset{\sim}{\Delta}^{(KL)} \qquad (4\text{-}24)$$

where

$$\underset{\sim}{\Delta}^{(KL)} = \underset{\sim}{\gamma}^{(KL)} \underset{\sim}{\varepsilon}^{(KL)} \underset{\sim}{\gamma}^{(KL)\dagger} \underset{\sim}{S}^{(KL)} \quad . \qquad (4\text{-}25)$$

Using Eqs. (4-13) and (4-24) in Eqs. (4-7) and (4-4) results in

$$\underset{\sim}{\Delta}\underset{\sim}{\Gamma} = \underset{\sim}{\Gamma}\underset{\sim}{E} \qquad (4\text{-}26)$$

where

$$\underset{\sim}{\Delta} = \underset{\sim}{S}^{-1}\underset{\sim}{H} = \sum_{K=1}^{N} \sum_{L>K}^{N} \underset{\sim}{\Delta}^{(KL)} - (N - 2) \sum_{K=1}^{N} \underset{\sim}{\Delta}^{(K)} \quad . \qquad (4\text{-}27)$$

The important results of this formalism are given by Eqs. (4-26) and (4-27). The adiabatic energies are found in part by solving the eigenvalue problem for the atoms and diatomics that make up the molecule. If the eigenvalues and eigenvectors for the fragments are known, the only electronic calculations that may have to be done are the overlap integrals.

## 4-3 The Eigenvalues

This section shall develop the DIM procedure to the $H_3^+$ molecular ion. Since the results are already available in the literature (Ellison, Huff and Patel, 1963) many of the details will be omitted. The approach to be used for this system will be more physical in nature that the general outline presented in the previous section. This will hopefully clarify some of the correlations between the DIM and valence bond procedures.

The $H_3^+$ system consists of three protons which will be labeled A, B and C and two electrons. An electronic function centered on nucleus A with an alpha spin will be designated as "a" and for beta spin "$\bar{a}$". Electronic functions centered on nuclei B and C are designated as $b(\bar{b})$ and $c(\bar{c})$ respectively. Instead of using a simple product of atomic orbitals for the electronic basis it is more convenient to use canonical valence bond structures. There are three such structures for $H_3^+$ and they are given by

$$\Phi_1 = |a\bar{b}| - |\bar{a}b| \quad , \tag{4-28}$$

$$\Phi_2 = |b\bar{c}| - |\bar{b}c| \tag{4-29}$$

and

$$\Phi_3 = |a\bar{c}| - |\bar{a}c| \tag{4-30}$$

where $\Phi_1$, $\Phi_2$ and $\Phi_3$ represent bonds between AB, BC, and AC respectively and $|---|$ represents a determinant. Since the electrons are assigned differently for each structure, the Hamiltonian will have a different form for each structure. The structures $\Phi_1$, $\Phi_2$ and $\Phi_3$ correspond to the Hamiltonians

$$\hat{H} = \hat{H}_{AB} + \hat{H}_{bc} + \hat{H}_{ac} - \hat{H}_{A} - \hat{H}_{B} \quad , \tag{4-31}$$

$$\hat{H} = \hat{H}_{BC} + \hat{H}_{ab} + \hat{H}_{ac} - \hat{H}_{B} - \hat{H}_{C} \tag{4-32}$$

and

$$\hat{H} = \hat{H}_{AC} + \hat{H}_{ab} + \hat{H}_{bc} - \hat{H}_{A} - \hat{H}_{C} \tag{4-33}$$

where AB, BC and AC refer to hydrogen molecules, A, B and C to hydrogen atoms and ab, bc and ac to hydrogen molecular ions. One notices from Eqs. (4-31) through (4-33) and from the discussion in the previous section that one needs valence bond functions that are eigenfunctions of the fragment Hamiltonians. For the isolated diatomic AB one has

$$\phi_1^{AB} = |a\bar{b}| - |\bar{a}b| \quad , \tag{4-34}$$

$$\phi_1^{ab} = (a + b) \quad , \tag{4-35}$$

$$\phi_2^{ab} = (\bar{a} + \bar{b}) \quad , \tag{4-36}$$

$$\phi_3^{ab} = (a - b) \quad , \tag{4-37}$$

$$\phi_4^{ab} = (\bar{a} - \bar{b}) \tag{4-38}$$

where the notation for the Hamiltonian also applies here. The first function, Eq. (4-34), corresponds to the $H_2$ bond and one has that

$$\hat{H}_{AB}\phi_1^{AB} = E_1^{AB}\phi_1^{AB} \tag{4-39}$$

where $E_1^{AB}$ is the ground state energy, ${}^1\Sigma_g^+$, for $H_2$ which depends on the distance between nuclei A and B. The functions defined by Eqs. (4-35) and (4-36) correspond to a $H_2^+$ bond and one has

$$\hat{H}_{ab}\phi_i^{ab} = E_1^{ab}\phi_i^{ab} \tag{4-40}$$

where i is either 1 or 2 and $E_1^{ab}$ is the ground state energy, ${}^2\Sigma_g^+$, of $H_2^+$ which is of course dependent on the distance between nuclei A and B. The final two functions given by Eqs. (4-37) and (4-38) correspond to the first excited state of $H_2^+$ so that

$$\hat{H}_{ab}\phi_i^{ab} = E_3^{ab}\phi_i^{ab} \tag{4-41}$$

where i is either 3 or 4 and $E_3^{ab}$ corresponds to the first excited state, ${}^2\Sigma_u^+$, of $H_2^+$ as a function of the distance between A and B. One notices that Eqs. (4-35) through (4-38) furnish a means of expressing the atomic orbitals in terms of the valance bond functions. For example, from Eqs. (4-35) and (4-37) one has that

$$a = (\phi_1^{ab} + \phi_2^{ab})/2 \qquad (4-42)$$

Similar results are obtained for the isolated diatomics BC and AC. As an example of how to construct matrix elements consider

$$\hat{A}_2\hat{H}_{ac}\phi_1 = \hat{A}_2\hat{H}_{ac}(a\bar{b}-\bar{a}b) \quad . \qquad (4-43)$$

From an analogous procedure that led to Eq. (4-42) one obtains

$$\begin{aligned} \hat{A}_2\hat{H}_{ac}\phi_1 &= \hat{A}_2\hat{H}_{ac}[(\phi_1^{ac} + \phi_3^{ac})\bar{b} - (\phi_2^{ac} + \phi_4^{ac})b]/2 = \\ &\hat{A}_2[(E_1^{ac}\phi_1^{ac} + E_3^{ac}\phi_3^{ac})\bar{b} - (E_1^{ac}\phi_2^{ac} + E_3^{ac}\phi_4^{ac})b]/2 \quad . \end{aligned} \qquad (4-44)$$

Re-expressing the valance bond states in terms of atomic orbitals, rearranging the terms and carrying through the antisymmetrization operation results in

$$\hat{A}_2\hat{H}_{ac}\phi_1 = (E_1^{ac}(\phi_1 + \phi_2) + E_3^{ac}(\phi_1 - \phi_2))/2 \quad . \qquad (4-45)$$

Carrying through the algebra for the other cases results in

$$\hat{A}_2\hat{H}_{bc}\phi_1 = [E_1^{bc}(\phi_1 + \phi_3) + E_3^{bc}(\phi_1 - \phi_3)]/2 \quad , \qquad (4-46)$$

$$\hat{A}_2\hat{H}_{ac}\phi_2 = [E_1^{ac}(\phi_1 + \phi_2) + E_3^{ac}(\phi_2 - \phi_1)]/2 \quad , \qquad (4-47)$$

$$\hat{A}_2\hat{H}_{ab}\phi_2 = [E_1^{ab}(\phi_2 + \phi_3) + E_3^{ab}(\phi_2 - \phi_3)]/2 \quad , \qquad (4-48)$$

$$\hat{A}_3\hat{H}_{bc}\phi_3 = [E_1^{bc}(\phi_1 + \phi_3) + E_3^{bc}(\phi_3 - \phi_1)]/2 \quad , \qquad (4-49)$$

$$\hat{A}_2\hat{H}_{ab}\phi_3 = [E_1^{ab}(\phi_2 + \phi_3) + E_3^{ab}(\phi_3 - \phi_2)]/2 \quad , \qquad (4-50)$$

$$\hat{A}_2\hat{H}_{AB}\phi_1 = E_1^{AB}\phi_1 \quad , \qquad (4-51)$$

$$\hat{A}_2\hat{H}_{BC}\phi_2 = E_1^{BC}\phi_2 \quad , \qquad (4-52)$$

and

$$\hat{A}_2\hat{H}_{AC}\phi_3 = E_1^{AC}\phi_3 \quad . \qquad (4-53)$$

Combining Eqs. (4-45) through (4-53) with Eqs. (4-31) through (4-33) results in the matrix elements of the Hamiltonian being defined by

$$\begin{aligned} <\phi_1|\hat{H}|\phi_1> = [(2E_1^{AB} + E_1^{ac} + E_3^{ac} + E_1^{bc} + E_3^{bc} - 4E_H)S_{11} \\ + (E_1^{ac} - E_3^{ac})S_{12} + (E_1^{bc} - E_3^{bc})S_{13}]/2 \quad , \end{aligned} \qquad (4-54)$$

$$<\phi_1|\hat{H}|\phi_2> = [(E_1^{ac} - E_2^{ac})S_{11} + (2E_1^{BC} + E_1^{ac} + E_2^{ac} + E_1^{ab}$$

$$+ E_2^{ab} - 4E_H)S_{12} + (E_1^{ab} - E_2^{ab})S_{11}]/2 \quad , \qquad (4\text{-}55)$$

$$<\phi_1|\hat{H}|\phi_1> = [(E_1^{bc} - E_2^{bc})S_{11} + (E_1^{ab} - E_2^{ab})S_{12}$$

$$+ (2E_1^{AC} + E_1^{bc} + E_2^{bc} + E_1^{ab} + E_2^{ab} - 4E_H)S_{11}]/2 \quad , \qquad (4\text{-}56)$$

$$<\phi_2|\hat{H}|\phi_1> = [(2E_1^{AB} + E_1^{ac} + E_2^{ac} + E_1^{bc} + E_2^{bc} - 4E_H)S_{21}$$

$$+ (E_1^{ac} - E_2^{ac})S_{22} + (E_1^{bc} - E_2^{bc})S_{11}]/2 \quad , \qquad (4\text{-}57)$$

$$<\phi_2|\hat{H}|\phi_2> = [(E_1^{ac} - E_2^{ac})S_{21} + (2E_1^{BC} + E_1^{ac} + E_2^{ac} + E_1^{ab}$$

$$+ E_2^{ab} - 4E_H)S_{22} + (E_1^{ab} - E_2^{ab})S_{21}]/2 \quad , \qquad (4\text{-}58)$$

$$<\phi_2|\hat{H}|\phi_2> = [(E_1^{bc} - E_2^{bc})S_{21} + (E_1^{ab} - E_2^{ab})S_{22}$$

$$+ (2E_1^{AC} + E_1^{bc} + E_2^{bc} + E_1^{ab} + E_2^{ab} - 4E_H)S_{21}]/2 \quad , \qquad (4\text{-}59)$$

$$<\phi_1|\hat{H}|\phi_1> = [(2E_1^{AB} + E_1^{ac} + E_2^{ac} + E_1^{bc} + E_2^{bc} - 4E_H)S_{11}$$

$$+ (E_1^{ac} - E_2^{ac})S_{12} + (E_1^{bc} - E_2^{bc})S_{11}]/2 \quad , \qquad (4\text{-}60)$$

$$<\phi_1|\hat{H}|\phi_2> = [(E_1^{ac} - E_2^{ac})S_{11} + (2E_1^{BC} + E_1^{ac} + E_2^{ac}$$

$$+ E_1^{ab} + E_2^{ab} - 4E_H)S_{12} + (E_1^{ab} - E_2^{ab})S_{11}]/2 \qquad (4\text{-}61)$$

and

$$\langle\phi_1|\hat{H}|\phi_3\rangle = [(E_1^{bc} - E_3^{bc})S_{31} + (E_1^{ab} - E_1^{ab})S_{12}$$

$$+ (2E_1^{AC} + E_1^{bc} + E_3^{bc} + E_1^{ab} + E_3^{ab} - 4E_H)S_{32}]/2 \qquad (4\text{-}62)$$

where

$$S_{ij} = \langle\phi_i|\phi_j\rangle \qquad (4\text{-}63)$$

One notices at this point that the main objective of DIM has been obtained, i.e. the Hamiltonian is expressed in terms of isolated fragment energies and overlaps. The overlaps are easily found to be given by

$$S_{11} = 2(1 + \langle a|b\rangle^2) \quad , \qquad (4\text{-}64)$$

$$S_{22} = 2(1 + \langle b|c\rangle^2) \quad , \qquad (4\text{-}65)$$

$$S_{33} = 2(1 + \langle a|c\rangle^2) \quad , \qquad (4\text{-}66)$$

$$S_{12} = S_{21} = 2(\langle a|c\rangle + \langle a|b\rangle\langle b|c\rangle) \quad , \qquad (4\text{-}67)$$

$$S_{23} = S_{32} = 2(\langle b|c\rangle + \langle a|c\rangle\langle a|b\rangle) \quad , \qquad (4\text{-}68)$$

and

$$S_{13} = S_{31} = 2(\langle a|b\rangle + \langle a|c\rangle\langle b|c\rangle) \qquad (4\text{-}69)$$

Most applications of DIM have assumed that atomic functions centered on different nuclei are orthogonal. This will also be assumed here so that the elements for the overlap matrix are given by

$$S_{ij} = 2\delta_{ij} \qquad . \qquad (4\text{-}70)$$

With the overlap defined by Eq. (4-70), the matrix elements of the Hamiltonian considerably simplify and one obtains

$$H_{11} = 2E_1^{AB} + E_1^{ac} + E_3^{ac} + E_1^{bc} + E_3^{bc} - 4E_H \quad , \qquad (4\text{-}71)$$

$$H_{12} = H_{21} = E_1^{ac} - E_3^{ac} \qquad , \qquad (4\text{-}72)$$

$$H_{22} = 2E_1^{aC} + E_1^{ac} + E_3^{ac} + E_1^{ab} + E_3^{ab} - 4E_H \qquad (4\text{-}73)$$

$$H_{23} = H_{32} = E_1^{ab} - E_3^{ab} \qquad , \qquad (4\text{-}74)$$

$$H_{13} = H_{31} = E_1^{bc} - E_3^{bc} \qquad , \qquad (4\text{-}75)$$

and

$$H_{33} = 2E_1^{AC} + E_1^{bc} + E_3^{bc} + E_1^{ab} + E_3^{ab} - 4E_H \qquad (4\text{-}76)$$

where

$$H_{ij} = \langle \phi_i | \hat{H} | \phi_j \rangle \qquad . \qquad (4\text{-}77)$$

One should mention that the Hamiltonian with matrix elements defined by Eqs. (4-54) through (4-62) is not Hermitian. However with the overlap defined by Eq. (4-70) the resulting Hamiltonian becomes Hermitian. In other words, the assumption for the overlap eliminates the non-Hermitian terms in the Hamiltonian.

Expressing the eigenfunctions of the total Hamiltonian as linear combinations of the canonical valence bond function i.e.

$$\Psi_i = \sum_j \Phi_j \Gamma_{ji} \tag{4-78}$$

one obtains in accordance with Eq. (4-4) the following matrix equation

$$\underline{\underline{H}}\,\underline{\underline{\Gamma}} = \underline{\underline{S}}\,\underline{\underline{\Gamma}}\,\underline{\underline{E}} \tag{4-79}$$

where the elements of the diagonal matrix $\underline{\underline{E}}$ correspond to the adiabatic eigenvalues and the matrix elements of $\underline{\underline{H}}$ were defined in Eq. (4-77). As is well known, the eigenvalues are found by solving

$$|(\underline{\underline{H}} - E\underline{\underline{S}})| = 0 \tag{4-80}$$

where again |---| indicates a determinant. From Eq. (4-80) it is straightforward to show that the eigenvalues are given by

$$-8E^3 + 4(H_{11} + H_{22} + H_{33})E^2 + 2(H_{12}^2 + H_{23}^2 + H_{13}^2$$

$$- H_{22}H_{33} - H_{11}H_{22} - H_{11}H_{33})E + H_{11}H_{22}H_{33} + 2H_{12}H_{23}H_{13}$$

$$- H_{11}H_{23}^2 - H_{12}^2H_{33} - H_{13}^2H_{22} = 0 \qquad (4-81)$$

which is a third order polynomial whose roots furnish the three adiabatic energies. It is a straightforward exercise to determine these roots analytically (Selby, 1964). The lowest two roots correspond to the two lowest surfaces for $H_3^+$ while the other root corresponds to an excited surface. This excited surface is energetically inaccessible and does not couple to the lower surfaces. Because of this, the excited surface will not be considered so that the problem involves only two surfaces.

4-4 The Eigenfunctions

Even though the adiabatic energies were found without determining the eigenvectors, these eigenvectors are necessary to form other quantities such as non-adiabatic couplings. As was mentioned in the previous section the upper excited surface does not couple to the two lower surfaces so that one has in essence a two-surface system.

In the following, the eigenvalue and eigenvector of the lowest surface will be designated as $E_1$ and $\Psi_1$ respectively. This is the surface that asymptotically corresponds to $H_2$. The other surface which asymptotically correlates to $H_2^+$ will have its eigenvalue and eigenvector designated as

$E_2$ and $\Psi_2$ respectively. Since $\Psi_1$ and $\Psi_2$ are linear combinations of the three canonical valence bond functions, there are a total of six coefficients to be determined. From Eq. (4-79) one has that

$$(H_{11} - 2E_1)\Gamma_{11} + H_{12}\Gamma_{21} + H_{13}\Gamma_{31} = 0 \quad , \qquad (4\text{-}82)$$

$$H_{21}\Gamma_{11} + (H_{22} - 2E_1)\Gamma_{21} + H_{23}\Gamma_{31} = 0 \quad , \qquad (4\text{-}83)$$

and

$$H_{31}\Gamma_{11} + H_{32}\Gamma_{21} + (H_{33} - 2E_1)\Gamma_{31} = 0 \quad . \qquad (4\text{-}84)$$

Defining

$$H_1 = H_{12}^2 - (H_{22} - 2E_1)(H_{11} - 2E_1) \quad , \qquad (4\text{-}85)$$

$$G_1 = H_{13}(H_{22} - 2E_1) - H_{12}H_{23} \quad , \qquad (4\text{-}86)$$

and

$$F_1 = H_{23}(H_{11} - 2E_1) - H_{12}H_{13} \qquad (4\text{-}87)$$

it is not difficult to show that

$$\Gamma_{31} = \frac{H_1}{G_1}\Gamma_{11} \qquad (4\text{-}88)$$

and

$$\Gamma_{21} = \frac{F_1}{G_1}\,\Gamma_{11} \quad . \tag{4-89}$$

The value of $\Gamma_{11}$ is found by requiring $\Psi_1$ to be normalized. Doing this results in

$$\Gamma_{11} = \frac{G_1}{\sqrt{2}}(H_1{}^2 + G_1{}^2 + F_1{}^2)^{-\frac{1}{2}} \tag{4-90}$$

The coefficients of $\Psi_2$ are determined by solving

$$(H_{11} - 2E_2)\Gamma_{12} + H_{12}\Gamma_{22} + H_{13}\Gamma_{32} = 0 \quad , \tag{4-91}$$

$$H_{12}\Gamma_{12} + (H_{22} - 2E_2)\Gamma_{22} + H_{23}\Gamma_{32} = 0 \quad , \tag{4-92}$$

and

$$\Gamma_{11}\Gamma_{12} + \Gamma_{21}\Gamma_{22} + \Gamma_{31}\Gamma_{32} = 0 \tag{4-93}$$

where Eq. (4-93) insures that the eigenfunctions are orthogonal. Defining

$$a_2 = \frac{\Gamma_{21}H_{12} - \Gamma_{11}(H_{22} - 2E_2)}{\Gamma_{31}(H_{22} - 2E_2) - \Gamma_{21}H_{23}} \tag{4-94}$$

and

$$G_2 = \frac{\Gamma_{21}H_{12} - \Gamma_{11}H_{22}}{\Gamma_{11}(H_{22} - 2E_2) - \Gamma_{21}H_{12}} \qquad (4\text{-}95)$$

one finds that

$$\Gamma_{12} = B_1\Gamma_{12} \qquad (4\text{-}96)$$

and

$$\Gamma_{22} = B_2G_2\Gamma_{12} \quad . \qquad (4\text{-}97)$$

The value of $\Gamma_{12}$ is obtained from the normalization of $\Psi_2$ and one finds that

$$\Gamma_{12} = \frac{1}{\sqrt{2}} \left(1 + B_2^2 \left(1 + G_2^2\right)\right)^{-\frac{1}{2}} \quad . \qquad (4\text{-}98)$$

One notices that the dependence of these coefficients on nuclear distance is contained solely in the adiabatic eigenvalues. Since these are given analytically by Eq. (4-81) these eigenvalues are also analytical functions of the internuclear variables. As will be seen in the next section, this will considerably simplify the problem of determining the non-adiabatic couplings.

## 4-5 Non-adiabatic Couplings

As was mentioned previously, one of the advantages of using DIM is that it is relatively easy to obtain the non-adiabatic couplings. Since eigenfunctions obtained from an ab initio or other semi-empirical approach are not analytic functions of the nuclear variables, at least two complete calculations would have to be done to obtain the coupling of one configuration of the nuclei. In DIM, however, the eigenfunctions depend analytically on the nuclear variables so that the couplings are readily obtained functions of the internuclear variables.

To simplify matters, the momentum operator will be assumed to have the form of Eq. (2-4). Furthermore, only one component of $\underset{\sim}{\hat{P}}_{\nu}$ will be considered which will be designated as $\frac{\partial}{\partial X}$ . Since from Eq. (2-19) the couplings from $\partial^2/\partial X^2$ can be expressed in terms of the couplings from $\partial/\partial X$, this section shall only treat the couplings that come from $\frac{\partial}{\partial X}$ . The matrix elements of interest are given by

$$\langle \Psi_i | \frac{\partial}{\partial X} | \Psi_j \rangle \tag{4-99}$$

where $\Psi_i$ was defined in Eq. (4-78). One can easily show by taking the partial derivative of $\langle \Psi_i | \Psi_j \rangle$ with respect to X that the matrix of these couplings is antisymmetric with diagonal elements equal to zero.

Two methods for obtaining the couplings given in Eq. (4-99) will be presented here. The first method will obtain the couplings directly from the expansion coefficients which depend analytically on X. The second method will employ partial derivatives of the Hamiltonian matrix with respect to X and it will be seen that this may have some advantages.

In general, the coupling matrix whose elements are defined by Eq. (4-99) is given by

$$\langle \underset{\sim}{\Psi} | \frac{\partial}{\partial X} | \underset{\sim}{\Psi} \rangle = \begin{pmatrix} 0 & \langle \Psi_1 | \frac{\partial}{\partial X} | \Psi_2 \rangle \\ -\langle \Psi_1 | \frac{\partial}{\partial X} | \Psi_2 \rangle & 0 \end{pmatrix} \qquad (4\text{-}100)$$

where its antisymmetric property has been used. From Eq. (4-78) and with the overlap given by Eq. (4-70) one finds that

$$\langle \Psi_1 | \frac{\partial}{\partial X} | \Psi_2 \rangle = 2(\Gamma_{11}\frac{\partial}{\partial X}\Gamma_{12} + \Gamma_{21}\frac{\partial}{\partial X}\Gamma_{22} + \Gamma_{31}\frac{\partial}{\partial X}\Gamma_{32}) \quad . \qquad (4\text{-}101)$$

This may at first glance seem to be a rather simple expression. However one notices from the equations for the expansion coefficients given in the previous section that they are fairly complicated expressions in terms of the matrix elements of the Hamiltonian and eigenvalues. Analytical expressions for the partial derivatives of these coefficients may be very complicated so that numerical procedures may be more appropriate for calculating Eq. (4-101).

The other method starts from the time independent Schrödinger equation. Taking the partial derivative with respect to X of this equation results in

$$\left(\frac{\partial \hat{H}}{\partial X}\right)\Psi_2 + \hat{H}\frac{\partial}{\partial X}\Psi_2 = \left(\frac{\partial}{\partial X}E_2\right)\Psi_2 + E_2\frac{\partial}{\partial X}\Psi_2 \quad . \qquad (4\text{-}102)$$

Multiplying from the left by $\Psi_1$ and integrating over electronic coordinates results in

$$<\Psi_1|\frac{\partial}{\partial X}|\Psi_2> = \frac{<\Psi_1|(\frac{\partial}{\partial X}\hat{H})|\Psi_2>}{E_2 - E_1} \qquad (4\text{-}103)$$

where the Hermitian property of $\hat{H}$ has been used. Using Eq. (4-78) in Eq. (4-103) results in

$$<\Psi_1|\frac{\partial}{\partial X}|\Psi_2> = \{\Gamma_{11}(\Gamma_{12}\frac{\partial}{\partial X}H_{11} + \Gamma_{22}\frac{\partial}{\partial X}H_{12} + \Gamma_{32}\frac{\partial}{\partial X}H_{13})$$

$$+ \Gamma_{21}(\Gamma_{12}\frac{\partial}{\partial X}H_{21} + \Gamma_{22}\frac{\partial}{\partial X}H_{22} + \Gamma_{32}\frac{\partial}{\partial X}H_{23})$$

$$+ \Gamma_{31}(\Gamma_{12}\frac{\partial}{\partial X}H_{31} + \Gamma_{22}\frac{\partial}{\partial X}H_{32} + \Gamma_{32}\frac{\partial}{\partial X}H_{33})\}(E_2 - E_1)^{-1}.$$

$$(4\text{-}104)$$

Equation (4-104) may seem to be more complicated than Eq (4-101) but one notices that the matrix elements of the Hamiltonian are linear functions of the fragment energies. If these energies are given by rather simple expressions, Eq. (4-104) may be determined analytically. This could bypass the use of numerical methods to determine the couplings or could provide a means to check their accuracy.

All the essential ingredients from the electronic problem to do a scattering calculation have now been obtained. The adiabatic surfaces are obtained by finding the lowest two roots of Eq. (4-81). The couplings are given by Eqs. (4-101) or (4-104) with the expansion coefficients obtained from Eqs. (4-88) through (4-90) and Eqs. (4-96) through (4-98). The numerical results for the surfaces and couplings will be presented in chapter six.

## CHAPTER 5

## THE NUCLEAR PROBLEM FOR COLLINEAR $H_3^+$

### 5-1 Hyperspherical Coordinates

Hyperspherical coordinates were originally introduced by Delves (Delves, 1960). Recently they have found increasing use in quantum mechanical calculations that involve rearrangement processes (Smith, 1962; Kuppermann, 1975; Hauke, Manz and Römelt, 1980). The reason for this is that they describe both reactants and products equally well. Using these coordinates avoids the necessity of having to make changes from, for example, one set of Jacobi coordinates that describe the initial state to another set that describe the final state during the collision. Instead, the problem is solved by matching, in the asymptotic regions, the solutions in terms of hyperspherical coordinates to the solutions of the asymptotic channel Hamiltonians. Thus the collision event is described by one set of coordinates.

This section is concerned with developing the quantum mechanical Hamiltonian operator in hyperspherical coordinates for a collinear system of three nuclei. Although the equations of motion developed in chapter three do not require the formation of this operator, constructing it is helpful for obtaining a more complete picture of the scattering problem.

To begin with, the positions of the nuclei are designated by $z_A$, $z_B$ and $z_C$ defined in a center of mass coordinate system such that $z_\alpha$, $-\infty \leq z_\alpha \leq +\infty$, is the position of nucleus $\alpha$ relative to the center of mass. In the collinear case there are two arrangement channels given by (A,BC) and (AB,C) which will be designated as channels 1 and 3 respectively. The Jacobi coordinates are defined for channel 1 as

$$Z_1 = z_A - \frac{m_B z_B + m_C z_C}{m_B + m_C} \qquad (5\text{-}1)$$

$$z_1 = z_B - z_C \qquad (5\text{-}2)$$

and for channel 3 as

$$Z_3 = z_C - \frac{m_A z_A + m_B z_B}{m_A + m_B} \qquad (5\text{-}3)$$

$$z_3 = z_A - z_B \qquad (5\text{-}4)$$

where $m_A$, $m_B$ and $m_C$ are the masses of nuclei A, B and C respectively. The Hamiltonian in channel 1 is given as

$$\hat{H} = \frac{-\hbar^2}{2m_{BC}} \frac{\partial^2}{\partial z_1^2} - \frac{\hbar^2}{2m_{A,BC}} \frac{\partial^2}{\partial Z_1^2} + \hat{H}_{el}(z_1, Z_1) \qquad (5\text{-}5)$$

where

$$m_{BC} = \frac{m_B m_C}{m_B + m_C} \qquad (5\text{-}6)$$

and

$$m_{A,BC} = \frac{m_A(m_B + m_C)}{m_A + m_B + m_C} \quad . \qquad (5\text{-}7)$$

A more symmetric form for the kinetic energy operator can be obtained by introducing mass weighted Jacobi coordinates defined in channel 1 as

$$X = \left(\frac{m_{A,BC}}{m_{BC}}\right)^{\frac{1}{2}} Z \qquad (5\text{-}8)$$

and

$$Y = z \qquad (5\text{-}9)$$

where the channel subscript has been suppressed. In these variables the Hamiltonian becomes

$$\hat{H} = \frac{-\hbar^2}{2m_{BC}} \left(\frac{\partial^2}{\partial X^2} + \frac{\partial^2}{\partial Y^2}\right) + \hat{H}_{el}(X,Y) \quad . \qquad (5\text{-}10)$$

Motivation for introducing hyperspherical coordinates is provided by considering the eigenvalue problem of the kinetic energy operation in Eq. (5-10). The solutions of this problem can be written as

$$e^{ik_1X}\, e^{ik_2Y} \tag{5-11}$$

where

$$\frac{\hbar^2 k_1}{2m_{BC}} + \frac{\hbar^2 k_2}{2m_{BC}} = E \tag{5-12}$$

and E is the continuous eigenvalue. Equation (5-11) points out one of the fundamental differences between the two and three body problems. Since $k_1$ and $k_2$ are continuous variables, the three body problem in this set of coordinates requires two sets of functions that depend on continuous variables. The two body problem, however, only requires one such set of functions. The following change of variables will reduce this to one set for the three body problem thus making it formally equivalent to a two body problem.

Hyperspherical coordinates for the case of three collinear nuclei are defined as

$$r = (X^2 + Y^2)^{1/2} \tag{5-13}$$

and

$$\phi = \arctan\ (Y/X) \tag{5-14}$$

where $0 \le r \le \infty$, $0 \le \phi \le \phi_{max}$ and

$$\phi_{max} = \arctan\{(\frac{m_B(m_A + m_B + m_C)}{m_A m_C})^{\frac{1}{2}}\} \qquad (5\text{-}15)$$

The Hamiltonian in this set of coordinates becomes

$$\hat{H} = \frac{-\hbar^2}{2m_{BC}}(\frac{1}{r}\frac{\partial}{\partial r}(r\frac{\partial}{\partial r}) + \frac{1}{r^2}\frac{\partial^2}{\partial\phi^2}) + \hat{H}_{e\ell}(r,\phi) \quad . \qquad (5\text{-}16)$$

Considering the eigenvalue problem for the kinetic energy operator one has

$$(\frac{1}{r}\frac{\partial}{\partial r}(r\frac{\partial}{\partial r}) + \frac{1}{r^2}\frac{\partial^2}{\partial\phi^2})\psi = w\psi \qquad (5\text{-}17)$$

where

$$w = \frac{2m_{BC}}{\hbar^2}E \quad . \qquad (5\text{-}18)$$

Expressing the solution as a product $\chi(r)\ \Theta(\phi)$ of a function of $r$ and a function of $\phi$ results in

$$\frac{r}{\chi(r)}\frac{\partial}{\partial r}(r\frac{\partial}{\partial r})\ \chi(r) - wr^2 = -\frac{1}{\Theta(\phi)}\frac{\partial^2}{\partial\phi^2}\Theta(\phi) \quad . \qquad (5\text{-}19)$$

Setting both sides of Eq.(5-19) equal to a constant A leads to

$$\frac{1}{r}\frac{\partial}{\partial r} r \frac{\partial}{\partial r} \chi(r) - w\chi(r) = \frac{\Lambda}{r^2} \chi(r) \qquad (5\text{-}20)$$

and

$$\frac{\partial^2}{\partial\phi^2} \Theta(\phi) = - \Lambda\Theta(\phi) \quad . \qquad (5\text{-}21)$$

The solutions of Eq. (5-21) can be written as a linear combination of sine and cosine functions. Requiring that $\Theta(0) = \Theta(\phi_{max}) = 0$ gives

$$\Lambda_n = \frac{n^2\pi^2}{\phi_{max}} \qquad (5\text{-}22)$$

and

$$\Theta_n(\phi) = C_n \sin\left(\frac{n\pi}{\phi_{max}}\right) \qquad (5\text{-}23)$$

where $C_n$ is a constant that could be determined through normalization. The full solution is expressed as

$$\psi \quad \sum_n \chi_n(r)\ \Theta_n(\phi) \qquad (5\text{-}24)$$

where $\chi_n$ satisfies Eq. (5-20) with $\Lambda$ equal to $\Lambda_n$. Equation (5-24) illustrates one of the advantages of using these coordinates is that the $\phi$ dependence is given by a denumerable (i.e. countable) set of functions. This formally reduces the problem to a two body problem as is apparent by noticing the similarity of Eq. (5-20) to the radial part of the two body problem in the center of mass coordinate system.

It is convenient to further define a variable $\theta$ such that

$$0 \leq \theta \leq \pi \quad . \tag{5-25}$$

Its relation to $\phi$ is given by

$$\theta = \frac{\phi\pi}{\phi_{max}} \tag{5-26}$$

so that the Hamiltonian becomes

$$\hat{H} = -\frac{\hbar^2}{2m_{BC}} \left(\frac{1}{r}\frac{\partial}{\partial r} r \frac{\partial}{\partial r} + \frac{\pi^2}{r^2\phi^2_{max}}\frac{\partial^2}{\partial\theta^2}\right) + \hat{H}_{el}(r,\theta) \quad . \tag{5-27}$$

One of the reasons for introducing this angle is that the regions of $\theta$ that correspond to breakup and rearrangement do not depend on the masses of the nuclei.

Another advantage of using these variables can be seen by considering Eqs. (5-5) and (5-27). The Hamiltonian given by Eq. (5-5) is channel dependent. Its coordinates are particularly useful for describing the asymptotic states in channel 1. If a rearrangement occurs, it becomes necessary to transform to another set of coordinates that are useful for describing the final states. This introduces practical problems such as when to make the transformation. Also since eigenstates corresponding to different channels are not necessarily orthogonal, overcompleteness can occur.

These difficulties are avoided by using hyperspherical coordinates. The collision process is handled by matching the eigenstates of the Hamiltonian in terms of hyperspherical coordinates to those of the initial channel Hamiltonian in the Jacobi coordinates of the asymptotic region. Hyperspherical coordinates are used throughout the collision. When rearrangements occur, $\theta$ simply goes from small values for A + BC to values that are close to $\pi$ for AB + C in the asymptotic region. Breakups would correspond to large values of r, and $\theta$ in the region of $\pi/2$. Thus all possible products are described by one set of coordinates so that it is no longer necessary to change coordinate systems during the collision process. Also, since the eigenstates that are functions of $\theta$ are orthogonal and complete, overcompleteness does not occur.

## 5-2 The Hamiltonian in the Almost Adiabatic Representation

This section shall be concerned with obtaining an expression for the Hamiltonian defined by Eq. (3-69) in hyperspherical coordinates with the electronic basis satisfying Eq. (2-22). The momentum in terms of hyperspherical coordinates is given by

$$\underset{\sim}{P} = P_r \underset{\sim}{u}_r + \frac{P_\theta}{r\kappa} \underset{\sim}{u}_\theta \qquad (5\text{-}28)$$

where $\underset{\sim}{u}_r$ is a unit vector in the direction of $\underset{\sim}{r}$, $\underset{\sim}{u}_\theta$ is a unit vector perpendicular to $\underset{\sim}{u}_r$ and

$$\kappa = \frac{\phi_{max}}{\pi} \quad . \tag{5-29}$$

In terms of these coordinates, the Hamiltonian becomes

$$\overline{H} = \frac{P_r^2}{2m} + \frac{P_\theta^2}{2mr^2\kappa^2} + \overline{W} \tag{5-30}$$

where for brevity the subscript MC for the masses has been suppressed.

Expressions for the Laplacian, divergence and gradient in this coordinate system will be needed later on. In general one has that

$$\nabla^2 f = \frac{1}{r}\frac{\partial}{\partial r} r \frac{\partial}{\partial r} f + \frac{1}{r^2\kappa^2}\frac{\partial^2}{\partial\theta^2} f \ , \tag{5-31}$$

$$\nabla\cdot\underline{F} = \frac{1}{r}\frac{\partial}{\partial r} rF_r + \frac{1}{r\kappa}\frac{\partial}{\partial\theta} F_\theta \tag{5-32}$$

and

$$\nabla f = \underline{u}_r \frac{\partial f}{\partial r} + \underline{u}_\theta \frac{1}{r\kappa}\frac{\partial f}{\partial\theta} \tag{5-33}$$

where f is an arbitrary function of r and θ and $\underline{F}$ is an arbitrary vector with components $F_r$ and $F_\theta$.

## 5-2a The Electronic Transformation

In Section 2-2c it was shown that the transformation from the adiabatic to the almost adiabatic electronic basis satisfies Eq. (2-22). By using Eqs. (5-31) through (5-33), it is straightforward to show that, in terms of hyperspherical coordinates, this transformation satisfies

$$\underset{\sim}{C}^{\dagger} \frac{\partial^2}{\partial r^2} \underset{\sim}{C} + \frac{1}{r} \underset{\sim}{C}^{\dagger} \frac{\partial}{\partial r} \underset{\sim}{C} + \frac{1}{r^2 K^2} \underset{\sim}{C}^{\dagger} \frac{\partial^2}{\partial \theta^2} \underset{\sim}{C} + \left(\frac{\partial}{\partial r} \underset{\sim}{C}^{\dagger}\right)\left(\frac{\partial}{\partial r} \underset{\sim}{C}\right)$$

$$+ \frac{1}{r^2 K^2}\left(\frac{\partial}{\partial \theta} \underset{\sim}{C}^{\dagger}\right)\left(\frac{\partial}{\partial \theta} \underset{\sim}{C}\right) + \frac{1}{r} \underset{\sim}{C}^{\dagger} \underset{\sim}{d}^{a}_{r} \underset{\sim}{C} + \underset{\sim}{C}^{\dagger}\left(\frac{\partial}{\partial r} \underset{\sim}{d}^{a}_{r}\right)\underset{\sim}{C}$$

$$+ \frac{1}{r^2 K^2} \underset{\sim}{C}^{\dagger}\left(\frac{\partial}{\partial \theta} \underset{\sim}{d}^{a}_{\theta}\right)\underset{\sim}{C} = \underset{\sim}{0} \qquad (5\text{-}34)$$

where

$$(d^{a}_{\alpha})_{ij} = \langle \phi_i | \frac{\partial}{\partial \alpha} | \phi_j \rangle \qquad (5\text{-}35)$$

and α is either r or θ. For two electronic states one has

$$\underset{\sim}{d}^{a}_{\alpha} = \begin{pmatrix} 0 & d^{a}_{\alpha} \\ -d^{a}_{\alpha} & 0 \end{pmatrix} \qquad (5\text{-}36)$$

where

$$d^{a}_{\alpha} = \langle \phi_1 | \frac{\partial}{\partial \alpha} | \phi_2 \rangle \qquad , \qquad (5\text{-}37)$$

α = r,θ and

$$\underset{=}{C} = \begin{pmatrix} \cos\lambda(r,\theta) & \sin\lambda(r,\theta) \\ -\sin\lambda(r,\theta) & \cos\lambda(r,\theta) \end{pmatrix} \qquad (5\text{-}38)$$

where the electronic basis is assumed to be real. By using Eqs. (5-36) and (5-38) in Eq. (5-34), it is not difficult to show that the transformation angle satisfies

$$\frac{\partial^2\lambda}{\partial r^2} + \frac{1}{r}\frac{\partial\lambda}{\partial r} + \frac{1}{r^2\kappa^2}\frac{\partial^2\lambda}{\partial\theta^2} + \frac{d_r^{a}}{r} + \frac{\partial d_r^{a}}{\partial r} + \frac{1}{r^2\kappa^2}\frac{\partial d_\theta^{a}}{\partial\theta} = 0 \; . \quad (5\text{-}39)$$

Equation (5-39) is a second order partial differential equation which could in principle be numerically solved. This is however far from being a trivial task. It becomes more convenient to make a transformation into time. This is accomplished by defining

$$\lambda(r(t),\theta(t)) = \Gamma(t) \quad . \qquad (5\text{-}40)$$

By taking the first and second total derivatives of $\Gamma$ with respect to t, one finds

$$\left(\frac{\partial\lambda}{\partial r}\right)_\theta = \frac{m}{P_r}\frac{d\Gamma(t)}{dt} \qquad (5\text{-}41)$$

$$\left(\frac{\partial\lambda}{\partial\theta}\right)_r = \frac{mr^2\kappa^2}{P_\theta}\frac{d\Gamma(t)}{dt} \qquad (5\text{-}42)$$

$$\left(\frac{\partial^2\lambda}{\partial r^2}\right)_\theta = \frac{m^2}{P_r^{\,2}}\,\frac{d^2\Gamma(t)}{dt^2} - \frac{m^2}{P_r^{\,3}}\,\frac{dP_r}{dt}\,\frac{d\Gamma(t)}{dt} \qquad (5\text{-}43)$$

and

$$\left(\frac{\partial^2\lambda}{\partial \theta^2}\right)_r = \frac{m^2 r^4 \kappa^4}{P_\theta^2}\,\frac{d^2\Gamma(t)}{dt^2} - \frac{m^2 r^4 \kappa^4}{P_\theta^3}\,\frac{dP_\theta}{dt}\,\frac{d\Gamma(t)}{dt} \qquad (5\text{-}44)$$

Using Eqs. (5-41) through (5-44) in Eq. (5-39) leads, with some rearrangement, to

$$\left(\frac{m^2}{P_r^{\,2}} + \frac{m^2 r^2 \kappa^2}{P_\theta^{\,2}}\right)\frac{d^2\Gamma(t)}{dt^2} + \left(\frac{m}{rP_r} - \frac{m^2}{P_r^{\,3}}\,\frac{dP_r}{dt} - \frac{m^2 r^2 \kappa^2}{P_\theta^{\,3}}\,\frac{dP_\theta}{dt}\right)\frac{d\Gamma(t)}{dt}$$

$$= S(r,\theta) \qquad (5\text{-}45)$$

where

$$S(r,\theta) = -\left(\frac{d_r^a}{r} + \frac{\partial d_r^a}{\partial r} + \frac{1}{r^2\kappa^2}\,\frac{\partial d^a}{\partial \theta}\right) \qquad . \qquad (5\text{-}46)$$

Defining

$$\frac{d\Gamma(t)}{dt} = A(t) \qquad (5\text{-}47)$$

one has that

$$\left(\frac{m^2}{P_r^2} + \frac{m^2r^2\kappa^2}{P_\theta^2}\right) \frac{d\Lambda(t)}{dt} + \left(\frac{m}{rP_r} - \frac{m^2}{P_r^3}\frac{dP_r}{dt} - \frac{m^2r^2\kappa^2}{P_\theta^3}\frac{dP_\theta}{dt}\right) \Lambda(t)$$

$$= S(r,\theta) \qquad (5\text{-}48)$$

and

$$\frac{d\Gamma(t)}{dt} - \Lambda(t) = 0 \qquad (5\text{-}49)$$

with boundary conditions

$$\Gamma(t_o) = 0 \qquad (5\text{-}50)$$

and

$$\Lambda(t_o) = 0 \qquad (5\text{-}51)$$

where $t_o$ is the initial time. Eqs. (5-48) and (5-49) are first order differential equations. They can be solved along with Hamiltonian's equation for the nuclear variables to give the transformation angle as a function of time.

### 5-2b The Equations of Motion

In order to determine the equations of motion an expression for the Hamiltonian must be obtained. From Eq. (5-30) one sees that the Hamiltonian is expressed as the sum of the kinetic energy and a potential energy W.

The expression for $\overline{W}$ depends on the electronic representation and on the form chosen for the nuclear expansion coefficients. Defining

$$\underline{\underline{D}} = \underline{\underline{V}} + \underline{\underline{P}}\cdot\underline{\underline{v}} + \frac{\pi}{2}\,\underline{\underline{v}}\cdot\underline{\underline{V}} \qquad (5\text{-}52)$$

there are three terms that need to be evaluated. The potential is given as

$$\underline{\underline{V}} = \underline{\underline{C}}^{\dagger}\underline{\underline{V}}^{e}\underline{\underline{C}} \qquad (5\text{-}53)$$

where $\underline{\underline{V}}^{e}$ is the adiabatic potential matrix. For the 2 × 2 case one finds

$$V_{11} = V_{11}^{a}\cos^2\Gamma(t) + V_{22}^{a}\sin^2\Gamma(t) \qquad (5\text{-}54)$$

$$V_{22} = V_{11}^{e}\sin^2\Gamma(t) + V_{22}^{e}\cos^2\Gamma(t) \qquad (5\text{-}55)$$

and

$$V_{12} = V_{21} = (V_{11}^{a} - V_{22}^{a})\cos\Gamma(t)\sin\Gamma(t) \qquad (5\text{-}56)$$

where $V_{11}^{e}$ and $V_{22}^{e}$ are defined in Eq. (2-11) and correspond to the two lowest surfaces of $H_3^+$.

Using Eqs. (2-21) and (5-33) in Eq. (3-23) leads to

$$\underset{\approx}{v} = \underset{\sim}{u}_r C^\dagger \underset{\approx}{v}^a_r \underset{\approx}{C} + \frac{\hbar \underset{\sim}{u}_r}{im} \underset{\approx}{C}^\dagger \frac{\partial}{\partial r} \underset{\approx}{C} + \frac{\underset{\sim}{u}_\theta}{r\kappa} \underset{\approx}{C}^\dagger \underset{\approx}{v}^a_\theta \underset{\approx}{C} + \frac{\underset{\sim}{u}_\theta}{r\kappa} \frac{\hbar}{im} \underset{\approx}{C}^\dagger \frac{\partial}{\partial \theta} \underset{\approx}{C} \qquad (5\text{-}57)$$

where

$$\underset{\approx}{v}^a_\alpha = \frac{\hbar}{im} \underset{\approx}{d}^a_\alpha \qquad (5\text{-}58)$$

and $\underset{\approx}{d}^a_\alpha$ was defined by Eq. (5-36). With $\underset{\approx}{C}$ defined by Eq. (5-38), one obtains after transforming into time

$$\underset{\approx}{v} = \underset{\sim}{u}_r \underset{\approx}{v}^a_r + \underset{\sim}{u}_r \frac{\hbar}{iP_r} \frac{d\Gamma}{dt} \underset{\approx}{I} + \frac{\underset{\sim}{u}_\theta}{r\kappa} \underset{\approx}{v}^a_\theta + \underset{\sim}{u}_\theta \frac{\hbar r\kappa}{iP_\theta} \frac{d\Gamma}{dt} \underset{\approx}{I} \qquad (5\text{-}59)$$

where

$$\underset{\approx}{I} = \begin{pmatrix} 0 & 1 \\ -1 & 0 \end{pmatrix} \qquad (5\text{-}60)$$

From Eqs. (5-28) and (5-59) the second term in the expression for $\underset{\approx}{D}$ becomes

$$\underset{\sim}{P} \cdot \underset{\approx}{v} = P_r \underset{\approx}{v}^a_r + \frac{P_\theta}{r^2\kappa^2} \underset{\approx}{v}^a_\theta + \frac{2\hbar}{i} \Lambda(t) \underset{\approx}{I} \qquad (5\text{-}61)$$

where Eq. (5-49) has been used. In a similar manner one obtains

$$\frac{m}{2} \underset{\approx}{v} \cdot \underset{\approx}{v} = \Big(\frac{\hbar^2}{2m} (d^a_r)^2 + \frac{\hbar^2}{P_r} d^a_r \Lambda(t) + \frac{\hbar^2 m}{2P_r^2} \Lambda(t)^2 + \frac{\hbar^2}{2mr^2\kappa^2} (d^a_\theta)^2$$

$$+ \frac{\hbar^2}{P_\theta} d^a_\theta \Lambda(t) + \frac{mr^2\kappa^2\hbar^2}{2P_\theta^2} \Lambda(t)^2\Big) \underset{\approx}{1} \qquad (5\text{-}62)$$

where

$$\underset{\sim}{1} = \begin{pmatrix} 1 & 0 \\ 0 & 1 \end{pmatrix} \qquad (5\text{-}63)$$

Using Eqs. (5-53), (5-61) and (5-62) in Eq. (5-52) and substituting the result into Eq. (5-30), one obtains an expression for the Hamiltonian of the form

$$\bar{H} = \frac{P_r^2}{2m} + \frac{P_\theta^2}{2mr^2\kappa^2} + \frac{\hbar^2}{2}\left(\frac{d_r^{a2}}{m} + \frac{2d_r^a}{P_r} A(t) + \frac{m}{P_r^2} A^2(t) + \frac{d_\theta^{a2}}{mr^2\kappa^2}\right.$$
$$\left. + \frac{2d_\theta^a}{P_\theta} A(t) + \frac{mr^2\kappa^2}{P_\theta^2} A(t)^2\right) + (\underset{\sim}{C}_N^\dagger \underset{\sim}{C}_N)^{-1} \underset{\sim}{C}_N^\dagger (\underset{\sim}{V} + P_r \underset{\sim}{v}_r^a$$
$$\frac{P_\theta}{r^2\kappa^2} \underset{\sim}{v}_\theta^a + \frac{2\hbar}{i} A(t) \underset{\sim}{I}) \underset{\sim}{C}_N \qquad (5\text{-}64)$$

where the subscript N has been added to the nuclear expansion coefficients to avoid confusion with the transformation matrix $\underset{\sim}{C}$.

The expression for $\bar{H}$ given in Eq. (5-64) is quite complicated and the final expression depends on the form chosen for the nuclear expansion coefficients. It is straightforward, given the form of the nuclear expansion coefficients, to determine the final form of the Hamiltonian. However, since the calculations were performed in a different electronic basis, they will not be presented here. If this representation were used, one would need to simultaneously solve a set of ten first order differential equations. Four of them would correspond to the nuclear positions and momenta and four would determine the nuclear expansion coefficients. The other two given by Eq. (5-48) and (5-49) are needed to determine the transformation angle.

## 5-3 The Hamiltonian in the Diabatic Representation

The diabatic representation is defined by requiring that the electronic basis satisfy Eq. (2-13). There are two main advantages in using this representation. The first is that the transformation angle is much easier to determine. The second is that this representation leads to a rather simple form for the Hamiltonian. Another apparent advantage is that it seems to help, from a computational point of view, if the couplings do not appear explicitly. The rest of this chapter will develop the electronic transformation and Hamiltonian in this representation.

### 5-3a The Electronic Transformation

As was discussed in section (2-2b), the electronic transformation satisfies Eq. (2-15). In hyperspherical coordinates, one has that

$$\underline{u}_r \frac{\partial \lambda}{\partial r} + \frac{\underline{u}_\theta}{r\kappa} \frac{\partial \lambda}{\partial \theta} = - \underline{u}_r d^a_r - \frac{\underline{u}_\theta}{r\kappa} d^a_\theta \qquad (5\text{-}65)$$

where the transformation was chosen of the form

$$= \begin{pmatrix} \cos(\lambda) & \sin(\lambda) \\ -\sin(\lambda) & \cos(\lambda) \end{pmatrix} \qquad (5\text{-}66)$$

and $d^a_\theta$ was defined in Eq. (5-37). By comparing the partial derivative of $d^a_r$ with respect to $\theta$ to the partial derivative of $d^a_\theta$ with respect to r, one finds that

$$\frac{\partial d^a_r}{\partial \theta} = \frac{\partial d^a_\theta}{\partial r} \quad . \qquad (5\text{-}67)$$

Letting

$$\lambda(r,\theta) = \lambda(r_o,\theta_o) - (\int_{\theta_o}^{\theta} d^a_\theta(r,\theta')d\theta' + \int_{r_o}^{r} d^a_r(r',\theta_o)dr') \qquad (5\text{-}68)$$

One has that

$$\frac{\partial \lambda(r,\theta)}{\partial \theta} = - d^a_\theta(r,\theta) \qquad (5\text{-}69)$$

and

$$\frac{\partial \lambda(r,\theta)}{\partial r} = - \int_{\theta_o}^{\theta} \frac{\partial}{\partial r} d^a_\theta(r,\theta')d\theta' - d^a_r(r,\theta_o) \quad . \qquad (5\text{-}70)$$

Using Eq. (5-67) in (5-70) results in

$$\frac{\partial\lambda}{\partial r} = - d_r^a(r,\theta) \qquad (5\text{-}71)$$

which shows that $\lambda$ defined by Eq. (5-68) is a solution of Eq. (5-65). One notices that Eq. (5-68) can be simplified if $\theta_0$ is chosen such that

$$d_r^a(r,\theta_0) = 0 \qquad (5\text{-}72)$$

for all r. In this case one has that

$$\lambda(r,\theta) = \lambda(r_0,\theta_0) - \int_{\theta_0}^{\theta} d_\theta^a(r,\theta')d\theta' \quad . \qquad (5\text{-}73)$$

This seems to be the most useful form for application. If $d_\theta^a$ could be expressed in terms of simple functions, one might be able to find analytic solutions of Eq. (5-73) so that a transformation into time could be avoided. This will be seen to be the case for the collinear $H_3^+$ system.

### 5-3b The Equations of Motion

The Hamiltonian considerably simplifies in the diabatic representation. Since all of the couplings are eliminated, the expression for $\overline{W}$ simplifies to

$$\overline{W} = (\underset{\sim}{C}^{\dagger}\underset{\sim}{C})^{-1}\underset{\sim}{C}^{\dagger}\underset{\sim}{V}^{d}\underset{\sim}{C} \qquad (5\text{-}74)$$

where

$$V_{11}^{d} = V_{11}^{a} \cos^{2}\lambda + V_{22}^{a} \sin^{2}\lambda \qquad (5\text{-}75)$$

$$V_{22}^{d} = V_{11}^{a} \sin^{2}\lambda + V_{22}^{a} \cos^{2}\lambda \qquad (5\text{-}76)$$

and

$$V_{12}^{d} = V_{21}^{d} = (V_{11}^{a} - V_{22}^{a}) \sin\lambda \cos\lambda \qquad (5\text{-}77)$$

where $\lambda$ is given by Eq. (5-73). If the symmetric form for the nuclear expansion coefficients is chosen, one has that

$$C_1 = \frac{(X_1 + iY_1)}{\sqrt{2\hbar}} \qquad (5\text{-}78)$$

and

$$C_2 = \frac{(X_2 + iY_2)}{\sqrt{2\hbar}} \qquad (5\text{-}79)$$

which results in, with $\underset{\approx}{C}^{\dagger}\underset{\approx}{C} = 1$

$$\overline{W} = \frac{1}{2\hbar}\,(V_{11}^{d}(X_1^2 + Y_1^2) + V_{22}^{d}(X_2^2 + Y_2^2) + 2V_{12}^{d}(X_1X_2 + Y_1Y_2)) \,. \qquad (5\text{-}80)$$

This essentially completes the development in that the Hamiltonian is found by using Eq. (5-80) in Eq. (5-30). Doing this results in a set of eight first order differential equations in time that need to be solved simultaneously. Explicitly, these equations are

$$\frac{dr}{dt} = \frac{\partial \overline{H}}{\partial P_r} = \frac{P_r}{m} \tag{5-81}$$

$$\frac{dP_r}{dt} = -\frac{\partial \overline{H}}{\partial r} \tag{5-82}$$

$$\frac{d\theta}{dt} = \frac{\partial \overline{H}}{\partial P_\theta} = \frac{P_\theta}{mr^2\kappa^2} \tag{5-83}$$

$$\frac{dP_\theta}{dt} = -\frac{\partial \overline{H}}{\partial \theta} \tag{5-84}$$

$$\frac{dX_1}{dt} = \frac{\partial \overline{H}}{\partial Y_1} = \frac{1}{\hbar}(V_{11}^d Y_1 + V_{12}^d Y_2) \tag{5-85}$$

$$\frac{dY_1}{dt} = -\frac{\partial \overline{H}}{\partial X_1} = -\frac{1}{\hbar}(V_{11}^d X_1 + V_{12}^d X_2) \tag{5-86}$$

$$\frac{dX_2}{dt} = \frac{\partial \overline{H}}{\partial Y_2} = \frac{1}{\hbar}(V_{22}^d Y_2 + V_{12}^d Y_1) \tag{5-87}$$

and

$$\frac{dY_2}{dt} = -\frac{\partial \overline{H}}{\partial X_2} = -\frac{1}{\hbar}(V_{22}^d X_2 + V_{12}^d X_1) \tag{5-88}.$$

The analytical expressions that determine $P_r$ and $P_\theta$ have been omitted because of their complexity. In practice it is found that they are easier to determine numerically.

## CHAPTER 6
## CALCULATIONS FOR $H_3^+$

### 6-1 Electronic Results

This section will be concerned with the numerical aspects of applying the equations developed in chapter four to the collinear $H_3^+$ system. It was shown in chapter four that the method of Diatomics in Molecules with zero differential overlap led to a solution of the electronic problem that depended solely on the diatomic potentials.

The following subsection will develope the diatomic potentials that are necessary for the Diatomics in Molecules treatment. These will be used in the following subsections to construct the potentials and couplings for the collinear $H_3^+$ system which will be given in terms of hypersperical coordinates.

### 6-1a The Diatomic Potentials

As was discussed in Section (2-3), for each pair of nuclei, three diatomic potentials are needed to determine the electronic problem. These correspond to the ground state potential, ${}^1\Sigma_g^+$, for $H_2$ and the ground state, ${}^2\Sigma_g^+$, and first excited state, ${}^2\Sigma_u^+$, potentials for $H_2^+$.

A Morse function (Morse, 1929) was chosen to represent the ground state for $H_2$. Explicitly one has

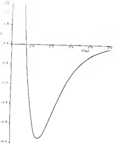

Fig. (12) The Morse potential, Eq. (6-1), for the ground state, $^1\Sigma_g^+$, of $H_2$. The parameters are defined in the text following Eq. (6-1).

$$^1\Sigma_g^+(r) = {}^1D(e^{-2\,^1a(r - {}^1r_o)} - 2e^{-\,^1a(r - {}^1r_o)}) \qquad (6\text{-}1)$$

where r is the internuclear distance. For $H_2$, the well depth, $^1D$, is 4.759 e.V., the position of the minimum, $^1r$ , is 1.402 $a_o$, and $^1a$ is 1.044 $a_o^{-1}$. The potential is shown in Fig. (12).

The ground state for $H_2^+$ was also given the form of a Morse potential so that

$$^2\Sigma_g^+(r) = {}^2D_g(e^{-2\,^2a_g(r - {}^2r_g)} - 2e^{-\,^2a_g(r - {}^2r_g)}) \qquad (6\text{-}2)$$

where $^2D_g$, $^2r_g$, and $^2a_g$ have the values 2.795 e V., 2.003 $a_o$, and .7194 $a_o^{-1}$ respectively. An anti-Morse potential, defined by

$$^2\Sigma_u^+(r) = {}^2D_u(e^{-2\,^2a_u(r - {}^2r_u)} + 2e^{-\,^2a_u(r - {}^2r_u)}) \qquad (6\text{-}3)$$

was used to describe the first excited state, $^2\Sigma_u^+$, of $H_2^+$. The values of the parameters were chosen to be 17.1 e.V., .344 $a_o$ and .8708 $a_o^{-1}$ for $^2D_u$, $^2r_u$ and $^2a_u$ respectively. The values of the parameters used in Eqs. (6-2) and (6-3) are essentially the same as those used by Petersen and Porter (Petersen and Porter, 1967). These potentials are shown in Fig. (13)

The use of Morse and anti-Morse potentials may seem to be a bit arbitrary in that more accurate diatomic

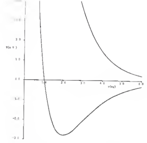

Fig. (13) The potentials for the ground state, $^2\Sigma_g^+$, (Eq. (6-2)) and first excited state, $^2\Sigma_u^+$, (Eq. (6-3)) for $H_2^+$. The parameters are given in the text following Eqs.(6-2) and (6-3).

potentials could be easily obtained. They are, however, convenient for making comparisons in that other theoretical studies (Tully and Preston, 1971; Top and Baer, 1977) have used potentials of this form.

### 6-1b Adiabatic Potential Surfaces

The adiabatic potential energy surfaces are found by solving for the roots of the third degree polynomial defined in Eq. (4-81). These can be determined analytically (Selby, 1964) and the lowest two roots correspond to the surfaces that are needed in the scattering calculations.

The diatomic potentials that were presented in the previous section depend on internuclear distance. In terms of hyperspherical coordinates, these internuclear distances become

$$r_{AB} = r\left[\left(\frac{m_{BC}}{m_{A,BC}}\right)^{\frac{1}{2}}\cos\left(\frac{\phi_{max}}{\pi}\,\theta\right) + \frac{m_B}{m_B + m_C}\,\sin\left(\frac{\phi_{max}}{\pi}\,\theta\right)\right] \qquad (6\text{-}4)$$

$$r_{BC} = r\,\sin\left(\frac{\phi_{max}}{\pi}\,\theta\right) \qquad (6\text{-}5)$$

$$r_{AC} = r\left[\left(\frac{m_{BC}}{m_{A,BC}}\right)^{\frac{1}{2}}\cos\left(\frac{\phi_{max}}{\pi}\,\theta\right) - \frac{m_C}{m_B + m_C}\,\sin\left(\frac{\phi_{max}}{\pi}\,\theta\right)\right] \qquad (6\text{-}6)$$

where $r_{\alpha\beta}$ is the distance from nucleus $\alpha$ to nucleus $\beta$ and the mass terms were defined in Section 5-1.

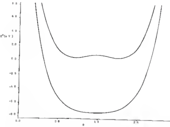

Fig. (14) The two lowest adiabatic potential energy surfaces for collinear $H_3^+$ in hyperspherical coordinates. $r = 4\ a_0$

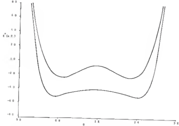

Fig. (15) The two lowest adiabatic potential energy surfaces for collinear $H_3^+$ in hyperspherical coordinates. $r = 6\ a_0$

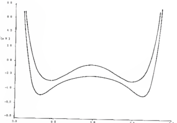

Fig. (16) The two lowest adiabatic potential energy surfaces for collinear $H_3^+$ in hyperspherical coordinates $r = 8\ a_0$

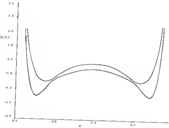

Fig. (17) The two lowest adiabatic potential energy surfaces for collinear $H_3^+$ in hyperspherical coordinates. $\rho = 10\ a_0$

Figures (14) through (17) show the $\theta$ dependence of the two lowest surfaces of collinear $H_3^+$ for different values of r. For r equal to 4 $a_o$ one notices the deep well of the lower surface which gives rise to the formation of long lived complexes. As r increases, the well turns into a barrier and the surfaces begin to approach each other at $\theta$ in the neighborhood of .8 and 2.2 radians. By r equal to 10 $a_o$, the surfaces approach very closely and we shall see in the next subsection that this is accompanied by large non-adiabatic couplings.

### 6-1c Non-adiabatic Couplings

In Section 4-5 it was shown that the non-adiabatic couplings could be obtained either through Eq. (4-101) which involved partial derivatives of the eigenvectors or Eq. (4-104) which involved partial derivatives of the matrix elements of the electronic Hamiltonian. In practice it was found easier to numerically differentiate Eq. (4-101) and the results were checked with Eq. (4-104) using analytical derivatives for the diatomic potentials. In hyperspherical coordinates, two coupling terms are present and one needs to evaluate,

$$d_\theta^a = <\phi_1^a|\frac{\partial}{\partial\theta}|\phi_2^a> \qquad (6-7)$$

and

$$d_r^a = <\phi_1^a|\frac{\partial}{\partial r}|\phi_2^a> \qquad (6-8)$$

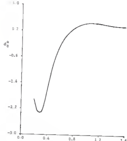

Fig. (18) Non-adiabatic couplings due to $\theta$, Eq. (6-7). $r = 4\ a_0$.

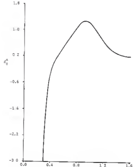

Fig. (19) Non-adiabatic couplings due to $\theta$, Eq. (6-7). $r = 6\ a_0$.

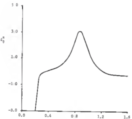

Fig. (20) Non-adiabatic couplings due to θ, Eq. (6-7). $r = 8\ a_0$.

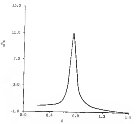

Fig. (21) Non-adiabatic couplings due to $\theta$, Eq. (6-7). $r = 10\ a_0$.

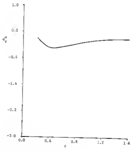

Fig. (22) Non-adiabatic couplings due to r, Eq. (6-8). $r = 4\ a_0$.

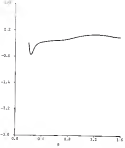

Fig. (23) Non-adiabatic couplings due to r, Eq. (6-8). $r = 6\ a_0$.

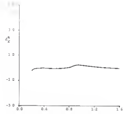

Fig. (24) Non-adiabatic couplings due to r, Eq. (6-8), $r = 8\ a_0$.

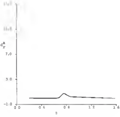

Fig. (25) Non-adiabatic couplings due to r, Eq. (6-8).
r = 10 $a_o$

The couplings due to $\theta$ given in Eq. (6-7) are shown in Figs. (18) through (21) as a function of $\theta$ for different values of r. Since the couplings are symmetric about $\pi/2$, only the results for $0 \leq \theta \leq \pi/2$ are shown. For r equal to $4a_0$, the surfaces are far apart and, as one would expect, the couplings are small except for small values of $\theta$. For small values of $\theta$ the surfaces are highly repulsive so that these couplings lie in a region that is in this study energetically inaccessible. As r increases, the coupling becomes stronger and more localized in the region where the potentials approach each other. For r equal to 10 $a_0$, the coupling is large and localized about the potential pseudocrossing and eventually, for r in the asymptotic region, the coupling becomes a delta function (Top and Baer, 1977).

The couplings due to r given by Eq. (6-8) are shown in Figs. (22) through (25) for different values of r. One notices that they have the same general behavior as the couplings due to $\theta$ but they are also much weaker. This is one of the advantages in using hyperspherical coordinates in that since the couplings due to r are much smaller than those due to $\theta$, it may be possible to neglect them.

### 6-1d Model of Non-adiabatic Couplings

The results to be presented in the next section were done in the diabatic electronic representation. In chapter five it was shown that the transformation from the adiabatic to the diabatic representation required only the non-adiabatic couplings due to θ. It was further suggested that if these couplings exhibit a rather simple behavior, it may be possible to model them with simple functions so that the integral in Eq. (5-73) could be determined analytically.

In the previous section it was seen in Figs. (18) through (21) that the couplings due to θ were fairly symmetric around the pseudocrossing. A function with this property is the Gaussian, so that the couplings were chosen to have the form

$$d_\theta^a(r,\theta) = B(r)e^{-b(r)(\theta - \theta_x(r))^2} \qquad (6\text{-}9)$$

where $\theta_x$ is the value of θ that corresponds to the maximum of the coupling. The range of θ in Eq. (6-9) is restricted to be between zero and π/2. The coupling for values of θ greater than π/2 are simply found by evaluating Eq (6-9) with θ equal to π − θ. B(r) was chosen to be

$$B(r) = Ae^{\alpha r} - .52e^{-(r - 8a_0)^2 a_0^{-2}} \qquad (6\text{-}10)$$

where A = .045, α = .55$a_0^{-1}$ and the second term on the right hand side was added to improve the agreement at r equal to 8$a_0$. $\theta_x$ was given the form

$$\theta_x(r) = a_x + b_x r + .034e^{-2a_0^{-2}(r - 8a_0)^2} \qquad (6\text{-}11)$$

where $a_x = 1.1684$, $b_x = -.04215\ a_0^{-1}$ and again the last term improved the agreement around r equal to $8a_0$. Finally, for $r \geq 6a_0$,

$$b(r) = ae^{cr^3} \tag{6-12}$$

where $a = 3.5067$ and $c = .00477a_0^{-3}$ and for r less than $6a_0$

$$b(r) = d + er \tag{6-13}$$

where $d = 1.7$ and $e = 1.355a_0^{-1}$. Although the derivative of b(r) is not continuous at $r = 6a_0$, b(r) is continuous so that the integral is still well defined. The results of the couplings defined by Eq. (6-9) are compared to the actual couplings in Figs. (26) through (29). In general the agreement is not bad The worst agreement occurs for r equal to $4a_0$ but the coupling is small in this region anyway.

6-2 Trajectory Calculations

Since the collision process occurs in a very short amount of time ($10^{-14}$ secs - $10^{-15}$ secs), it is convenient to choose a set of units that reflect this. There are four units that need to be defined and they correspond to units for mass, energy, length and time. A convenient unit for length is the atomic unit, $a_0$, which is equal to .5292 Å. A natural choice for the unit of mass is the proton rest

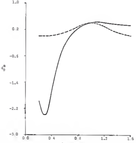

Fig. (26) A comparison of the modeled couplings (---) due to $\theta$ to the actual ones (——). $r = 4\ a_0$.

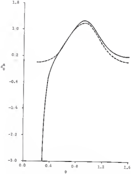

Fig. (27) A comparison of the modeled couplings (---) due to $\theta$ to the actual ones (——). $x = 6\ s_o$.

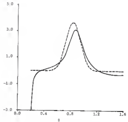

Fig. (28) A comparison of the modeled couplings (---) due to $\theta$ to the actual ones (——). $r = 8\ a_0$.

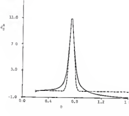

Fig. (29) A comparison of the modeled couplings (----) due to $\theta$ to the actual ones (——). $r = 10\ a_0$.

mass, $m_p$ ($1.6726 \times 10^{-24}$g), and electron volts, e.V. ($1.6022 \times 10^{-12}$ergs), will be chosen for the unit of energy. The unit of time, $\tau$, corresponding to the above units is given by

$$\tau = \sqrt{\frac{m_p a}{e.V.}} \qquad (6\text{-}14)$$

which gives $\tau$ equal to $5.407 \times 10^{-15}$ secs. The value of Planck's constant in these units is found to be .121733 $m_p a_o^2 \tau^{-1}$.

As will become apparent later, it is necessary to define transformations between Jacobi and hyperspherical variables. In terms of the hyperspherical coordinates $(r,\theta)$, the Jacobi coordinates in channel 1 (A,BC) are given by

$$z_1 = r \sin(\kappa\theta) \qquad (6\text{-}15)$$

and

$$Z_1 = \left(\frac{m_{BC}}{m_{A,BC}}\right)^{\frac{1}{2}} r \cos(\kappa\theta) \qquad (6\text{-}16)$$

where $m_{BC}$ and $m_{A,BC}$ were defined in Eqs. (5-6) and (5-7) and $\kappa$ was defined by Eq. (5-29). In terms of the Jacobi coordinates, r and $\theta$ are found to be

$$r = (Z_1^2 + \frac{m_{A,BC}}{m_{BC}} z_1^2)^{\frac{1}{2}} \qquad (6\text{-}17)$$

and

$$\theta = \frac{1}{\kappa} \arctan( \frac{z_1}{Z_1} (\frac{m_{BC}}{m_{A,BC}})^{\frac{1}{2}}) \qquad (6\text{-}18)$$

The Jacobi momenta are given by

$$P_{z_1} = \frac{m_D Z_1}{\kappa r^2} P_\theta + \frac{z_1}{r} P_r \qquad (6\text{-}19)$$

and

$$P_{Z_1} = \frac{m_D}{r} (m_D Z_1 P_r - \frac{z_1}{r\kappa} P_\theta) \qquad (6\text{-}20)$$

where

$$m_D = (\frac{m_{A,BC}}{m_{BC}})^{\frac{1}{2}} \quad . \qquad (6\text{-}21)$$

Finally one has that

$$P_\theta = \kappa (m_D Z_1 P_{z_1} - \frac{z_1}{m_D} P_{Z_1}) \qquad (6\text{-}22)$$

and

$$P_r = \frac{1}{r} (z_1 P_{z_1} - Z_1 P_1) \quad . \qquad (6\text{-}23)$$

It will also be found useful to define the Jacobi variables in channel 3 (AB,C) and these are found to be

$$z_3 = Z_1 - \frac{m_C}{m_B + m_C} z_1 \quad , \qquad (6\text{-}24)$$

$$Z_3 = - \frac{m_A}{m_A + m_B} Z_1 - \frac{m_B(m_A + m_B + m_C)}{(m_A + m_B)(m_B + m_C)} z_1 \; , \qquad (6\text{-}25)$$

$$P_{Z_3} = \frac{m_B(m_A + m_B + m_C)}{(m_A + m_B)(m_B + m_C)} P_{Z_1} - \frac{m_A}{m_A + m_B} P_{z_1} \quad , \qquad (6\text{-}26)$$

and

$$P_{z_3} = - \frac{m_C}{m_B + m_C} P_{Z_1} - P_{z_1} \quad . \qquad (6\text{-}27)$$

### 6-2e Test Cases

Before attempting to do a calculation on a two-surface system some preliminary studies were done on systems that consisted of only one electronic surface. There are two main reasons for doing this. The first is to make sure that the computer programs are working properly. The second is to gain some experience in working with hyperspherical coordinates. Two of the test cases that were studied will be the subject of the rest of this subsection.

The first system consisted of a rigid diatomic molecule colliding with an atom under the influence of the repulsive potential $az_1^{-2}$. The two masses of the diatomic were chosen to be 1 $m_p$ and the separation distance was set equal to 1.402 $a_o$. The mass of the incoming atom was 1 $m_p$ and its initial distance, $Z_1$, was chosen to be 10 $a_o$. With the internal energy of the diatomic set to zero and with a total energy of 1 e.V. the initial momenta $P_{Z_1}$ can be determined. The momenta $P_{z_1}$ is of course equal to zero. With these initial conditions in terms of Jacobi coordinates, Eqs. (6-17), (6-16), (6-22) and (6-23) are used to determine the initial conditions in terms of hyperspherical variables. The Hamiltonian is found to be

$$H(r,\theta) = \frac{P_r^2}{2m_{BC}} + \frac{P_\theta^2}{2m_{BC}r^2\kappa^2} + a\,\frac{m_{A,BC}}{m_{BC}}\,(r\cos(\kappa\theta))^{-2} \qquad (6\text{-}28)$$

where Eq. (6-16) was used. The equations of motion are given by

$$\frac{dr}{dt} = \frac{P_r}{m_{BC}} \quad , \qquad (6\text{-}29)$$

$$\frac{dP_r}{dt} = \frac{P_\theta^2}{m_{BC}r^3\kappa^2} + 2a\,\frac{m_{A,BC}}{m_{BC}}\,r^{-3}\cos^{-2}\kappa\theta \quad , \qquad (6\text{-}30)$$

$$\frac{d\theta}{dt} = \frac{P_\theta}{m_{BC}r^2\kappa^2} \qquad (6\text{-}31)$$

and

$$\frac{dP_\theta}{dt} = - \frac{2am_{A,BC}\sin\kappa\theta}{m_{BC}r^2\cos^3\kappa\theta} \qquad . \qquad (6\text{-}32)$$

Eqs. (6-29) through (6-32) were solved simultaneously using a standard subroutine based on the Runge, Kutta, Gill procedure (Shampine and Allen, 1973) to do the integration. The value of a in these calculations was set equal to $1\ m_p a_o^4 \tau^{-2}$. The results of these calculations are shown in Figs. (30) and (31). In Fig. (30) the coordinates r and θ are plotted as a function of time. One sees that r is initially around 11 $a_o$ and it steadily decreases until it reaches a turning point at a time of about 5.75 τ. After the turning point, r increases as the particles recede. The behavior of θ is also quite simple. Initially it is small and it increases to somewhat larger than 2.5 at the turning point. After the turning point it decreases back to small values. This behavior is what one would expect from a repulsive potential in that since rearrangements and complexes do not occur θ must initially and finally have small values. Also shown in Fig. (19) is the potential as a function of time. In the interaction zone it increases to a value of 1 e.V. at the turning point. This, of course, coincides with the kinetic energy being zero.

In Fig. (31) plots of $P_r$ and $P_\theta$ versus time are shown. $P_r$ initially is negative as the particles approach each

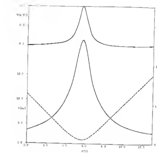

Fig. (30) Plots of r (——) and θ (---) as a function of t for the case of a repulsive potential, $\alpha Z_1^{-2}$. $E_{tot}$ = 1.0 e. V. The potential is shown in the upper figure.

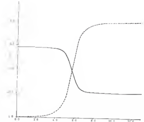

Fig. (31) Plots of $P_r$ (——) and $P_s$ (----) as a function of t for the case of a replusive potential, $\propto Z_1^{-2}$, $E_{tot}$= 1.0 e.V.

other, goes to zero at the turning point and becomes positive as the particles recede. $F_\theta$ is initially positive as $\theta$ increases, goes to zero at the turning point and becomes negative as $\theta$ becomes small.

Although this was a very simple test case, some of the general behavior for these variables will still be observed for the more complicated cases. One of the differences between this case and the more complicated cases is the oscillatory behavior of $\theta$ and $F_\theta$ due to the vibrational motion of the diatomic.

The second test case to be considered here is the collinear collision of a proton with a hydrogen molecule with only the lowest electronic surface present. Since this case includes vibrational motion and rearrangements and inelastic collisions are possible, this study should offer some insight in what to expect for the behavior of the hyperspherical variables when two surfaces are present.

This system is also convenient for determining the quickest numerical method for integrating the equations. A comparison was made between the Runge, Kutta, Gill procedure used in the previous test case and a predictor corrector method based on Adam's formula (Shampine and Gordon, 1975). Trajectories were run with both procedures using the same initial conditions and error tolerances. It was found that the trajectories obtained from the procedure based on Adam's formula used about an order of magnitude less computing time than the corresponding ones obtained from the Runge, Kutta, Gill procedure. This result did not depend on the initial vibrational level. The integration subroutines based on Adam's formula were therefore used to do all further calculations.

The initial conditions for the trajectories were chosen in the following way. They were all done at the same total energy. This was chosen to be −1.9175 e.V. which is about 1 e.V. above the n=4 vibrational level of $H_2$ (the zero of energy corresponds to two hydrogen atoms and a proton, all infinitely separated and at rest). The value of the initial relative distance, $Z_1$, was chosen to be large enough so that the interactions between the proton and $H_2$ were negligible. In practice it was set equal to 14 $a_0$. Choosing the initial vibrational level of $H_2$ to be n, $0 \leq n \leq 4$, the initial internal energy of $H_2$ is given by

$$E^{i}_{int} = -{}^{1}D + \hbar\,{}^{1}a\left(\frac{2\,{}^{1}D}{m_{BC}}\right)^{\frac{1}{2}}(n + \tfrac{1}{2}) - \frac{\hbar^{2}\,{}^{1}a^{2}}{m_{BC}}(n + \tfrac{1}{2})^{2} \qquad (6\text{-}33)$$

where the parameters were defined in Eq. (6-1). The initial value of the relative momentum, $P^{i}_{Z_1}$, is found to be

$$P^{i}_{Z_1} = \sqrt{2m_{A,BC}(E_{tot} - E^{i}_{int})} \qquad (6\text{-}34)$$

where $E_{tot}$ is the total energy. What remains is to choose the initial values of the vibrational coordinate, $z_1^i$, and momentum $P_{z_1}^i$. The value of the initial vibrational momentum was chosen to be either plus or minus some fraction of the maximum initial vibrational momentum, $P_{z_1}^{max}$, which is given by

$$P_{z_1}^{max} = \sqrt{2m_{BC}({}^1D + E_{int}^i)} \quad . \tag{6-35}$$

The initial values of the coordinate are found to be

$$z_{1,\mp}^i = {}^1r_0 - \frac{1}{{}^1\alpha} \ln(1 \pm \sqrt{1 + a}) \tag{6-36}$$

where

$$a = \frac{E_{int}^i - (P_{z_1}^i)^2/2m_{BC}}{{}^1D} \tag{6-37}$$

and the $\mp$ indicates initial values that are less than (-) or greater than (+) the equilibrium distance.

The first set of trajectories to be considered here originated in the n=0 vibrational level. From Eqs. (6-33) and (6-34) the relative momentum, $P_{z_1}^i$, was found to be $-1.85\ m_p a_0 \tau^{-1}$. The maximum value of the diatomic momentum,

$P_{z_1}^{max}$, was obtained from Eq. (6-35) which gave 0.5189 $m_p a_o \tau^{-1}$. The initial value of the diatomic momentum, $P_{z_1}$, was chosen to be +.5189 $m_p a_o \tau^{-1}$ which gave the initial value of the vibrational coordinate, $z_1$, of 1.402 $a_o$, the equilibrium distance. The initial values of the hyperspherical variables were found by using Eqs. (6-17), (6-18), (6-22) and (6-23). The Hamiltonian was given by Eq. (5-30) with $\overline{W}$ equal to the lowest electronic surface which was designated as $E_1$ in Section (4-4). The equations of motion were found to be

$$\frac{dr}{dt} = \frac{P_r}{m_{BC}} \qquad (6\text{-}38)$$

$$\frac{dP_r}{dt} = \frac{P_\theta^2}{m_{BC} r^3 \kappa^2} - \frac{\partial E_1^a}{\partial r} \qquad (6\text{-}39)$$

$$\frac{d\theta}{dt} = \frac{P_\theta}{m_{BC} r^2 \kappa^2} \qquad (6\text{-}40)$$

and

$$\frac{dP_\theta}{dt} = - \frac{\partial E_1^a}{\partial \theta} \qquad (6\text{-}41)$$

where the superscript "a" indicates the adiabatic surface and

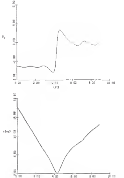

Fig. (32) Plots of r and $P_r$ as a function of t for the adiabatic collision of $H^+$ with $H_2$ on the lowest $H_3^+$ surface. n=0, $E_{tot}$= -1.9175 e.V. and $P_{z_1}^i$ is .5189 $m_p a_o \tau^{-1}$.

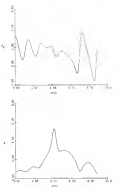

Fig. (33) Plots of $\theta$ and $P_\theta$ as a function of t for the adiabatic collision of $H^+$ with $H_2$ on the lowest $H_3^+$ surface. n=0, $E_{tot}$=-1.9175 e.V. and $P^i_{Z_1}$= .5189 $m_p a_0 \tau^{-1}$.

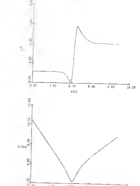

Fig. (34) Plots of $Z_1$ and $P_{Z_1}$ as a function of time for the adiabatic collision of $H^+$ with $H_2$ on the lowest $H_3^+$ surface. n=0, $E_{tot}$=-1.9175 e.V. and $P^1_{Z_1}$ is .5189 $m_p a_o \tau^{-1}$.

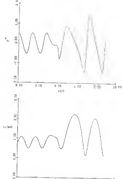

Fig. (35) Plots of $z_1$ and $P_{z_1}$ for the adiabatic collision of $H^+$ with $H_2$ on the lowest $H_3^+$ surface. n=0, $E_{tot}$=-1.9175 e.V. and $P^i_{z_1}$=.5189 $m_p a_o \tau^{-1}$.

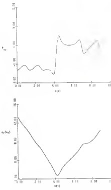

Fig. (36) Plots of $z_3$ and $P_{z_3}$ for the adiabatic collision of $H^+$ with $H_2$ on the lowest $H_3^+$ surface. n=0, $E_{tot}$= -1.9175 e.V. and $P_{z_1}^i$ = .5189 $m_p a_o \tau^{-1}$.

where the terms involving partial derivatives were evaluated numerically.

The results of Eqs. (6-38) through (6-41) are shown in Figs. (32) and (33). One notices that they exhibit the same general behavior as in the previous test case. The essential difference is their oscillatory nature due to the vibrational motion. This is especially evident in the trajectories for $\theta$ and $P_\theta$. One also notices that initially $\theta$ has small oscillations but that after the collision its oscillations are noticeably larger. This of course corresponds to a transfer of energy from the translational to vibrational modes. Since $\theta$ returns to small values after the collision, this is an example of a process that doesn't involve rearrangements.

The results are also given in terms of Jacobi variables in Figs. (34) through (36). One sees in Fig. (34) that $P_{z_1}$ becomes constant both before and after the collision. This constant behavior served as a criteria for terminating the calculation. The gain in vibrational energy is also evident from the plots of $z_1$ and $P_{z_1}$ given in Figs. (35). As will be seen shortly, the trajectories of $z_3$ given in Fig. (36) and of $z_1$ serve as an aid in understanding the collision process.

A particularly informative quantity is the potential energy as a function of time shown in Fig. (37). Before the collision there are small oscillations in $E_1^e$ due to the vibrational motion of BC (for brevity the nuclei will be

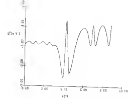

Fig. (37) Plot of $E_1^a$ vs. t for the adiabatic collision of $H^+$ with $H_2$ on the lowest $H_3^+$ surface. n=0, $E_{tot}$= -1.9175 e.V. and $P_{z_1}^i = .5189\ m_p a_o \tau^{-1}$.

referred to as A, B and C and the diatomics as AB and BC). As A approaches B, there is a sharp decrease in $E_I^a$ followed by a strong repulsion when the distance between A and B is at a minimum. As A and B separate there is another large decrease in $E_I^a$ and eventually A escapes leaving BC with greater vibrational energy.

Further insight is obtained by considering Figs. (35) and (36). One sees in Fig. (35) that in the initial part of the collision around $t = 3.5\ \tau$, BC is contracting. Due to the large attraction between A and B, the contraction is slower for a while. As A and B separate, BC further contracts and then undergoes a large expansion. One might expect that if BC were initially expanding in the collision, the repulsion between B and C would be strong enough to cause a rearrangement.

The second set of trajectories shown in Figs. (38) through (44) were done with the same set of initial conditions that were used for the previous ones with the exception that the sign of the diatomic momentum $P_{z_1}$ was changed, i.e. $P_{z_1} = -.5189 \frac{m_F a_0}{\tau}$. Since $\theta$ in Fig. (39) goes from small values to values close to $\pi$, this is an example of a rearrangement. One notices in Fig. (42) that $P_{z_3}$ is constant after the collision and this was used to terminate the calculation. In practice $P_{z_1}$ and $P_{z_3}$ were

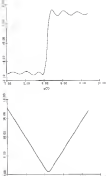

Fig. (38) Plots of r and $P_r$ vs. t for the adiabatic collision of $H^+$ with $H_2$ on the lowest $H_3^+$ surface, n=0, $E_{tot}$ = -1.9175 e.V. and $P_{z_1}^i = -.5189\ m_p a_0 \tau^{-1}$.

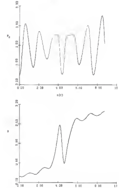

Fig. (39) Plots of θ and $P_\theta$ vs. t for the adiabatic collision of $H^+$ with $H_2$ on the lowest $H_3^+$ surface. n=0, $E_{tot}$= -1.9175 e.V. and $P^i_{z_1}$ = -.5189 $m_p a_o \tau^{-1}$.

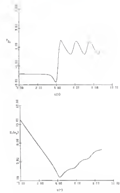

Fig. (40) Plots of $Z_1$ and $P_{Z_1}$ vs. t for the adiabatic collision of $H^+$ vs. $H_2$ on the lowest $H_3^+$ surface. n=0, $E_{tot}$= -1.9175 e.V. and $P^i_{z_1}$ = -.5189 $m_p a_o \tau^{-1}$.

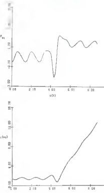

Fig. (41) Plots of $z_1$ and $P_{z_1}$ vs. t for the adiabatic collision of $H^+$ with $H_2$ on the lowest $H_3^+$ surface. n=0, $E_{tot}$= -1.9175 e.V. and $P_{z_1}^i$ = -.5189 $m_p a_0 \tau^{-1}$.

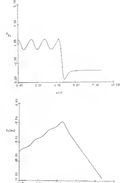

Fig.(42) Plots of $Z_3$ and $P_{Z_3}$ vs. t for the adiabatic collision of $H^+$ with $H_2$ on the lowest $H_3^+$ surface. m=0, $E_{tot}$= -1.9175 e.V. and $P_{Z_1}^i$ = -.5189 $m_p a_0 \tau^{-1}$.

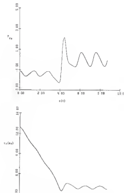

Fig. (43) Plots of $z_3$ and $P_{z_3}$ vs. t for the adiabatic collision of $H^+$ with $H_2$ on the lowest $H_3^+$ surface. n=0, $E_{tot}$= -1.9175 e.V. and $P_{z_1}^{i}$ = $-.5189\ m_p a_0 \tau^{-1}$.

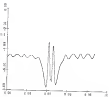

Fig. (44) Plot of $E_1^a$ vs. t for the adiabatic collision of $H^+$ with $H_2$ on the lowest $H_3^+$ surface. n=0, $E_{tot}$= -1.9175 e.V. and $P_{z_1}^1 = -.5189\ m_p a_o \tau^{-1}$.

calculated throughout the collision and the calculation was stopped if either $P_{Z_1}$ or $P_{Z_3}$ was constant when $P_r$ was positive and r was greater than some value which was chosen to be 10 $a_0$.

In Fig. (41) one notices that during the initial part of the collision around t = 3.5 $\tau$, BC is expanding. Since B is strongly attracted to A, this expansion is somewhat greater which corresponds to an increase in the vibrational energy of BC. When B and C contract, they get close enough to undergo a strong repulsion which gives rise to the second sharp increase in $E_1$ shown in Fig. (44). Due to the increased vibrational energy of BC, this repulsion is strong enough so that C escapes and AB is formed.

The previous two examples offer some insight into why and how rearrangements take place. The rearrangement process seems to depend mainly on whether there is a substantial increase in the vibrational energy of BC during the initial part of the collision. If BC is contracting during the initial part of the collision, the attraction between A and B causes this contraction to be slower for a while. Consequently there is no initial increase in the vibrational energy of BC so that A escapes and BC remains bound. If, however, BC is initially expanding during the collision, the attraction between A and B causes BC to expand to greater distances. This enhanced expansion corresponds to an increase in the vibrational energy of BC which is great enough for C to escape and for AB to form.

Calculations were also done at the same total energy for the n=4 vibrational level. These results along with the n=0 results seem to indicate that the mechanism discussed above is almost always capable of predicting the correct final nuclear configuration. As is expected, it can give incorrect predictions in cases where long lived complexes are formed. It will be seen later that, since this mechanism only depends on the initial part of the collision, it will still be of use when the upper surface is included.

As is clearly seen in Fig. (37), this system has the ability to transfer energy between translational and vibrational modes. Figs. (35) and (43) help in understanding why this is so. One sees in Fig. (35) that as A is leaving the collision region, around $t = 4.2\ \tau$ the diatomic is expanding. The attraction between A and B causes BC to expand to greater distances which increases its vibrational energy. The opposite case is shown in Fig. (43) where, at around $t = 4.5\ \tau$, AB is contracting. The attraction between B and C slows down this contraction for a while leaving AB with a lower amount of vibrational energy.

As a check in the calculations, the total energy, $\bar{H}$, was calculated throughout the collision and it was found to remain constant. Time reversal studies were also done and they led to the same results.

### 6-2b $H_3^+$ Results

This section shall report the results of some typical trajectories that were obtained by including both electronic surfaces for the collinear $H_3^+$ system. The calculations were done in the diabatic electronic representation so that the results were obtained by integrating Eqs. (5-81) through (5-88). The electronic coupling terms were modeled according to Eq. (6-9) so that the angle, Eq. (5-73), that determines the transformation between the adiabatic and diabatic representations is given in terms of error functions as in Section (2-5).

Common to all trajectories are the initial value of $Z_1$ and the total energy. As in the previous adiabatic test case, the initial value of $Z_1$ was chosen to be 14 $a_0$ and the total energy was set equal to -1.9175 e V. (1 e.V. above the n=4 vibrational level of $H_2$). Also common to all trajectories were the initial values of the electronic amplitudes. $X_1$ was set equal to $\sqrt{2\hbar}$ and $Y_1$, $X_2$ and $Y_2$ were all chosen to be zero From Eqs. (3-103), (3-106) and (3-107) this corresponds to an initial value of $P_1 = 1$ and to initial values of $\gamma_1$ and $P_2$ of zero. $\gamma_2$ was also set equal to zero.

The remaining initial conditions were chosen in a fashion similar to the previous adiabatic test case.

Selecting the initial vibrational energy level, the initial internal energy is found from Eq. (6-33). This is used in Eq. (6-34) to determine the initial value of $P_{z_1}$. Choosing an initial value of $z_1$ between the turning points, the initial value of $P_{z_1}$ is given by

$$P^{i}_{z_1} = \pm \sqrt{2m_{BC}(E^{i}_{int} - {}^{1}E_{g}{}^{+}(z_1))} \quad . \qquad (6\text{-}42)$$

The initial values of the hyperspherical variables were determined by using Eqs. (6-17), (6-18), (6-22) and (6-23).

The first set of trajectories consists of an example of a non-rearrangement process that initiates in the n equal to zero vibrational level. From Eqs. (6-33) and (6-34) the initial value of $P_{z_1}$ is $-1.85 \frac{m_p a_0}{\tau}$ . With an initial value of $z_1$ of 1.45 $a_0$, Eq (6-42) gives the value of $P^{i}_{z_1}$ of $.508 \frac{m_p a_0}{\tau}$ where the plus sign was chosen.

The results of r, $P_r$ and θ, $P_\theta$ are shown in Figs. (45) and (46) respectively. Their behavior is similar to the adiabatic test case involving non-rearrangement. Initially r decreases monotonically and $P_r$ is negative and undergoes small oscillations. As the particles collide, r reaches a minimum and begins to increase and $P_r$ goes from negative to positive. For r greater than about 6 τ, r

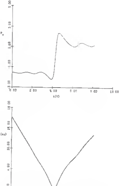

Fig. (45) Plots of r and $P_r$ vs. t for the non-adiabatic collision of $H^+$ with $H_2$ on the lowest two $H_3^+$ surfaces. n=0, $E_{tot}$ = -1.9175 e.V., $z_1^i$=1.45 $a_o$ and $P_{z_1}^i$ = .508 $m_p a_o \tau^{-1}$.

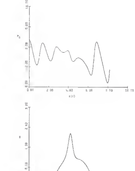

Fig. (46) Plots of θ and $P_\theta$ vs. t for the non-adiabatic collision of $H^+$ with $H_2$ on the lowest two $H_3^+$ surfaces. n=0, $E_{tot}$= -1.9175 e.V., $z_1^i$=1.45 $a_o$ and $P_{z_1}^i$=-.508 $m_p a_o \tau^{-1}$.

monotonically increases and $P_r$ oscillates around a positive value. The final rate of increase of r is less than its initial rate of decrease which signifies an increase in vibrational energy. This is also seen by considering the behavior of $\theta$ and $P_\theta$. Initially $\theta$ is small and undergoes small oscillations. It increases to about 2 when the particles are all close together and then returns to small values but with significantly larger oscillations.

The results of $Z_1$, $P_{Z_1}$ and $z_1$, $P_{z_1}$ are shown in Figs (47) and (48) respectively. One notices that for t greater than 6 $\tau$, $P_{Z_1}$ becomes constant and this was used to terminate the calculation. One also sees in Fig. (48) that during the initial part of the collision, $t \lesssim 3\tau$, BC is undergoing a contraction. Since this is a non-rearrangement process, the mechanism described for the adiabatic test cases might apply to this system also. This subject will be discussed again a little later.

Fig. (49) shows the time dependence of $\overline{W}$. The diabatic potentials $E_1$, $E_2$ and $E_{12}$ used to calculate $\overline{W}$ are shown in Figs. (50), (51) and (52) respectively. The adiabatic potentials $E_1^a$ and $E_2^a$ are shown in Figs. (53) and (54) respectively and the transformation angle, $\lambda$, is depicted in Fig. (55). One notices the similarity in the figures for $\overline{W}$, $E_1$ and $E_1^a$. Initially they undergo small oscillations characteristic of the lowest vibrational level. As $\lambda$ approaches $\pi$, there is a large decrease in energy and the

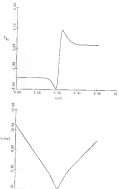

Fig. (47) Plots of $Z_1$ and $P_{z_1}$ vs. t for the non-adiabatic collision of $H^+$ with $H_2$ on the lowest two $H_3^+$ surfaces. n=0, $E_{tot}$= -1.9175 e.V., $z_1^i$=1.45 $a_o$ and $P_{z_1}^i$=.508 $m_p a_o \tau^{-1}$.

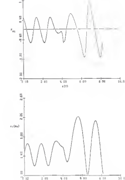

Fig. (48) Plots of $z_1$ and $P_{z_1}$ vs. t for the non-adiabatic collision of $H^+$ with $H_2$ on the lowest two $H_3^+$ surfaces. n=0, $E_{tot}$= -1.9175 e.V., $z_1^i$=1.45 $a_0$ and $P_{z_1}^i$=.508 $m_p a_0 \tau^{-1}$.

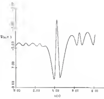

Fig. (49) Plot of $\overline{W}$ vs. t for the non-adiabatic collision of $H^+$ with $H_2$ on the lowest two $H_3^+$ surfaces. n=0, $E_{tot}$=-1.9175 e.V., $z_1^i$=1.45 $a_o$ and $P_{z_1}^i$=.508 $m_p a_o \tau^{-1}$.

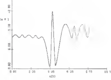

Fig. (50) Plot of the diabatic potential $E_1$ vs. t for the collision of $H^+$ with $H_2$ on the lowest two $H_3^+$ surfaces. n=0, $E_{tot}$=-1.9175 e.V., $z_1^i$=1.45 $a_o$ and $P_{z_1}^i$=.508 $m_p a_o \tau^{-1}$.

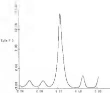

Fig. (51) Plot of the diabatic potential $E_2$ vs. t for the collision of $H^+$ with $H_2$ on the lowest two $H_3^+$ surfaces. n=0, $E_{tot}$= -1.9175 e.V., $z_1^i$=1.45 $a_o$ and $P_{z_1}^i$ =.508 $m_p a_o \tau^{-1}$.

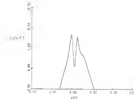

Fig. (52) Plot of the diabatic potential $E_{12}$ vs. t for the collision of $H^+$ with $H_2$ on the lowest two $H_3^+$ surfaces. n=0, $E_{tot}$= -1.9175 e.V., $z_1^i$=1.45$a_o$ and $P_{z_1}^i$=.508 $m_p a_o \tau^{-1}$.

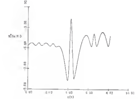

Fig. (53) Plot of the adiabatic potential $E_1^a$ vs. t for the collision of $H^+$ with $H_2$ on the lowest two $H_3^+$ surfaces. $m=0$, $E_{tot}= -1.9175$ e.V., $z_1^i=1.45\ a_o$ and $P_{z_1}^i=.508\ m_p a_o \tau^{-1}$.

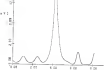

Fig. (54) Plot of the adiabatic potential $E_2^a$ vs. t for the non-adiabatic collision of $H^+$ with $H_2$ on lowest two $H_3^+$ surfaces. n=0, $E_{tot}$= -1.9175 a.v. $z_1^i$=1.45 $a_o$ and $P_{z_1}^i$=.508 $m_p a_o \tau^{-1}$.

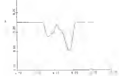

Fig. (55) Plot of the transformation angle, λ, vs. t for the non-adiabatic collision of $H^+$ with $H_2$ on the lowest two $H_3^+$ surfaces. n=0, $E_{tot}$= -1.9175 e.V., $s_1^i$=1.45 $a_o$ and $P_{s_1}^i$ =.508 $m_p a_o \tau^{-1}$.

system is in the well region of the lowest surface. As A gets closer to B a strong repulsion occurs which corresponds to the sharp increase in the potentials. As A and B separate there is another large decrease in the potentials as the system goes through the well region. The large final oscillations indicate a significant increase in vibrational energy. On close inspection one finds that initially and finally $E_1$ and $E_1^s$ coincide and that in the collision region $E_1$ is greater than $E_1^s$ as it should be. Due to the similarity between $E_1$ and $\bar{W}$ after the collision one would expect a low probability for electronic transition.

The results of $P_1$, $\gamma_1$ and $P_2$, $\gamma_2$ are shown in Figs. (56) and (57) respectively and $\gamma_1$ and $\gamma_2$ are seen to oscillate very rapidly. The behavior of the probabilities can be better understood by considering the graphs of $z_1$ and $P_{z_1}$. It is well known from the semi-classical treatment of this system (Tully and Preston, 1971) that the derivative of the amplitude for the upper surface is proportional to the velocity. It has also been shown (Tully and Preston, 1971) that the main contribution to this derivative comes from the velocity of the diatomic that is crossing the seam. Thus, if the diatomic crosses the seam in an expansion mode this would correspond to going to the upper surface so that $P_1$ should decrease and $P_2$ should increase. If the diatomic is contracting when going through the seam, the system ends up on the lower surface so that $P_1$ should increase and $P_2$ should decrease. Considering the results for $P_2$ (Fig. 57)

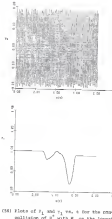

Fig. (56) Plots of $P_1$ and $\gamma_1$ vs. t for the non-adiabatic collision of $H^+$ with $H_2$ on the lowest two $H_3^+$ surfaces. n=0, $E_{tot}$= -1.9175 e.V., $z_1^i$=1.45 $a_o$ and $P_{z_1}^i$=.598 $m_p a_o \tau^{-1}$.

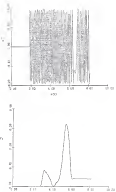

Fig. (57) Plots of $P_2$ and $\gamma_2$ vs. t for the non-adiabatic collision of $H^+$ with $H_2$ on the lowest two $H_3^+$ surfaces. n=0, $E_{tot}$= -1.9175 e.V., $z_1^i$=1.45 $a_o$ and $P_{z_1}^i$=.508 $m_p a_o \tau^{-1}$.

one sees that $P_2$ increases rapidly to about .1 for t around 3 τ. From Fig. (48) this corresponds to positive values of $P_{z_1}$. BC then begins to contract so that $P_{z_1}$ is negative and $P_2$ decreases. This is followed by another increase in $P_2$ to about .3 for t around 6 τ. From Fig. (48) $P_{\theta_1}$ is seen to be positive during the increase and zero at the maximum. As BC contracts, $P_2$ decreases and attains a final value of about .05. The larger increase in $P_2$ is seen to correspond to a greater expansion of BC.

Two important inferences about trajectories that originate in the n equal to zero vibrational level can be made. First, non-adiabatic effects should only be important as the particles exit the collision region. This is so because before the collision the oscillations of BC are small and do not enter the seam and because the couplings are small for small values of r. Second, the mechanism that determined whether or not rearrangement should take place should apply here too. This is because the mechanism depended on the initial part of the collision where non-adiabatic effects are small.

The second set of trajectories to be considered here also originate in the n equal zero vibrational level. The initial values of $z_1$ and $P_{z_1}$ are 1.25 $a_0$ and -4261 $\frac{m_p a_0}{\tau}$ respectively. The results of r, $P_r$ and θ, $P_\theta$ are shown in Figs. (58) and (59) respectively. One sees that the final values of θ are close to π so that this is an example of a rearrangement process. The larger oscillations of [illegible] after the collision indicates an increase in vibrational energy.

The results of $Z_1$, $P_{Z_1}$ and $z_1$, $P_{z_1}$ are plotted in Figs (60) and (61) respectively. One notices that during the initial part of the collision BC is expanding, which based on previous discussions results in a rearrangement. The results for $Z_3$, $P_{Z_3}$ and $z_3$, $P_{z_3}$ are shown in Figs. (62) and (63) respectively. As seen in Fig. (62), $P_{Z_3}$ becomes constant after the collision and this was used as the criterion to terminate the calculation.

$\bar{\bar{W}}$ is shown in Fig. (64) and the diabatic potentials $E_1$ and $E_2$ are shown in Figs. (65) and (66) respectively. One sees that there is considerable vibrational excitation in $\bar{\bar{W}}$ and $E_1$ after the collision. One also notices that $E_1$ and $E_2$ are close to each other at around t equal to 6 $\tau$ and it will be seen that $P_1$ and $P_2$ undergo large changes in this region.

The results of $P_1$ and $P_2$ are shown in Fig. (67). From Figs. (61) and (63) one sees that the small initial increase in $P_2$ is due to the expansion of BC. Then as A approaches B it passes through the seam and $P_2$ decreases to very small values. For t between 4 $\tau$ and 5 $\tau$ the particles are close together and the couplings are small so that $P_2$ remains small. At around 5 $\tau$ $P_2$ begins to sharply increase and from Figs. (61) and (63) this is seen to result from both AB and BC expanding. A passes through the seam and exits and a maximum in $P_2$ occurs at around 6 $\tau$. This is seen to

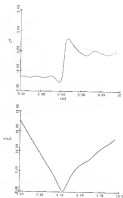

Fig (58) Plots of r and $P_r$ vs. t for the non-adiabatic collision of $H^+$ with $H_2$ on the lowest two $H_3^+$ surfaces. n=0, $E_{tot}$= -1.9175 e.V., $z_1^i$=1.25 $a_o$ and $P_{z_1}^i$=-.4261 $m_p a_o \tau$-1.

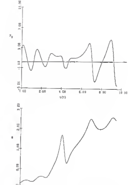

Fig. (59) Plots of θ and $P_\theta$ vs. t for the non-adiabatic collision of $H^+$ with $H_2$ on the lowest two $H_3^+$ surfaces. n=0, $E_{tot}$= -1.9175 e.V., $z_1^i$=1.25 $a_o$ and $P_{z_1}^i$=.4261 $m_p a_o \tau^{-1}$.

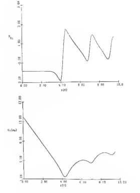

Fig. (60) Plots of $Z_1$ and $P_{Z_1}$ vs. t for the non-adiabatic collision of $H^+$ with $H_2$ on the lowest two $H_3^+$ surfaces. m=0, $E_{tot}$= -1.9175 e.V., $Z_1^i$=2.25 $a_o$ and $P_{Z_1}^i$=.4261 $m_p a_o \tau^{-1}$.

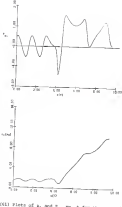

Fig. (61) Plots of $z_1$ and $P_{z_1}$ vs. t for the non-adiabstic collision of $H^+$ with $H_2$ on the lowest two $H_3^+$ surfaces. n=0, $E_{tot}$= -1.9175 e.V., $z_1^i$=1.25 $a_o$ and $P_{z_1}^i$=.4261 $m_p a_o \tau^{-1}$.

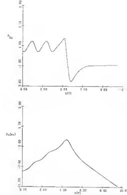

Fig. (62) Plots of $Z_3$ and $P_{Z_3}$ vs. t for the non-adiabatic collision of $H^+$ with $H_2$ on the lowest two $H_3^+$ surfaces. n=0, Etot= -1.9175 e.V., $z_1^i$=1.25 $a_o$ and $P_{z_1}^i$=.4261 $m_p a_o \tau^{-1}$.

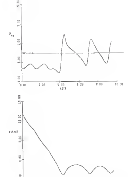

Fig. (63) Plots of $z_3$ and $P_{z_3}$ vs. t for the non-adiabatic collision of $H^+$ with $H_2$ on the lowest two $H_3^+$ surfaces. n=0, $E_{tot}$= -1.9175 e.V., $z_1^i$=1.25 $a_o$ and $P_{z_1}^i$=.4261 $m_p a_o \tau^{-1}$.

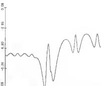

Fig. (64) Plot of $\overline{W}$ vs. t for the non-adiabatic collision of $H^+$ with $H_2$ on the lowest two $H_3^+$ surfaces. n=0, $E_{tot}$= -1.9175 e.V., $z_1^i$=1.25 $a_o$ and $P_{z_1}^i$ = .4261 $m_p a_o \tau^{-1}$.

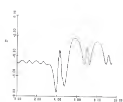

Fig. (65) Plot of the diabatic potential $E_1$ vs. t for the collision of $H^+$ with $H_2$ on the lowest two $H_3^+$ surfaces. n=0, $E_{tot}$= -1.9175 e.V., $z_1^1$=1.25 $a_o$ and $P_{z_1}^1$=.4261 $m_p a_o \tau^{-1}$.

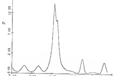

Fig. (66) Plot of the diabatic potential $E_2$ vs. t for the non-adiabatic collision of $H^+$ with $H_2$ on the lowest two $H_3^+$ surfaces. n=0, $E_{tot}$= -1.9175 e.V., $z_1^i$=1.25 $a_o$ and $P_{z_1}^i$=.4261 $m_p a_o T^{-1}$.

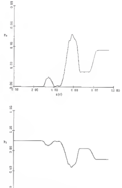

Fig. (67) Plots of $P_1$ and $P_2$ vs. t for the non-adiabatic collision of $H^+$ with $H_2$ on the lowest two $H_3^+$ surfaces. n=0, $E_{tot}$= -1.9175 e.V., $z_1^i$=1.25 $a_o$ and $P_{z_1}^i$=.4261 $m_p a_o \tau^{-1}$.

coincide with a zero of $P_{z_3}$. As AB contracts $P_2$ decreases and becomes constant when AB is away from the seam. There is a final increase in $P_2$ at around 8 $\tau$ and this is due to an AB expansion. The reason that this is not followed by another decrease in $P_2$ is that as r gets larger the seam becomes narrower so that by the time AB has fully expanded it is no longer in the seam.

The final two sets of trajectories to be discussed here originate in the n = 4 vibrational level. From Eqs. (6-33) and (6-34) one finds that $P^i_{z_1}$ is equal to $-1.15 \frac{m_p a_0}{\tau}$. The values of $z_1$ and $P_{z_1}$ for the first set of trajectories were chosen to be 2.17 $a_0$ and .635 $\frac{m_p a_0}{\tau}$ respectively.

The results of r, $P_r$ and $\theta$, $P_\theta$ are shown in Figs. (68) and (69) respectively. As is to be expected, the initial oscillations in $P_r$, $\theta$, and $P_\theta$ are noticeably larger than in the previous examples. One sees that the final rate of increase of r is less than its initial rate of decrease so that the internal energy of BC has increased. However, the final oscillations of $P_\theta$ are smaller so that the increase is probably due to an electronic transition.

The results of $Z_1$, $P_{Z_1}$ and $z_1$, $P_{z_1}$ are shown in Figs. (70) and (71) respectively. The invariance in the final values of $P_{Z_1}$ was used to terminate the calculation. One notices that as A and B begin to interact at around 4 $\tau$ BC is contracting which again leads to non-rearrangement

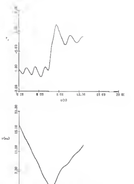

Fig. (68) Plots of $r$ and $P_r$ vs. $t$ for the non-adiabatic collision of $H^+$ with $H_2$ on the two lowest $H_3^+$ surfaces. $n=4$, $E_{tot}= -1.9175$ e.V., $z_1^i=2.17\ a_0$ and $P_{z_1}^i = .635\ m_p a_0 \tau^{-1}$.

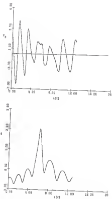

Fig. (69) Plots of θ and $P_\theta$ vs. t for the non-adiabatic collision of $H^+$ with $H_2$ on the lowest two $H_3^+$ surfaces. n=4, $E_{tot}$= -1.9175 e.V., $z_1^i$=2.17 $a_o$ and $P_{z_1}^i$=.635 $m_p a_o \tau^{-1}$.

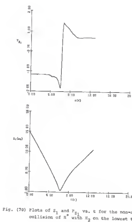

Fig. (70) Plots of $Z_1$ and $P_{z_1}$ vs. t for the non-adiabatic collision of $H^+$ with $H_2$ on the lowest two $H_3^+$ surfaces. n=4, $E_{tot}$= -1.9175 e.V., $z_1^i$=2.17 $a_o$ and $P_{z_1}^i$=.635 $m_p a_o \tau^{-1}$.

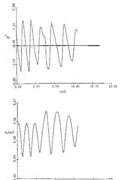

Fig. (71) Plots of $z_1$ and $P_{z_1}$ vs. t for the non-adiabatic collision of $H^+$ with $H_2$ on the two lowest $H_3^+$ surfaces. n=4, $E_{tot}$= -1.9175 e.V., $z_1^i$=2.17 $a_o$ and $P_{z_1}^i$=.635 $m_p a_o \tau^{-1}$.

$z_3$ and $P_{z_3}$ are presented in Fig. (72) and will be used later to help understand the behavior of $P_2$.

$\overline{W}$ is shown in Fig. (73) and one sees that after the collision there is a substantial increase in $\overline{W}$ with smaller oscillations which indicates that the motion is taking place on the upper surface. The diabatic potentials $E_1$ and $E_2$ are shown in Figs. (74) and (75) and one notices that there are crossings between $E_1$ and $E_2$ at around 5 $\tau$.

The results of $P_1$ and $P_2$ are given in Fig. (76). One notices a considerable increase in structure but some understanding can be achieved by considering the general trends. From Fig. (71), one sees that the initial increase in $P_2$ is due to an expansion of BC. $P_2$ decreases somewhat as BC contracts and then begins oscillating rapidly between value of zero and 8. From Figs. (71) and (72) one sees that the oscillations increase as BC expands across the seam and then decrease as A crosses the seam. The increase in the next set of oscillations is due to A crossing the seam as it exits and this followed by a decrease due to the contraction of BC. As BC expands $P_2$ starts to oscillate between zero and one and attains a value of about 0.6 when BC has contracted out of the seam. As in the previous example there is a final increase in $P_2$ as BC again expands into the narrowing seam.

Thus even though there is an enormous amount of structure in the results for the probabilities their

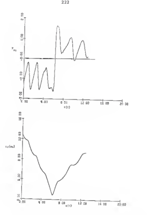

Fig. (72) Plots of $z_3$ and $P_{z_3}$ vs. t for the non-adiabatic collision of $H^+$ with $H_2$ on the lowest two $H_3^+$ surfaces. n=4, Etot= -1.9175 e.V., $z_1^i$=2.17 $a_o$ and $P_{z_1}^i$ = .635 $m_p a_o \tau^{-1}$.

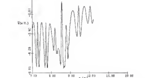

Fig. (73) Plot of $\overline{W}$ vs. t for the non-adiabatic collision of $H^+$ with $H_2$ on the lowest two $H_3^+$ surfaces. n=4, $E_{tot}$= -1.9175 e.V., $x_1^i$=2.17 $a_o$ and $P_{x_1}^i$=.635 $m_p a_o \tau^{-1}$.

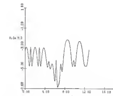

Fig. (74) Plot of the diabatic potential $E_1$ vs. t for the non-adiabatic collision of $H^+$ with $H_2$ on the lowest two $H_3^+$ surfaces. n=4, $E_{tot}= -1.9175$ e.V., $z_1^i=2.17\ a_o$ and $P_{z_1}^i=.635\ m_p a_o \tau^{-1}$.

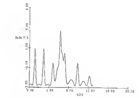

Fig. (75) Plot of the diabatic potential $E_2$ vs. t for the non-adiabatic collision of $H^+$ with $H_2$ on the lowest two surfaces of $H_3^+$. n=4, $E_{tot}$= -1.9175 e.V., $z_1^i$=2.17 $a_o$ and $P_{z_1}^i$=.635 $m_p a_o \tau^{-1}$.

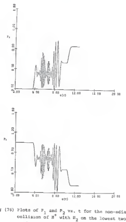

Fig (76) Plots of $P_1$ and $P_2$ vs. t for the non-adiabatic collision of $H^+$ with $H_2$ on the lowest two $H_3^+$ surfaces. n=4, $E_{tot}$= -1.9175 e.V., $z_1^i$=2.17 $a_o$ and $P_{z_1}^i$=-.635 $m_p a_o \tau^{-1}$.

general behavior can still be understood in terms of simple seam crossings. One also notices that the non-adiabatic effects before the collision are substantially larger than in the previous n = 0 cases. This somewhat puts into question whether the mechanism that determined whether or not rearrangement would occur is valid here. However from the cases that have been studied, it still seems to work.

The final set of trajectories also start in the n equal 4 vibrational level. The initial values of $z_1$ and $P_{z_1}$ are 2.17 $a_0$ and -.635 $\frac{m_p a_0}{\tau}$ respectively. The results for $r$, $P_r$ and $\theta$, $P_\theta$ are shown in Figs. (77) and (78). One notices a substantial increase in the absolute value of $P_r$ after the collision which indicates that internal energy has been lost. Thus one would expect that the probability for a transition to the upper surface to be small. One notices that the final values of $\theta$ are close to $\pi$ so that this is an example of a rearrangement process.

Fig. (79) displays the results for $z_1$ and $P_{z_1}$. The only difference in boundary conditions between this example and the previous one is the sign of $P^1_{z_1}$. Based on the mechanism introduced earlier, one would predict that a rearrangement would occur and it is gratifying to see that it indeed does. The results for $z_3$ and $P_{z_3}$ are shown in Fig. (80) and will be used later when the probabilities are discussed.

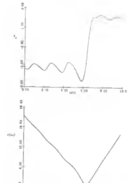

Fig. (77) Plots of r and $P_r$ vs. t for the non-adiabatic collision of $H^+$ with $H_2$ on the lowest two $H_3^+$ surfaces. n=4, $E_{tot}$= -1.9175 e.V., $z_1^i$=2.17 $a_0$ and $P_{z_1}^i$ = -.635 $m_p a_0 \tau^{-1}$.

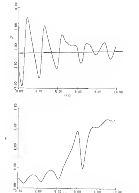

Fig. (78) Plots of θ and $P_\theta$ vs. t for the non-adiabatic collision of $H^+$ with $H_2$ on the lowest two $E_3^+$ surfaces. n=4, $E_{tot}$= -1.9175 e.V., $z_1^i$=2.17 $a_o$ and $P_{z_1}^i$ = -.635 $m_p a_o \tau^{-1}$.

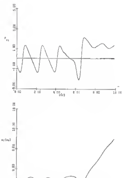

Fig. (79) Plots of $z_1$ and $P_{z_1}$ vs. t for the non-adiabatic collision of $H^+$ with $H_2$ on the lowest two $H_3^+$ surfaces. n=4, $E_{tot}$= -1.9175 e.V., $z_1^i$=2.17 $a_o$ and $P_{z_1}^i$ = -.635 $m_p a_o \tau^{-1}$.

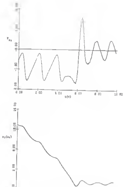

Fig. (80) Plots of $z_3$ and $P_{z_3}$ vs. t for the non-adiabatic collision of $H^+$ with $H_2$ on the lowest two $H_3^+$ surfaces. n=4, $E_{tot}$= -1.9175 e.V., $z_1^i$=2.17 $a_o$ and $P_{z_1}^i$ = -.635 $M_p a_o \tau^{-1}$.

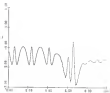

Fig. (81) Plot of $\overline{W}$ vs. t for the non-adiabatic collision of $H^+$ with $H_2$ on the lowest two $H_3^+$ surfaces. n=4, $E_{tot}$= -1.9175 e.V., $z_1^i$=2.17 $a_o$ and $P_{z_1}^i$ = -.635 $m_p a_o \tau^{-1}$.

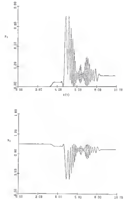

Fig. (82) Plots of $P_1$ and $P_2$ vs. t for the non-adiabatic collision of $H^+$ with $H_2$ on the lowest two $H_3^+$ surfaces. n=4, $E_{tot}$= -1.9175 e.V., $x_1^i$= 2.17 $a_o$ and $P_{z_1}^i$ = -.635 $m_p a_o \tau^{-1}$.

$\overline{W}$ is shown in Fig. (81) and one sees that after the collision $\overline{W}$ undergoes small oscillations. Thus one would expect a small final value of $P_2$.

$P_1$ and $P_2$ are shown in Fig (82) and again there is considerable structure. From Fig. (79) one sees that the initial increase in $P_2$ is due to an expansion of BC. BC then contracts and $P_2$ remains constant. As BC again expands across the seam $P_2$ starts to oscillate between small values and values that are close to 0.7. The oscillations in $P_2$ begin to decrease as A crosses the seam. The second set of oscillations are due to an expansion of AB followed by a contraction of BC. The oscillations are small since the couplings in this region are small. The increase in the final set of oscillations is due to C crossing the seam as it exits. The oscillations decrease as AB contracts and $P_2$ attains a final value of about 0.1.

As a final comment one notices that the non-adiabatic effects are much more pronounced in the initial part of the collision. This gives support to the mechanism that predicts rearrangement since its prediction is correct even when the non-adiabatic effects are large

### 6-3 Experimental Studies

The earlier experimental studies involving the collision of a proton with $H_2$ focused on obtaining probabilities of electron transfer as a function of the initial energy of the proton at a fixed laboratory angle (Ziemba, Lockwood, Morgan and Everhart, 1960). The range of energy of the proton was between one and 200 KeV and the laboratory angle was in the neighborhood of 5°. For such large proton energies this angle corresponds to almost head on collisions. The study done by Ziemba et al. (Ziemba, Lockwood, Morgan and Everhart, 1960) showed that the system exhibited a resonant electron capture, i.e. the probability oscillated around a value of about .4. When the probability was plotted versus the reciprocal velocity it was found that the spacings between adjacent resonances were almost the same. A comparison of the probability of electron transfer for the systems $H^+$, $H_2$ and $H^+$, H was done by Lockwood and Everhart (Lockwood and Everhart, 1962) and their results showed that the resonances for the two systems occurred at nearly the same energies. The positions of the resonances for the system $H^+$, H is well understood and can be simply related to the number of times the electron jumps from one proton to the other. This suggests a similar mechanism for $H^+$, $H_2$.

The next series of experiments to be considered here used a much lower kinetic energy for the incoming ion. The study by Krenos and Wolfgang (Krenos and Wolfgang, 1970) measured the relative yields in the forward direction of the reactive products (products corresponding to rearrangement, electron transfer and electron transfer with rearrangement) with the initial kinetic energy of the ion between 1 and 8 e.V. As expected, their results showed that below the threshold for molecular ion formation, about 1.8 e.V., reactive products due to rearrangement only were observed and their relative yields decreased as the energy increased up to about 6 e.V. As the energy increased above threshold, the relative yields for electron transfer processes increased sharply and then began to decrease in the neighborhood of 3 e.V. Between 2 and 5 e.V. the relative yields for the electron transfer processes were comparable to the one for rearrangement only and in some cases were even dominant.

One of the hopes of this experiment was to find a simple mechanism, i.e. complex formation or direct interaction, that would account for the results. In the study of $D^+$ colliding with HD it was found that the ratio of the relative yield of $HD^+$ to $D_2^+$ was roughly 2.1. This is what one would expect if a long lived complex were formed. However in the study of $H^+$ colliding with $D_2$ the relative yield of $D_2^+$ was about twice that of $HD^+$ which indicated a more direct mechanism. This led to their conclusion that only one simple mechanism would not be able to account for all of the results. Another observation worth noting is that there was a large tendency to transfer energy from translational to vibrational modes.

Similar results were obtained by Holliday et. al. (Holliday, Muckerman and Friedman, 1971). They measured cross sections for the reactive products of collisions of $D^+$ with $H_2$, $H^+$ with $D_2$ and $D^+$ with HD with the incident ion energy between 1 and 8 e.V. They again found that some results indicated the formation of a complex while others seemed to involve direct processes. Their conclusions were that complex formation was important for incoming ion energies less that 4 e.V. but that direct processes dominated at higher energies. They also found a large tendency to transfer energy from translational to vibrational modes.

Cross sections for the reactive products resulting from the collisions between $H^+$ and $D_2$ with the incident proton energy between .3 and 100 e.V. were measured by Maier (Maier, 1971). The increased range of proton energy allows the investigation of the effect of the breakup channel which has a center of mass threshold of about 5 e.V. They found that the total reaction cross section was much smaller than the Langevin cross section (Gioumousis and Stevenson, 1958). The values smaller that theoretically predicted were also observed by the previous authors.

Also obtained in this study were the branching ratios for the reactive products. The branching ratio is defined as the cross section for the particular reactive product divided by the sum of the cross sections for all reactive products. As was expected, the branching ratio for $D^+$ below the threshold for molecular ion formation was one. Above threshold it sharply decreased and reached a minimum at a center of mass energy of about 5 e.V. It then increased by a factor of three between 5 and 10 e.V. and remained fairly constant above 10 e.V. This increase is probably due to $D^+$ formed through a breakup process. The branching ratio for $D_2^+$ is zero for center of mass proton energies less than about 2 e.V. It increases rapidly between 2 and 5 e.V. and levels off at a value greater than .5 for energies greater than 5 e.V. Thus electron transfer is the dominant process above 5 e.V The branching ratio for $HD^+$ rises sharply as the energy is increased above threshold. It reaches a maximum in the neighborhood of 2.5 e.V. and quickly decreases to small values as the energy increases. This is further evidence that complex formation is important for low energies but that at higher energies direct processes dominate.

A rather extensive study of this system with the collision energy between 1 and 8 e.V. was done by Krenos et al. (Krenos, Preston, Wolfgang and Tully, 1974). They studied the collisions of $H^+$ with $D_2$, $D^+$ with HD and $D^+$ with $D_2$ and obtained the cross sections for the various reactive products. They compared these with those obtained in the previous studies and found that there was fairly good agreement.

A crossed molecular beam arrangement was used in this study to obtain a velocity analysis of the products at several lab angles. These results were compared to theoretical calculations (to be discussed in the next section) to give a better understanding of the mechanics that govern the reactions as a function of the initial collision energy. In general they found that, for the initial diatomic in the lowest vibrational level, non-adiabatic effects were not important as the particles approached each other. This is because the vibrations of the diatomic are not large enough to reach the avoided crossing. As the particles get close together they enter the deep well region of the lower surface. Since the surfaces are far apart in this region non-adiabatic effects are again unimportant so that the nuclear motions take place on the lowest surface. This well region was responsible for complex formation and for the conversion of kinetic to internal energy. As the particles separated, non-adiabatic affects became important and in some cases there were numerous crossings of the seam.

Some insights into the mechanisms that led to final nuclear configurations were also obtained. It was found that above a center of mass collision energy of 4.5 e.V. complexes no longer formed. This was expected since the dissociation energy of the initial diatomic is 4.5 e.V. and for a collision energy above this there is no way that energy can be shared among the three particles to give a stable complex. It was shown that above 7 e.V. velocity contours from theoretical calculations using hard sphere potentials agreed fairly well with experimental ones. This indicated that, in this region of energy, nuclear motion is governed mostly by repulsive forces and that direct processes, i.e. knockout, etc., led to rearrangement. The theoretical calculations also showed that as the energy decreased below 4.5 e.V. the collision time increased which indicated that complex formation was important.

A further experiment done by Ochs and Teloy (Ochs and Teloy, 1974) focused on obtaining more accurate cross sections for the reactive products. The interesting aspect of this work was that the agreement with previous experimental studies was only fair but the agreement with the theoretical results was excellent.

The crossed beam experiment done by Lees and Rol (Lees and Rol, 1975) concentrated on obtaining energy distributions for the reactive products. Their agreement with the theoretical predictions was also excellent. The added feature in this experiment was that the initial diatomic could have a vibrational quantum number of up to seven. Their results indicated that the higher vibrational levels noticeably enhanced the formation of molecular ions.

## 6-4 Theoretical Studies

Since the $H_3^+$ system has only two electrons, it is possible to obtain the potential energy surfaces by using ab initio methods. This is of particular importance in trajectory calculations because comparing experimental results to ab initio theoretical results should give some indication of the validity of using classical trajectories as a tool to study chemical reactions. This was one of the primary incentives for the calculations done by Csizmadia et al. (Csizmadia, Polanyi, Roach and Wong, 1969) They calculated differential cross sections for the production of $H^+$ from the reaction of $D^+$ with $H_2$ for initial center of mass relative energies of 3 and 4.5 e.V. The three dimensional classical trajectories were calculated using the lowest adiabatic surface which was determined by ab initio means. When compared to experimental results it was found that the cross sections were too large. This was not too surprising since this calculation neglected the energetically open channels corresponding to electron transfer processes. This work was important however because it gave motivation for the experiments to be done.

A calculation referred to in the previous section that incorporated the upper surface was done by Tully and Preston (Tully and Preston, 1971) Comparison to experimental results were also made (Krenos, Preston, Wolfgang and Tully, 1974). The theoretical approach, termed the Trajectory Surface Hopping model, handled the dynamics of the reaction in the following way Initially, the diatomic ($D_2$) was in a low vibrational level so that seam crossings did not occur prior to the collision. In this region, nuclear motion evolved on the lower surface only. When the incoming ion ($H^+$) closely approaches the diatomic, the particles are in the deep well region of the lower potential end, since the couplings are small, nuclear motion is again governed by the lowest surface. As the particles separate, seam crossings can occur so that non-adiabatic effects must be included. If a seam crossing occurs the trajectory splits into two trajectories corresponding to motion on each surface. The trajectories are assigned probabilities that are determined from the non-adiabatic couplings. These couplings are rather easy to obtain since the surfaces are obtained from a Diatomics in Molecules approach. Further seam crossings result in further splitting of the trajectories so that a unique initial trajectory usually evolves into a number of weighted final trajectories all of which have unique final conditions. Cross sections are obtained by a Monte Carlo averaging over the initial conditions. Other details such as the assignment of positions and moments after a surface crossing has occurred are discussed in the articles referred to above.

The excellent agreement between theory and experiment was very encouraging since it showed that trajectory calculations could still be used for multi-surface systems if the couplings could be incorporated in a reasonable way.

As is apparent from the previous section, this is important because trajectory calculations combined with experimental data often lead to a better understanding of the dynamics of the reaction.

A quantum mechanical calculation for the collinear $H_3^+$ system was done by Top and Baer (Top and Baer, 1977). They used a diabatic electronic representation and the total energy was in the few e.V. range. Their study showed that for a given total energy, the probability for electron transfer was greatly enhanced if the diatomic was initially in a higher (≥4) vibrational level. Since the n = 4 vibrational level of $H_2$ is nearly coincident in total internal energy with the n = 0 vibrational level of $H_2^+$, this behavior was attributed to a resonance between these two levels. For lower initial vibrational levels they argued that the deep well in the lower surface caused vibrational excitation which populated the upper vibrational levels. As the particles leave the reaction zone resonances between these populated levels and those of the $H_2^+$ lead to electronic transitions. We shall return to some of the more numerical aspects of this study in the next section.

## 6-5 Comparisons

Since this work only considers the collinear configurations of the $H_3^+$ system no direct quantitative comparisons can be made with either the Trajectory Surface Hopping studies or the experimental studies discussed in Section 6-3.

It is encouraging to see however that some of their conclusions are borne out in this study also. The calculations discussed in Section 6-2 also indicate that non-adiabatic effects are most important as the particles are leaving the collision region. In other words, the nuclear motions before the collision and while the particles are all close together are governed by the lowest surface. The simple mechanism suggested in Section 6-2a, that determines whether rearrangements take place for the adiabatic test case, seems to hold for the two-surface case also. This supports the conclusions discussed in Sections 6-3 and 6-4 that the lowest surface determines whether rearrangements occur. In concurrence with the experimental and trajectory studies, the results of Section 6-2 also indicate that there is a large tendency to transfer energy between vibrational and translational modes. Finally the results of Section 6-2 indicate that they can not be toatally explained in terms of either direct mechanisms or complex formation. This is not unexpected since the total energy used in this study is between the higher energies where direct processes dominate and lower energies where complex formation is important.

The quantum mechanical calculation by Top and Baer determined the total electronic transition probabilities for a number of total energies. As discussed in Section 3-7, it is possible to construct total electron transfer probabilities using this formalism if appropriate averages are taken over the initial conditions.

For the $H_3^+$ system, the initial conditions for the diatomic that need to be averaged over are the vibrational coordinate and momenta of the initial $H_2$ diatomic. The vibrational distributions for the coordinate are proportional to the eigenfunctions of the Morse potential (Morse, 1929). The reason why they are only proportional to these functions is that some of the quantum mechanical distribution lies outside of the classical turning points which is physically meaningless in this formalism. Instead one must require that the Morse eigenfunctions are normalized between the classical turning points. This is easily done by determining the integral of $|\psi_n|^2$ between the turning points, where $\psi_n$ is the Morse eigenfunction for the $n^{th}$ vibrational level. The normalization constant is then defined as the inverse square root of this integral.

There still remains the problem of averaging over the initial momentum of the diatomic. In actuality the charge transfer probability should be found by integrating $P_{2\to1}(E,E_n,z,P)|\psi_n(z)|^2|\psi_n(P)|^2$ over the curve of constant $E_n$ in classical phase space. However it was assumed for simplicity that, for a given value of the vibrational coordinate, the corresponding momentum may be either positive or negative with equal probability. With this assumption, the total electron transfer probability is defined as

$$P_{2+1}(E,E_n,Z) = \frac{1}{2}\{ \int dz P^{+}_{2+1}(E,E_n,z,Z)|\psi'_n(z)|^2$$

$$+ \int dz P^{-}_{2+1}(E,E_n,z,Z)|\psi'_n(z)|^2 \} \tag{6-43}$$

where $P^{+}$($P^{-}$) corresponds to a positive (negative) initial diatomic momenta and the prime over $\psi_n$ indicates that it is normalized between the turning points. Z is the initial relative Jacobi coordinate Obviously the integrals are taken between the turning points.

As seen in Eq. (6-43), the total electron transfer probability still depends on the initial relative distance Z. It is shown in Appendix three that averaging over Z leads to

$$P_{2+1}(E , E_n) = \frac{1}{2(z_+ - z_-)} \int_{z_-}^{z_+} \{ P^{+}_{2+1}(E , E_n, Z_0, z)$$

$$+ P^{-}_{2+1}(E, E_n, Z_0, z)\} dz \tag{6-44}$$

where $z_+$($z_-$) is the outer (inner) turning point and $Z_0$ is the initial relative distance which is large enough so that the interaction between A and BC is negligible. If the integral in Eq. (6-44) is found using N equally spaced points of z, $z_- \leq z \leq z_+$ , a convenient variable for displaying results is given by

$$y = 1 + \frac{(N - 1)}{(z_+ - z_-)} (z - z_-) \tag{6-45}$$

Each equally spaced value of z corresponds to an integer value of y between 1 and N .

The results for the integrands $P^{\rightarrow}_{2\leftarrow 1}$ and $P^{\leftarrow}_{2\leftarrow 1}$ in Eq. (6-44) for n = 0 to n = 4 are shown in Figs. (83) through (87) respectively. In each case 50 equally spaced values of z were used so that y goes from 1 to 50. A logarithmic scale for the probabilities was used in order to show more of their behavior when the probabilities are small. The points labeled with a Δ correspond to cases where dissociation of the complex did not occur within a time of 50 τ. When necessary, lines between adjacent points were drawn so that the behavior of the probabilities would be easier to follow. All calculations were done at a total energy of -1.918 e.V and the initial conditions were determined as in Section 6-2. The R|N notation significies that one is going from a region where rearrangements occur to a region where non-rearrangements occur. N|R has a similar meaning.

One sees in Figs. (83) through (85) that, for $n \leq 2$, there are two fairly localized regions where the probability is larger than 0.1. As is seen in Figs. (86) and (87) this is no longer the case for $n \geq 3$. One notices that the regions where the probability is greater than 0.1 are considerably more extensive for $n \geq 3$ which should give rise to substantially larger total electron transfer probabilities. A rough estimate of the behavior of the total electron transfer probability as a function of n can be made by simply counting the number of times the integrand in Eq. (6-44) is greater than 0.1. For $n = 0, 1, 2, 3$ and 4, one finds a value greater than 0.1 for the integrand 23, 16, 18, 32 and 57 times respectively. This indicates that the total electron transfer probability should not change very much for $n \leq 2$ and that it should noticeably increase for $n \geq 3$.

Total electron transfer probabilities were obtained by integrating the results shown in Figs. (83) through (87) using the trapezoidal rule. The final probabilities for trajectories that did not dissociate within 50 τ, i.e. points labeled by Δ in the figures, were assigned a value of $0.5 \pm 0.5$. The results of this work are compared to those estimated from Fig. (11) in the paper by Top and Baer (Top and Baer, 1977) in Table I. The error estimates arise from trajectories that did not dissociate. The agreement for $n = 0$ and 4 is quite good and well within the estimated errors. For $n = 1$ the agreement is not so good but the results are still within 40% of each other. It is encouraging to see that both sets of results show relatively little change in the probability for n going from 0 to 1. It is also pleasing to see that both studies show a sharp increase in the probability for $n = 4$. Sources of disagreement could arise from excluding the region of configuration space beyond the turning points and from not using enough initial values of the diatomic coordinate. The approximations used in obtaining Eq. (6-43) could also be a source

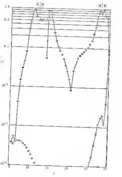

Fig. (83) The results for $P^+_{2+1}$ (——) and $P^-_{2+1}$ (---) as a function of $s^i_1$. n=0 and $E_{tot}$= -1.9175 e.V.

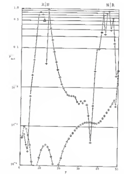

Fig. (84) The results for $P^{+}_{2+1}$ (——) and $P^{-}_{2+1}$ (---) as a function of $z_1^1$. n=1 and $E_{tot}$= -1.9175 e.V.

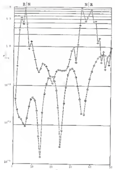

Fig. (85) The results for $P^{+}_{2+1}$ (——) and $P^{-}_{2+1}$ (----) as a function of $a^{i}_{1}$. n=2 and $E_{tot}$ = -1.9175 e.V.

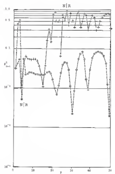

Fig. (86) The results for $P^{+}_{2+1}$ (——) and $P^{-}_{2+1}$ (---) as a function of $z^{1}_{1}$. n=3 and $E_{tot}$= -1.9175 e.V.

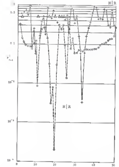

Fig. (87) The results for $P^{+}_{2+1}$ (——) and $P^{-}_{2+1}$ (---) as a function of $z^{i}_{1}$. n=4 and $E_{tot}$= -1.9175 e.V.

TABLE I

| n | $P_{2+1}$ a) | $P_{2+1}$ b) |
|---|---|---|
| 0 | .15±.02 | .14 |
| 1 | .09±.01 | .16 |
| 2 | .12±.01 | — |
| 3 | .22±.02 | .07 |
| 4 | .29±.04 | .29 |

a) This work
b) Estimated from Fig. (11) in the paper by Top and Baer (Top and Baer, 1977)

of error. All of these sources of error can be numerically checked and could be the subject of future studies.

The most noticeable disagreement in the results occurs for n = 3. This was called an "intermediate case" (intermediate in the sense that the mechanism for charge transfer is neither totally due to resonances for $n \geq 4$ nor to populating the upper vibrational levels via the deep well for $n \leq 2$) in the quantum mechanical study and was not further considered. The reason for such a low probability is not clear. It would seem that an "intermediate case" would lead to results somewhere between the ones for $n \leq 2$ and the ones for $n \geq 4$.

## 6-6 Conclusions

This work primarily addressed two fundamental problems in scattering theory. One of the problems centered around the electronic basis used in the expansion for the full solution. The other problem focused on how to handle the problem for the nuclear degrees of freedom when more than one electronic basis function is included in the expansion.

In chapter two it was shown that the Hamiltonian for the nuclear degrees of freedom was not hermitian in the adiabatic electronic representation. This is of little consequence when only one electronic state is energetically accessible. However, when it became necessary to include more than one electronic state it was pointed out that other electronic representations could be more suitable.

The diabatic and almost adiabatic representations discussed in sub-sections 2-2b and 2-2c respectively were shown to restore hermiticity to the Hamiltonian. The minimization procedure discussed in Section 2-3 was shown to lead to well behaved potentials but its usefulness depended on whether the coupling terms after transformation could be neglected or not.

Given a suitable electronic basis, the nuclear problem was the subject matter of chapter three. It was shown that if the nuclear expansion coefficients for the time independent Schrödinger equation are written in the form of a common eikonal and the short wavelength approximation is used, a transformation from coordinate to the time variable led to a set of coupled first order differential equations that determined the nuclear positions, momenta and expansion coefficients. It was seen that this set of coupled equations is formally equivalent to Hamilton's equations of motion where the independent variables now include the real and imaginary parts of the nuclear expansion coefficients. One of the principal advantages that this formalism provided was that lengthy expansions in internal nuclear states were avoided.

An application to the collinear $H_3^+$ system was made in chapters four through six. The trajectories presented in Section 6-2 indicated how useful they can be in obtaining a better understanding of the basic mechanisms involved in chemical reactions. It was very encouraging to see that many of the conclusions about the mechanisms of the $H^+ + H_2$ reaction made from the experimental and Trajectory Surface Hopping studies were supported by this work also. The reasonable agreement with the quantum mechanical study indicated that this approach is capable of yielding physically meaningful results even when light nuclear masses are involved.

As was pointed out in chapter three, one of the consequences of using a common eikonal is that the final trajectories evolve on an average potential energy surface. Although expressions such as Eq. (3-108) allow one to determine total electron probabilities, one still needs to determine cross sections in order to make direct comparisons with experiment. The problem that arises is that cross sections are defined with quantum mechanical initial and final states that evolve on their appropriate potential energy surfaces. The corresponding trajectories should evolve initially and finally on only one surface. As was seen in Section 6-2 this was rarely the case.

This problem could in principle be solved by finding an expression that relates the initial conditions to the final conditions. The initial and final conditions correspond to points in phase space that lie on constant energy curves of the initial and final internal energies respectively.

Once these expressions have been found the cross sections can be obtained in a straightforward manner (Micha, 1982) by either conservation of flux or from transition matrix elements. The cross sections obtained from transition matrix elements should be more reliable since they include interference terms.

In closing, it should be pointed out that this work is rather preliminary and much more remains to be done. In particular, an extension to three dimensions would be important because it would allow more direct comparisons to experiments and Trajectory Surface Hopping studies. This would also allow one to address the problem of obtaining cross sections. It has also recently been shown (Micha, 1982) that the equations obtained in chapter three correspond to the first term in the expansion of the nuclear wave function in powers of the local deBroglie wavelength. Inclusion of the next term in this collinear case should give some indication of the error introduced by using the short wavelength approximation. Finally an extension to systems with more than two surfaces would also be of value.

# APPENDIX 1
## HYPERSPHERICAL COORDINATES

Fairly recently, a number of studies of reactive three-body collisions have been made that employ hyperspherical coordinates (Kuppermann, 1975; Hauke, Manz and Römelt, 1980). As was discussed in chapter five, the reason for this is that these coordinates describe both reactants and products so that coordinate transformations are avoided except in the asymptotic regions. This appendix will extend the developments of Section (5-1) to three dimensions. The development will somewhat follow the one given by Delves (Delves, 1960).

To begin with we will consider three particles, A, B and C with masses $m_A$, $m_B$ and $m_C$ respectively in the center of mass coordinate system. In this coordinate system there are six degrees of freedom which can be defined by the Jacobi coordinates. Introducing the Jacobi coordinates for channel 1, (A,BC), one has

$$\underset{\sim}{r} = \underset{\sim}{r}_B - \underset{\sim}{r}_C \qquad (A1-1)$$

and

$$\underset{\sim}{z} = \underset{\sim}{r}_A - \frac{m_B\underset{\sim}{r}_B + m_C\underset{\sim}{r}_C}{m_B + m_C} \qquad \text{(A1-2)}$$

where $\underset{\sim}{r}_A$, $\underset{\sim}{r}_B$ and $\underset{\sim}{r}_C$ are vectors from the center of mass of the three particles to particles A, B and C respectively and the channel subscript 1 has been suppressed. The time independent Schrödinger equation in this coordinate system is given by

$$\left\{-\frac{\hbar^2}{2m}\nabla^2_{\underset{\sim}{z}} - \frac{\hbar^2}{2M}\nabla^2_{\underset{\sim}{Z}} + V(\underset{\sim}{z},\underset{\sim}{Z}) - E\right\}\psi(\underset{\sim}{z},\underset{\sim}{Z}) = 0 \qquad \text{(A1-3)}$$

where

$$m = \frac{m_B m_C}{m_B + m_C} \qquad \text{(A1-4)}$$

and

$$M = \frac{m_A(m_B + m_C)}{m_A + m_B + m_C} \qquad \text{(A1-5)}$$

and for simplicity we have assumed only one electronic state is needed in the Born-Oppenheimer expansion. Letting $\underset{\sim}{z} = (z,\Omega_1)$ and $\underset{\sim}{Z} = (Z,\Omega_2)$ and expanding the solution as

$$\psi(\underset{\sim}{z},\underset{\sim}{Z}) = \sum_{\ell_1}\sum_{\ell_2} R^{\ell_1\ell_2}(z,Z)\; Y_{\ell_1}(\Omega_1)\; Y_{\ell_2}(\Omega_2) \qquad \text{(A1-6)}$$

where

$$\int d\Omega_1 d\Omega_2 Y^*_{\ell_1'}(\Omega_1)\ Y^*_{\ell_2'}(\Omega_2)\left\{ -\frac{\hbar^2}{2m}\nabla^2_{\underset{\sim}{z}} - \frac{\hbar^2}{2M}\nabla^2_{\underset{\sim}{Z}} \right\} Y_{\ell_1}(\Omega_1) Y_{\ell_2}(\Omega_2)$$

$$= \delta_{\ell_1\ell_1}\delta_{\ell_2\ell_2}\left\{ -\frac{\hbar^2}{2mz^2}\frac{\partial}{\partial z}\left(z^2\frac{\partial}{\partial z}\right) - \frac{\hbar^2}{2MZ^2}\frac{\partial}{\partial Z}\left(Z^2\frac{\partial}{\partial Z}\right) \right. \tag{A1-7}$$

$$\left. + \frac{\hbar^2\ell_1(\ell_1+1)}{2mz^2} + \frac{\hbar^2\ell_2(\ell_2+1)}{2MZ^2} \right\}$$

gives

$$\left\{-\frac{\hbar^2}{2mz^2}\frac{\partial}{\partial z}\left(z^2\frac{\partial}{\partial z}\right) - \frac{\hbar^2}{2MZ^2}\frac{\partial}{\partial Z}\left(Z^2\frac{\partial}{\partial Z}\right) + \frac{\hbar^2\ell_1(\ell_1+1)}{2mz^2}\right.$$

$$\left. + \frac{\hbar^2\ell_2(\ell_2+1)}{2MZ^2} - E\right\} R^{\ell_1\ell_2}(z,Z) + \sum_{\ell_1'}\sum_{\ell_2'} W^{\ell_1\ell_2\ell_1'\ell_2'}(z,Z)\ R^{\ell_1'\ell_2'}(z,Z) = 0 \tag{A1-8}$$

where

$$W^{\ell_1\ell_2\ell_1'\ell_2'}(z,Z) = \int d\Omega_1 d\Omega_2 Y^*_{\ell_1}(\Omega_1) Y^*_{\ell_2}(\Omega_2) V(z,Z,\Omega_1,\Omega_2)$$

$$\times\ Y_{\ell_1'}(\Omega_1) Y_{\ell_2'}(\Omega_2) \quad . \tag{A1-9}$$

If $W^{\ell_1\ell_2\ell_1'\ell_2'}$ is zero the solutions of Eq. (A1-8) could be written in terms of a product of functions of z and Z but their eigenvalue spectrum would both be continuous. Defining

$$z = \left(\frac{M}{m}\right)^{\frac{1}{2}} r \sin\alpha \qquad \text{(A1-10)}$$

and

$$Z = \left(\frac{m}{M}\right)^{\frac{1}{2}} r \cos\alpha \qquad \text{(A1-11)}$$

Eq. (A1-8) becomes

$$\Big\{ -\frac{1}{r^5}\frac{\partial}{\partial r}\left(r^5\frac{\partial}{\partial r}\right) - \frac{1}{r^2\sin^2\alpha\cos^2\alpha}\frac{\partial}{\partial\alpha}\left(\sin^2\alpha\cos^2\alpha\,\frac{\partial}{\partial\alpha}\right)$$

$$+ \frac{\ell_1(\ell_1+1)}{r^2\sin^2\alpha} + \frac{\ell_2(\ell_2+1)}{r^2\cos^2\alpha} - k^2\Big\} \overset{\ell_1\ell_2}{R}(r,\alpha) \qquad \text{(A1-12)}$$

$$+ \sum_{\ell'_1}\sum_{\ell'_2} \overset{\ell_1\ell_2\ell'_1\ell'_2}{W}(r,\alpha)\ \overset{\ell'_1\ell'_2}{R}(r,\alpha) = 0$$

where

$$k^2 = \frac{\sqrt{mM}}{\hbar^2}\,E \qquad \text{(A1-13)}$$

and r and α are the hyperspherical coordinates. The volumn element is

$$d\underset{\sim}{z}\,d\underset{\sim}{Z} = r^5\sin^2\alpha\,\cos^2\alpha\,d\Omega_1 d\Omega_2\,dr\,d\alpha \quad . \qquad \text{(A1-14)}$$

Letting

$$\overset{\ell_1\ell_2}{R}(r,\alpha) = r^{-5/2}\sin^{-1}\alpha\,\cos^{-1}\alpha\,\overset{\ell_1\ell_2}{\Lambda}(\alpha)\,\overset{\ell_1\ell_2}{R}(r) \qquad \text{(A1-15)}$$

where $\overset{\ell_1\ell_2}{A}$ satisfies

$$\left\{ \frac{d^2}{d\alpha^2} + 4 - \frac{\ell_1(\ell_1+1)}{\sin^2\alpha} - \frac{\ell_2(\ell_2+1)}{\cos^2\alpha} \right\} \overset{\ell_1\ell_2}{A}(\alpha) = -B \overset{\ell_1\ell_2}{A}(\alpha) \qquad \text{(A1-16)}$$

results in $\overset{\ell_1\ell_2}{R}(r)$ satisfying an ordinary differential equation. The solutions of Eq. (A1-16) that are regular at $\alpha=0$ and $\pi/2$ are given by

$$\overset{\ell_1\ell_2}{A}(\lambda;\alpha) = A \sin\alpha^{\ell_1+1} \cos\alpha^{\ell_2+1} {}_2F_1(-\lambda, \ell_1+\ell_2+\lambda+2; \ell_1+\tfrac{3}{2}; \sin^2\alpha) \qquad \text{(A1-17)}$$

with

$$B = (\ell_1+\ell_2+\lambda)(\ell_1+\ell_2+2\lambda+4) \qquad \text{(A1-18)}$$

where A is a normalization constant, $\lambda=0,1,2,\cdots$ and ${}_2F_1$ is the confluent hypergeometric function (Bucholtz, 1969). As is apparent from Eq. (A1-17), introducing hyperspherical coordinates allows one to expand the solution, $\overset{\ell_1\ell_2}{R}(r)$ in a set of functions of $\alpha$ that have a discrete spectrum. The ordinary differential equation that $\overset{\ell_1\ell_2}{R}(r)$ satisfies is given by

$$\left\{ \frac{d^2}{dr^2} - \frac{\ell(\ell+1)}{r^2} + k^2 \right\} \overset{\ell_1\ell_2\lambda}{R}(r) - \sum_{\ell_1'} \sum_{\ell_2'} \sum_{\lambda'} \overset{\ell_1\ell_2\lambda\ell_1'\ell_2'\lambda'}{G}(r) \overset{\ell_1'\ell_2'\lambda'}{R}(r) = 0 \qquad \text{(A1-19)}$$

where

$$s = \ell_1 + \ell_2 = 2k + \frac{3}{2} \tag{A1-20}$$

and

$$\overset{\ell_1 \ell_2 \lambda \ell_1' \ell_2' \lambda'}{G(r)} = \int d\Omega_1 d\Omega_2 d\alpha \overset{\ell_1 \ell_2}{A}(\lambda;\alpha) Y^*_{\ell_1}(\Omega_1) Y^*_{\ell_2}(\Omega_2)$$

$$\times \quad V(r,\alpha,\Omega_1,\Omega_2,) Y_{\ell_1'}(\Omega_1) Y_{\ell_2'}(\Omega_2) \overset{\ell_1' \ell_2'}{A}(\lambda';\alpha) \quad . \tag{A1-21}$$

One sees in Eq. (A1-19) that $\overset{\ell_1 \ell_2 \lambda}{R}$ satisfies an equation that is formally equivalent to the two body problem. The essential difference is that the potential in the three body problem is considerably more complicated.

## APPENDIX 2
## COMPUTER PROGRAM

Main Program-

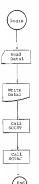

Datal consists of the parameters for the model coupling, the parameters for the diatomic potentials, certain physical constants such as the masses of the particles, the value of h, etc. and the parameters used to terminate the calculation.

SCCST is a subroutine that calculates certain mass dependent constants used throughout the program.

SCTRJ is a subroutine that determines the initial conditions and calls the integration subroutine.

Subroutine SCTRJ:

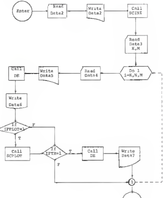

Data2 contains information for taking numerical derivatives, parameters needed in the integration subroutine, DE, and information about the initial state such as its total energy, the vibrational state, the initial relative distance, the number of initial states, etc.

Subroutine SCINI determines the initial conditions for the nuclear variables in terms of both hyperspherical and Jacobi coordinates. The initial conditions are stored in an array and used in the Do loop.

Data3 contains two integers K and M. If M=2 and K=1, only trajectories with positive initial values of the diatomic momentum will be run. If M=2 and K=2 only negative initial values will be run. For K=1 and M=1, all trajectories will be run.

Data4 consists of two sets of data. The first set contains arguments for time reversal and arguments used in the integration subroutine, DE, to print intermediate values of the trajectories and energies. The second set determines which trajectories will be plotted in subroutine SCPLOT.

Data5 are the initial conditions in both hyperspherical and Jacobi coordinates.

Subroutine DE is a well documented subroutine (Shampine and Gordon, 1975) that integrates the equations. Some modifications were made in order to print intermediate values of the trajectories and energies and form arrays used for plotting. The procedure for terminating the calculations discussed in Section 6-2 was also implemented. Subroutine SCPLOT plots, based on the information in Data4, any or all of the trajectories.

Data7 contains the final values of the trajectories for the time reversed studies.

# APPENDIX 3
## THE TOTAL ELECTRON TRANSFER PROBABILITY

In Section E-5, the electron transfer probability as a function of the initial relative distance was defined as

$$P_{2+1}(E_T,E_n,Z) = \frac{1}{2}\int_{z_-}^{z_+} dz\, |\phi_n(z)|^2 (P^+_{2+1}(E_T,E_n,Z,z)$$

$$+ P^-_{2+1}(E_T,E_n,Z,z)) \qquad \text{(A3-1)}$$

where Z and z are the initial Jacobi coordinates, $z_-$ and $z_+$ are the turning points, $P^+_{2+1}$ and $P^-_{2+1}$ are the electron transfer probabilities for positive and negative values of the initial diatomic momentum and $\phi_n$ is the vibrational wave function for the diatomic in its initial vibrational state. In order to obtain the total electron transfer probability which depends only on the total energy ($E_T$) and the initial internal energy ($E_n$) an averate of $P_{2+1}(E_n,E_T,z)$ must be taken over the initial relative distance Z. This gives

$$P_{2+1}(E_T,E_n) = \frac{1}{2(Z_2 - Z_1)}\int_{z_-}^{z_+} dz|\phi_n(z)|^2 \int_{Z_1}^{Z_2} dZ$$

$$\{(P^+_{2+1}(E_T,E_n,Z,z) + P^-_{2+1}(E_T,E_n,Z,z))\} \qquad \text{(A3-2)}$$

where $Z_2 >> Z_1$ and $Z_1$ is large enough so that the interaction between the incoming particle and the diatomic is negligible. Defining

$$P_{2+1}^{\pm}(E_T,E_n,Z,z) = P_{2+1}^{+}(E_T,E_n,Z,z) + P_{2+1}^{-}(E_T,E_n,Z,z)$$

Eq. (A3-2) becomes

$$P_{2+1}(E_T,E_n) = \frac{1}{2(Z_2 - Z_1)} \int_{z_-}^{z_+} dz\,|\psi_n(z)|^2 \int_{Z_1}^{Z_2} dZ P_{2+1}^{\pm}(E_T,E_n,Z,z). \qquad \text{(A3-4)}$$

Initially the diatomic molecule is vibrating in the nth vibrational level. The frequency of the vibration is given by

$$\omega = \frac{E_n}{\hbar} \qquad \text{(A3-5)}$$

where $E_n$ is the vibrational energy measured from the bottom of the well. The essential point to recognize is that, for Z in the asymptotic region, the diatomic will return to its initial values in phase space, $z(t_1)$, $P_z(t_1)$ when t equals $t_1 + \omega^{-1}$, $t_1 + 2\omega^{-1}$, etc With this in mind, consider the following two trajectories The first trajectory begins at the initial time $t_1$ and initial conditions given by $Z_1$ and $z_1$. The second trajectory starts at $t_2 = t_1 - \omega^{-1}$ with initial conditions $Z_1 + \Delta$ and $z_1$ where

$$\Lambda = V_Z \nu^{-1} \qquad \text{(A3-6)}$$

and $V_Z$ is the relative velocity. One sees that $\Lambda$ is just the distance that A travels during a complete vibration of BC. When the time of the second trajectory equals $t_1$, one has that the relative distance is $Z_1$ and the diatomic distance is $z_1$ (See Fig. (38)). Thus the second trajectory that started at $t_2$ passes through the initial conditions of the first trajectory at the time $t_1$ which means that they must give the same result of $P^{\pm}_{2+1}$. Since the results do not depend on the origin of time one has that, in general,

$$P^{\pm}_{2+1}(E_T,E_n,Z_1 + N\Lambda,z_1) = P^{\pm}_{2+1}(E_T,E_n,Z_1 z_1) \qquad \text{(A3-7)}$$

where $N = 0,1,2,\ldots.$ This argument is true for all initial values of Z so that

$$\frac{\int_{Z_1}^{Z_1 + N\Lambda} dZ P^{\pm}_{2+1}(E_T,E_n,Z,z)}{N\Lambda} = \frac{\int_0^{\Lambda} dX P^{\pm}_{2+1}(E_T,E_n,X,z)}{\Lambda} \qquad \text{(A3-8)}$$

where

$$X = Z - Z_1 \quad . \qquad \text{(A3-9)}$$

The essential question is whether the integral in Eq. (A3-8) depends on z. Intuitively, it would seem that it would not,

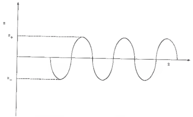

Fig. (88) Schematic illustration of the asymptotic behavior of the Jacobi coordinates.

since the integral over X contains all possible values of $F^{\pm}_{2+1}$. Changing z would change the values of the integrand but leave the integral unchanged. To see this assume that

$$\int_0^{\Lambda} dXF^{\pm}_{2+1}(X,z_1) = \int_0^{\Lambda} dXF^{\pm}_{2+1}(X,z_2) \qquad \text{(A3-10)}$$

where the arguments $E_T$ and $E_n$ have been suppressed. The point $(X,z_2)$ can be expressed in terms of $z_1$ by setting

$$X' = X - \alpha \qquad \text{(A3-11)}$$

where

$$a = \frac{(z_2 - z_1)}{(z_+ - a_-)} V_z\omega^{-1} \quad . \qquad \text{(A3-12)}$$

Then

$$dX = dX' \qquad \text{(A3-13)}$$

so that

$$\int_0^{\Lambda} dXF^{\pm}_{2+1}(X,z_2) = \int_{-a}^{\Lambda-a} dX'F^{\pm}_{2+1}(X',z_1) = \int_0^{\Lambda} dyF^{\pm}_{2+1}(y,z_1) \qquad \text{(A3-14)}$$

where

$$y = X' + a \quad . \qquad \text{(3-15)}$$

Thus Eq. (A3-10) is satisfied so that the integral in Eq. (A3-10) does not depend on the initial value of z. Since the vibrational wave functions are normalized, Eq. (A3-4) becomes

$$P_{2+1}(E_T,E_n) = \frac{1}{2\Lambda}\int_0^{\Lambda} P^{\pm}_{2+1}(E_T,E_n,X,z_o)\,dX \qquad \text{(A3-16)}$$

where $z_o$ is the initial diatomic separation. Instead of averaging over X, one could just as well average over the initial coordinate of the diatomic which gives

$$P_{2+1}(E_T,E_n) = \frac{1}{2(z_+ - z_-)}\int_{z_-}^{z_+} P^{\pm}_{2+1}(E_T,E_n,X_o,z)\,dz$$

where $X_o$ is an arbitrary large initial relative distance

# REFERENCES

Abramowitz, M., and Stegun, I. A., *Handbook of Mathematical Functions*, New York: Dover, 1972.

Baer, M., Chem. Phys. Lett. 35, 112 (1975).

Baer, M., Drolshagen, G. and Toennies, J. P., J. Chem. Phys. 73, 1690 (1980).

Born, M. and Huang, K., *Dynamical Theory of Crystal Lattices*, Oxford Univ. Press, 1954, Appendix VIII.

Born, M. and Oppenheimer, J. R., Ann. Phys. 84, 457 (1927).

Briggs, J. S., Re. Prog. Phys. 39, 217 (1976).

Child, M. S., *Atom-Molecule Collision Theory. A Guide for the Experimentalist*, ed. R. R. Bernstein, New York: Plenum Press, 1979, ch. 13.

Csizmadia, I. G., Polanyi, J. C., Roach, A. C. and Wong, W. H., Can. J. of Chem. 47, 4097 (1969).

Delos, J. B., Rev. Mod. Phys. 53, 287 (1981)

Delos, J. B. and Thorson, W. R., J. Chem. Phys. 70, 1774 (1979).

Delves, L. M., Nucl. Phys. 20, 275 (1960).

Ellison, F. O., J. Am. Chem. Soc. 85, 3540 (1963).

Ellison, F. O., Huff, N. T. and Patel, J. C., J. Am. Chem. Soc. 85, 3544 (1963).

Evans, S. A., Cohen, J. S. and Lane, N. F., Phys. Rev. A4, 2235 (1971).

Gabriel, H. and Taulbjerg, K., Phys. Rev. A10, 741 (1974).

Garrett, B. C. and Truhlar, D. G. in *Modern Theoretical Chemistry: Advances and Perspectives*, 6, ed. D. Henderson, New York: Academic Press, 1980.

Gioumousis, G. and Stevenson, D. P., J. Chem. Phys. **29**, 294 (1958).

Hauke, G., Manz, J. and Romelt, J., J. Chem. Phys. **73**, 5040 (1980).

Holliday, M. G., Muckerman, J. T. and Friedman, L., J. Chem. Phys. **54**, 1058 (1971).

Krenos, J. R., Preston, R. K., Wolfgang, R. and Tully, J. C., J. Chem. Phys. **60** 1634 (1974)

Krenos, J. R. and Wolfgang, R., J. Chem. Phys. **52**, 5961 (1970).

Kuntz, P. J. and Roach, A. C., J. Chem. Soc., Faraday Trans. II, **68**, 259 (1972).

Kuppermann, A., Chem. Phys. Letts. **32**, 374 (1975).

Landau, L. D., Physik. Z. Sowjetunion **2**, 46 (1932).

Lees, A. B. and Rol, P. K., J. Chem. Phys. **63**, 2461 (1975).

Lichten, W., Phys. Rev. **131**, 229 (1963).

Lockwood, G. J. and Everhart, E., Phys. Rev. **125**, 567 (1962).

Maier, W. B., J. Chem. Phys. **54**, 2732 (1971).

McCarroll, R. in *Atomic Processes and Applications*, ed. P. G. Burke and B. L. Moiseiwitsch, Amsterdam: North-Holland, 1976, ch. 13.

McDowell, M. R. C. and Coleman, J. P., *Introduction to the Theory of Ion-Atom Collisions*. Amsterdam. North-Holland, 1970.

Messiah, A., *Quantum Mechanics*, Vol. I, New York: Wiley, 1966.

Meyer, H. and Miller, W. H., J. Chem. Phys. **75**, 2156 (1979).

Micha, D. A., to be published (1982).

Moffitt, W., Proc. Roy. Soc. (London) **A210**, 279 (1931).

Moiseiwitsch, B. L., in Quantum Theory I. Elements, ed. D. R. Bates; New York, Academic Press, 1961.

Morse, P., Phys. Rev. 34, 57 (1929).

Newton, R. G., Scattering Theory of Particles and Waves, New York: McGraw-Hill, 1966.

Nikitin, E. E., Theory of Elementary Atomic and Molecular Processes in Gases, Ely House, London: Oxford University Press, 1970.

Nimrich, R. W. and Truhlar, D. J., J. Phys. Chem. 79, 2745 (1975).

Ochs, G. and Teloy, E., J. Chem. Phys. 61, 4930 (1974).

O'Malley, T. F., Phys. Rev. 162, 98 (1967).

Rebentrost, F. and Lester, W. A. Jr., J. Chem. Phys. 67, 3367 (1977)

Redmon, M. J. and Micha, D. A., Int. J. Quantum Chem. Symp. 8, 253 (1974).

Selby, S. M., Standard Mathematical Tables, Cleveland: The Chemical Rubber Co., 1968.

Shampine, L. F. and Allen, R. C. Jr., Numerical Computing: An Introduction, London Saunders Co., 1973.

Shampine, L. F. and Gordon, M. K., Computer Solution of Ordinary Differential Equations: The Initial Value Problem, San Francisco Freeman, 1975.

Slater, J. C., Int. J. Quantum Chem., 5, 403 (1971).

Smith, F. T., J. Math. Phys. 3, 735 (1962).

Smith, F. T., Phys. Rev. 179, 111 (1969).

Stueckelberg, E. C. G., Helv. Phys. Acta 5, 369 (1932).

Top, Z. H. and Baer, M., J. Chem. Phys. 66, 1363 (1977a).

Top, Z. H. and Baer, M., Chem. Phys. 25, 1 (1977).

Tully, J. C., J. Chem. Phys. 59, 5122 (1973a).

Tully, J. C., J. Chem. Phys. 58, 1396 (1973b).

Tully, J. C., in Dynamics of Molecular Collisions, Part B, ed. W. B. Miller, New York: Plenum Press, 1976, pgs. 217-267.

Tully, J. C., in Semiempirical Methods of Electron Structure Calculations, Part A, ed. G. A. Segal, New York: Plenum Press, 1977.

Tully, J. C., Adv. Chem. Phys. 42, 63 (1980).

Tully, J. C. and Preston, R. K., J. Chem. Phys. 55, 562 (1971).

Zerner, C., Proc. Roy. Soc. (London) A137, 696 (1932).

Ziemba, F. P., Lockwood, G. J., Morgan, G. H. and Everhart, E., Phys. Rev 118, 1552 (1960)

# BIOGRAPHICAL SKETCH

John Albert Olson was born on October 11th, 1946 in Bloomington, Illinois. He attended high school in Jacksonville, Florida, and graduated in 1964. Later that year he enlisted in the United States Navy and was honorably discharged in 1967 as a third class boatswains-mate.

He enrolled at the University Of Florida in the winter of 1968 where he received a Bachelor of Science degree in 1971. He began his graduate work in the Department of Chemistry at the University of Florida in the fall of 1971. He joined the Quantum Theory Project in 1972. In 1974 he received the Dag Hammarskjöld award and attended the International Summer Institute in Quantum Chemistry, Solid State Physics and Quantum Biology held in Uppsala, Sweden and Dalseter, Norway. After a leave of absence beginning in 1977, he returned to the Quantum Theory Project in 1979.

I certify that I have read this study and that in my opinion it conforms to acceptable standards of scholarly presentation and is fully adequate, in scope and quality, as a dissertation for the degree of Doctor of Philosophy.

David A. Micha, Chairman
Professor of Chemistry and
Physics

I certify that I have read this study and that in my opinion it conforms to acceptable standards of scholarly presentation and is fully adequate, in scope and quality, as a dissertation for the degree of Doctor of Philosophy.

Yngve N. Öhrn
Professor of Chemistry

I certify that I have read this study and that in my opinion it conforms to acceptable standards of scholarly presentation and is fully adequate, in scope and quality, as a dissertation for the degree of Doctor of Philosophy.

Thomas L. Bailey

Thomas L. Bailey
Professor of Physics

I certify that I have read this study and that in my opinion it conforms to acceptable standards of scholarly presentation and is fully adequate, in scope and quality, as a dissertation for the degree of Doctor of Philosophy.

Lenart R. Peterson

Lenart R. Peterson
Professor of Physical Sciences

I certify that I have read this study and that in my opinion it conforms to acceptable standards of scholarly presentation and is fully adequate, in scope and quality, as a dissertation for the degree of Doctor of Philosophy.

EE Muschlitz Jr

Earle E. Muschlitz, Jr.
Professor of Chemistry

This dissertation was submitted to the Graduate Faculty of the Department of Chemistry in the College of Arts and Sciences and to the Graduate Council, and was accepted as partial fulfillment of the requirements for the degree of Doctor of Philosophy.

August 1982

Dean, Graduate School